AD 264 925

WADD TECHNICAL REPORT 59-22
VOLUME II

AERODYNAMIC AND STRUCTURAL ANALYSES OF RADOME SHELLS

VOLUME II. STRUCTURAL ANALYSIS

BY

MARTIN H. BLOOM
DENNIS EISEN
MELVIN EPSTEIN
LAWRENCE GALOWIN
ANDREW G. HAMMITT
ERNEST D. KENNEDY
FRANK LANE
DANIEL E. MAGNUS
ALFRED A. MARINO
HAROLD S. PERGAMENT

GENERAL APPLIED SCIENCE LABORATORIES, INC.

FEBRUARY 1961

WRIGHT AIR DEVELOPMENT DIVISION

Best
Available
Copy

NOTICES

AF-WP-B-MAY 60 1M

WADD TECHNICAL REPORT 59-22
VOLUME II

AERODYNAMIC AND STRUCTURAL ANALYSES OF RADOME SHELLS

VOLUME II. STRUCTURAL ANALYSIS

BY

MARTIN H. BLOOM
DENNIS EISEN
MELVIN EPSTEIN
LAWRENCE GALOWIN
ANDREW G. HAMMITT
ERNEST D. KENNEDY
FRANK LANE
DANIEL E. MAGNUS
ALFRED A. MARINO
HAROLD S. PERGAMENT

GENERAL APPLIED SCIENCE LABORATORIES, INC.

FEBRUARY 1961

ELECTRONIC TECHNOLOGY LABORATORY
CONTRACT Nr AF 33(616)-3956
PROJECT Nr 4158
TASK Nr 41538

WRIGHT AIR DEVELOPMENT DIVISION
AIR RESEARCH AND DEVELOPMENT COMMAND
UNITED STATES AIR FORCE
WRIGHT-PATTERSON AIR FORCE BASE, OHIO

McGregor & Werner, Inc., Dayton, O.
100 - October 1961 - 2-9

AERODYNAMIC AND STRUCTURAL ANALYSES OF RADOME SHELLS

VOLUME II

STRUCTURAL ANALYSIS

CHAPTER IV - PART A

STRUCTURAL ANALYSIS OF HOMOGENEOUS AXISYMMETRIC RADOME SHELLS UNDER MECHANICAL, THERMAL AND INERTIAL LOADING

by Frank Lane

TABLE OF CONTENTS

A. STRUCTURAL ANALYSIS OF HOMOGENEOUS AXISYMMETRIC RADOME SHELLS UNDER MECHANICAL, THERMAL AND INERTIAL LOADING

1. INTRODUCTION

Up to the present time shell analyses carried to the point of numerical calculation have been restricted to membrane-type approximations, shallow-shell type approximations, or to shell analyses limited to axisymmetrical loadings. The present development combines the techniques of tensor analysis, differential geometry, and variational calculus with the capabilities of large-scale digital computing machinery to permit solution of the shell problems encountered in radome applications without restriction on geometry or form of loading distribution, and with complete consideration of both membrane and flexural effects. The variational approach permits treatment of static and dynamic or vibratory loadings by related methods and permits introduction of thermal effects (both material property variation and initial stress effects) without major complication.

The present report describes the formulation of the radome problem for homogeneous radome shell types with particular emphasis on ogive, cone, and hemispherical shapes. The techniques developed are, however, equally applicable to other shapes with completely general loading distributions and subject to arbitrary temperature variations. Within the framework of the tensor methods used, the internal displacements (and velocities in dynamic problems) are expressed as first-order tensors, stresses and strains in terms of second-order tensors, and stress-strain relations, in terms of fourth-order tensors, all in curvilinear coordinates appropriate to the radome shell middle surface. All elastic, thermal, and in dynamic applications, inertial aspects of the problem are formulated in general tensor notation as is the differential geometry of the shell middle surface.

Actual numerical computations are rendered feasible by utilizing the above-described intrinsic shell theory in conjunction with an energy or variational method. Final computation reduces to the solution of an algebraic problem, non-homogeneous in the case of response to static, dynamic, or thermal loading, and homogeneous in the case of free vibration. The entire development, for certain conditions, proceeding from the prescription of initial shell geometry and loading to the final resulting deformation and stress distribution is to be programmed for execution upon the IBM 704 digital computer.

The present section describes the analytical phases of an investigation whose ultimate objective is the development of an efficient and accurate program for the structural analysis of thermally and mechanically loaded axisymmetric, homogeneous radome shell structures by means of high-speed digital computing equipment. The end-product sought is a program which requires but a minimum of input data describing the shell geometry and the imposed thermal and mechanical loading distributions and which utilizes this data to generate solutions of the structural problem. The solutions are to include adequately detailed descriptions of the distributions of deformation and stress throughout the shell. Moreover, the program is to be sufficiently general to permit inclusion of varying degrees of edge fixity as well as the presence or absence of an elastic central boom.

The analysis is based on a general formulation of the axisymmetric shell problem in curvilinear coordinates and takes advantage, from the very outset, of the knowledge that the problem is to be solved numerically. This permits an approach which relies upon a minimum of physical assumptions or approximations. The only such assumptions introduced are the following: (a) The shell-type assumption that the normal stress component in the direction normal to the shell middle surface may be neglected relative to the other induced stresses; (b) The shell-type assumption that normals to the middle surface remain straight under deformation; (c) The calculation of the slopes of the above normals under the assumption that normals to the middle surface remain normal under deformation; (d) The assumption that Young's modulus ϵ and Poisson's ν may be considered constant throughout the shell and equal to their respective mean values over the temperature range experienced by the shell for any given problem. This last assumption may be dropped when axisymmetrical loading is considered, but results in an essential simplification for asymmetric conditions.

The fact that it is recognized in advance that numerical methods are to be used makes it unnecessary to use any of the standard shell approximations of expanding in powers of the normal coordinate, and neglecting various terms as small. Incidentally, it is this type of approximation which accounts for the major portion of the discrepancies noted between the linear shell theories of various investigators[2].

In view of the current interest in the unified antenna-radome concept, the analysis presented herein is made sufficiently general to encompass the case of the truncated axisymmetric radome with central boom. The formulation, however, is completely general and, aside from certain problems which arise at the apex of a complete shell, suffers from no essential complications when applied to general shells of revolution with or without a central boom.

The technique employed herein hinges on the energy approach to structural analysis and requires first an extension of the energy principle to permit inclusion of thermal effects. For this purpose the so-called "free energy" of Hemp[1] is utilized and is specialized from the general thermo-elastic three-dimensional form given by Hemp to the form appropriate to shell analysis. The use of the energy technique together with a general tensorial formulation of the energy expression in curvilinear coordinates appropriate to the shell middle surface virtually eliminates all possibility of error due to neglect of terms or inaccurate or incomplete resolution of forces required by equilibrium methods. Correspondingly, the macroscopic stresses or stress-resultants of the usual shell theory are by-passed, the entire problem being formulated in terms of displacements. Furthermore, the difference approximation required by the numerical solution technique is viewed as a direct method in the calculus of variations: The difference approximation is introduced directly into the energy integral (thereby converting this integral to a summation) and the equilibrium problem reduces to a minimum problem with respect to the mesh-point values of the displacements. This technique has several advantages: First, it insures that the numerical problem, in difference form, has a positive-definite matrix, thereby guaranteeing the convergence of iterative solution techniques. Second, it makes the introduction of quite general boundary conditions extremely simple and nearly automatic, and finally, it eliminates any necessity of performing the operation of first-variation to obtain the Euler equations and boundary conditions of the variational problem, followed by differencing of these equations. Rather, the differencing in the energy expression proper provides the matrix of the numerical problem directly and automatically insures the appropriate expression of boundary conditions in difference form whether these correspond to fixed, partially fixed, or free-edge situations.

2. GEOMETRY AND COORDINATE DEFINITION

Figure 1 shows, for the general shell of revolution, the y^i coordinate system utilized together with the associated covariant metric tensor (a_{ij}) components. The metric tensor elements are expressible completely in terms of meridian slope, β, and the two principal radii of curvature R_1 and R_2. The orthogonality of the coordinates insures the diagonal nature of the metric tensor and the simple relations for the contravariant form a^{ij}. The quantity J, which is equal to the square root of the determinant of a_{ij}, gives the volume element for the y^i coordinate system and will be needed for formulation of the energy integrals. The coordinate y^3 gives the inward distance locally normal to the shell middle surface, y^2 gives meridional distance along the middle surface from the apex of the middle surface (extended, if the actual shell is truncated), and y^1 is the longitude angle in radians.

Figure 2 illustrates the same data specialized to the case of the truncated cone. In this case the variable radii of curvature R_1 and R_2 are replaced, respectively, by $y^2 \tan \lambda$ and ∞, while the generally variable meridian-tangent angle, β, becomes simply the constant semi-vertex angle λ. The metric elements simplify correspondingly.

The contravariant form of the displacement vector corresponding to the y^i coordinate system is denoted by ξ^i and is to be distinguished from the physical displacement vector (u^1 u^2 u^3). The reason for introducing both tensorial and physical components of the displacement vector is that the strain-displacement relations are natural in the tensor form, whereas the shell-assumption of u^3 independent of y^3 while u^1 and u^2 vary linearly with y^3 is expressed in terms of physical displacements. The entire problem will be cast ultimately in terms of physical displacements.

The relation between physical and tensorial displacements is well-known:

$$u^i = \xi^i \sqrt{a_{ii}} = \xi_i \sqrt{a^{ii}} \qquad (1)$$

not summed on i

It is to be noted that, in view of the orthogonality of the coordinate system, there is no need to distinguish between contravariant and covariant forms of the physical displacements u^i.

3. STRESS-STRAIN AND STRAIN-DISPLACEMENT RELATIONS

The covariant form of the strain-displacement law for any coordinate system, within linear theory, is given simply as [3]

$$\eta_{ij} = \frac{1}{2} (\xi_{i,j} + \xi_{j,i}) \tag{2}$$

wherein commas denote covariant derivatives and the ξ_i are merely the covariant components of the displacement tensor. The η_{ij} are the covariant, linear strain components.

The stress-strain law for an isotropic material in general curvilinear coordinates, including thermal stress effects, is given by

$$\tau^{ij} = \frac{\epsilon}{1+\nu} \left(a^{ik} a^{jl} + \frac{\nu}{1-2\nu} a^{ij} a^{kl}\right) \eta_{kl} - \frac{\epsilon\alpha}{1-2\nu} (T - T_o) a^{ij} \tag{3}$$

wherein τ^{ij} is the contravariant form of the stress tensor, ϵ is Young's Modulus, ν is Poisson's Ratio, α is the linear coefficient of thermal expansion and $(T-T_o)$ is temperature relative to the temperature T_o associated with the unstressed state. Repeated indices imply summation throughout unless otherwise specified.

4. SHELL ASSUMPTIONS

At this point, the shell assumptions are introduced. These may be summarized as follows:

(a) $T^{33} = 0$ (4)

i.e., the normal stress (normal to the middle surface) is small of higher order relative to other stress components.

(b)
$$u^1 = u^1_{(o)}(y^1, y^2) + y^3\, u^1_{(1)}(y^1, y^2)$$
$$u^2 = u^2_{(o)}(y^1, y^2) + y^3\, u^2_{(1)}(y^1, y^2) \tag{5}$$
$$u^3 = u^3_{(o)}(y^1, y^2)$$

i.e., the in-plane displacements are assumed linear in y^3 while u^3 is assumed independent of y^3.

Finally

(c) the $u^1_{(1)}$ $u^2_{(2)}$ are to be computed on the assumption that normals to the middle-surface remain normal at the middle surface.

This process is clearly discussed by Novozhilov[4]. It is to be emphasized that the foregoing three assumptions, (a) (b) (c), together with the use of constant mean values of ϵ and ν, are the only ones introduced into the analysis until the difference method is introduced to permit numerical solution. No intermediate approximations, such as the common expansion of contravariant metric elements in powers of y^3, are utilized.

The assumption (4) of vanishing T^{33} is utilized to eliminate η_{33} from the stress-strain relation (3). Hereafter, Latin indices i, j, k, l ... will range over 1, 2, 3, while Greek indices $\alpha, \beta, \gamma, \delta$ ... will range over only the middle-surface indices 1, 2. The elimination of η_{33} from the general stress-strain law (3) gives the following shell stress-strain relations for the stress components parallel to the middle surface:

$$T^{\alpha\beta} = \frac{\epsilon}{1+\nu}\left(a^{\alpha\delta}a^{\beta\gamma} + \frac{\nu}{1-\nu}a^{\alpha\beta}a^{\gamma\delta}\right)\eta_{\gamma\delta} - \frac{\epsilon\,\alpha\, a^{\alpha\beta}(T - T_o)}{1-\nu} \tag{6}$$

This is the stress-strain law, including thermal effects, which governs the general shell-of-revolution problem.

Next is invoked the assumption (c) of normals at the middle surface remaining normal for purposes of computing the $u^{\alpha}_{(1)}$. This is equivalent to assuming that

$$\eta_{\alpha 3}\Big|_{y^3 = 0} = 0 \quad \text{for purposes of computing the } u^{\alpha}_{(1)}.$$

The consequences of this condition are as follows:

$$0 = \eta_{\alpha 3}\Big|_{y^3 = 0} = \frac{1}{2}(\xi_{\alpha,3} + \xi_{3,\alpha})\Big|_{y^3 = 0} \tag{7}$$

Expanding the indicated covariant differentiation, this becomes:

$$\begin{aligned} 0 &= \left[\frac{\partial \xi_\alpha}{\partial y^3} + \frac{\partial \xi_3}{\partial y^\alpha} - \begin{Bmatrix} k \\ \alpha \quad 3 \end{Bmatrix}\xi_k - \begin{Bmatrix} k \\ 3 \quad \alpha \end{Bmatrix}\xi_k\right]_{y^3 = 0} \\ &= \left[\frac{\partial \xi_\alpha}{\partial y^3} + \frac{\partial \xi_3}{\partial y^\alpha} - 2\begin{Bmatrix} k \\ \alpha \quad 3 \end{Bmatrix}\xi_k\right]_{y^3 = 0} \end{aligned} \tag{8}$$

where the bracketed expressions are the Christoffel symbols of the second kind based on a_{ij} and where the well-known symmetry of these symbols in the lower indices has been utilized. It is easily ascertained for the present metric that all Christoffel symbols with more than one index equal to 3 must vanish. Hence,

$$0 = \left[\frac{\partial \xi_\alpha}{\partial y^3} + \frac{\partial \xi_3}{\partial y^\alpha} - 2 \begin{Bmatrix} \beta \\ \alpha \quad 3 \end{Bmatrix} \xi_\beta \right]_{y^3 = 0} \tag{9}$$

Utilizing relations (1) and the fact that $a^{33} = a_{33} = 1$, this may be expressed in terms of the physical displacements

$$0 = \left[\sqrt{a_{\alpha\alpha}}\, \frac{\partial u^\alpha}{\partial y^3} + u^\alpha \frac{\partial \sqrt{a_{\alpha\alpha}}}{\partial y^3} + \frac{\partial u^3}{\partial y^\alpha} - 2\sqrt{a_{\beta\beta}}\, u^\beta \begin{Bmatrix} \beta \\ \alpha \quad 3 \end{Bmatrix}\right]_{y^3 = 0} \tag{10}$$

no sum on α

Now the relation between Christoffel symbols of the first and second kinds is given by

$$\begin{Bmatrix} i \\ j \quad k \end{Bmatrix} = a^{il} \left[j\, k, l\right] \tag{11}$$

Hence
$$\begin{Bmatrix} \beta \\ \alpha \quad 3 \end{Bmatrix} = a^{k\beta} \left[\alpha\, 3, k\right] = a^{\gamma\beta} \left[\alpha\, 3, \gamma\right] \tag{12}$$

due to the vanishing of Christoffel symbols with more than one index equal to 3. Invoking once again the diagonal character of a_{ij}, and the defining relations[3] for the Christoffel symbols of the first kind;

$$\left[i\, j, k\right] = \frac{1}{2}\left(\frac{\partial a_{ik}}{\partial y^j} + \frac{\partial a_{jk}}{\partial y^i} - \frac{\partial a_{ij}}{\partial y^k}\right) \tag{13}$$

the relation (10) may be put into its final form:

$$\frac{\partial u^{\alpha}}{\partial y^{3}} = u^{\alpha}_{(1)} = \left[\frac{1}{2}\, a^{\alpha\alpha}\; u^{\alpha}\; \frac{\partial a_{\alpha\alpha}}{\partial y^{3}} - \sqrt{a^{\alpha\alpha}}\; \frac{\partial u^{3}}{\partial y^{\alpha}} \right]_{y^{3}=0} \tag{14}$$

no sum on α

$\alpha = 1, 2$

This pair of equations serves to eliminate from all further considerations the quantities $u^{\alpha}_{(1)}$ in favor of the middle-surface deflections $u^{\alpha}_{(o)}$ and gradients of $u^{3}_{(o)}$. With this relation, the direct consequences of the shell-assumptions are concluded.

5. EXPRESSION OF STRAINS IN TERMS OF PHYSICAL DISPLACEMENTS

Equations (1) and (2), together with the well-known properties of the Christoffel symbols, permit the expression of the strains $\eta_{\alpha\beta}$ in terms of physical displacements u^i. These take the following form, for the case of the metric tensor corresponding to Figure 1:

$$
\begin{aligned}
\eta_{11} &= \sqrt{a_{11}}\,\frac{\partial u^1}{\partial y^1} + \frac{\sqrt{a^{22}}}{2}\,u^2\,\frac{\partial a_{11}}{\partial y^2} + \frac{1}{2}\,\frac{\partial a_{11}}{\partial y^3}\,u^3 \\
\eta_{22} &= \sqrt{a_{22}}\,\frac{\partial u^2}{\partial y^2} + \frac{u^3}{2}\,\frac{\partial a_{22}}{\partial y^3} \qquad (15) \\
\eta_{12} &= \frac{\sqrt{a_{11}}}{2}\,\frac{\partial u^1}{\partial y^2} - \frac{u^1}{4}\,\sqrt{a^{11}}\,\frac{\partial a_{11}}{\partial y^2} + \frac{\sqrt{a_{22}}}{2}\,\frac{\partial u^2}{\partial y^1}
\end{aligned}
$$

These strain expressions may then be given in terms of middle-surface values $u^i_{(o)}$ of displacements by simply substituting from (5) and (14) into the general displacements u^i of (15). The substitution, while routine, is somewhat lengthy and need not be reproduced at this point.

6. ENERGY FORMULATION

The energy formulation sought for the shell problem under both thermal and mechanical loading may be developed by extending to general curvilinear coordinates the "free energy" considered by Hemp in Reference (1). Hemp proposes a thermodynamic explanation of this quantity, but it suffices to consider the free energy as simply equal to the variational integral whose Euler's equations provide the proper equilibrium equations of thermoelasticity as well as the proper boundary conditions. In this sense, the free energy serves as the thermoelastic analog of the strain energy in ordinary isothermal elasticity, and this is the context in which it will be utilized in the present analysis.

Hemp's free energy, extended to general curvilinear coordinates y^i, takes the form:

$$F_{(general)} = \iiint J d_y^1 \, d_y^2 \, d_y^3 \left\{ \left[\frac{\epsilon}{2(1+\nu)} \left(a^{ik} a^{jl} + \frac{\nu}{1-2\nu} a^{ij} a^{kl} \right) \eta_{ij} \, \eta_{kl} - \frac{\epsilon \alpha}{1-2\nu} (T - T_o) \, a^{ik} \eta_{ik} \right] \right\} \tag{16}$$

Under the shell assumptions (a), (b), (c) of the present analysis, the expression for F may be re-derived with the following result:

$$F_{shell} = F = \iiint J d_y^1 \, d_y^2 \, d_y^3 \left\{ \left[\frac{\epsilon}{2(1+\nu)} \left(a^{\alpha\delta} a^{\beta\gamma} + \frac{\nu}{1-\nu} a^{\alpha\beta} a^{\gamma\delta} \right) \eta_{\alpha\beta} \, \eta_{\gamma\delta} - \frac{\epsilon \alpha (T - T_o)}{1 - \nu} a^{\alpha\beta} \eta_{\alpha\beta} \right] \right\} \tag{17}$$

This relation in conjunction with a work integral W forms the basis for the shell analysis developed herein. The work integral for the shell, assuming the mechanical loading to be due to a normal pressure distribution, $p(y^1, y^2)$, is given by

$$W = \iint dy^1 dy^2 \; J(y^1, y^2, o) \; p(y^1 \; y^2) \; u^3(y^1 \; y^2) \tag{18}$$

where p is considered positive when directed inward; i.e., p is actually the local value of (outer pressure minus inner pressure).

The combined problem of mechanical and thermal loading of a shell is then stated in variational form: The solution distribution of deflections u^i is such that (F-W) is stationary, i.e.,

$$\delta(F - W) = 0 \tag{19}$$

However, the fact that linear theory is used throughout implies that superposition of thermally and mechanically induced stresses is valid. Hence, the thermal response resulting from the temperature term in F and the mechanical response resulting from W may be calculated separately and added. Care must be taken, however, to insure that the proper mean values of ϵ and ν are used in the pressure problem if the pressure loading is to occur under high temperature conditions.

7. ELIMINATION OF y^1-DEPENDENCE BY FOURIER ANALYSIS

The thermoelastic response problem defined by relations (17), (18), and (19) is of three-dimensional character in its present form. The purpose of the present section is to reduce the problem to a series of two-dimensional problems in which the y^1-dependence is lacking. The following section will describe the technique for reducing each of these two-dimensional problems in turn to a one-dimensional problem by integration through the shell thickness with consequent elimination of y^3-dependence.

The reduction to two dimensions is straightforward and is accomplished by Fourier resolution of mechanical and thermal loading distributions as well as of the corresponding response deformation distributions. Thus, the independent variable y^1 is, for reasons of clarity, denoted by θ and the pressure load $p(y^1 y^2)$ is expressed as a cosine series in θ:

$$p(y^1, y^2) = p(y^2, \theta) = \sum_{m=0}^{\infty} {}_m p(y^2) \cos m\theta \qquad (20)$$

The use of a cosine series is but a minor restriction since the origin of θ may be chosen at will, and the radome loads to be expected will generally exhibit symmetry about some meridian plane.

Similarly, the temperature loading may be expanded in a cosine series with respect to θ where, due to the validity of superposition, the origin for this θ need not correspond to that of the θ used in the pressure expansion, provided the responses are obtained separately and superimposed correctly. Thus,

$$\alpha(T - T_0) = \sum_{m=0}^{\infty} {}_m T(y^2, y^3) \cos m\theta \qquad (21)$$

where the coefficient of expansion, α, which is in general temperature-dependent, is included with $(T-T_0)$ to simplify the analysis. Corresponding to loading expansions (20) and (21), not necessarily considered simultaneously, the displacements u^i are resolved into Fourier components as follows:

$$u^3_{(o)} = u^3 = \sum_{m=0}^{\infty} {}_m u^3 \cos m\theta$$

$$u^2_{(o)} = \sum_{m=0}^{\infty} {}_m u^2 \cos m\theta \qquad (22)$$

$$u^1_{(o)} = \sum_{m=1}^{\infty} {}_m u^1 \sin m\theta$$

where ${}_m u^i = {}_m u^i(y^2)$

Now, from equations (5) and (14), together with the fact that all geometric properties are θ-independent, it follows that $u^1_{(1)}$ depends linearly upon $u^1_{(o)}$ and $\frac{\partial u^3}{\partial y^1}$, both of which are given by sine series. Similarly, $u^2_{(1)}$ is linear in $u^2_{(o)}$ and $\frac{\partial u^3}{\partial y^2}$, both of which are given by cosine series. Hence u^3 and u^2 are expressed as cosine series in θ while u^1 is a sine series, which state of affairs corresponds to the even character of the loading (thermal or mechanical) in θ.

An examination of strain expressions (15) in the light of the above remark reveals that η_{11} and η_{22} must be pure cosine series while η_{12} must be a pure sine series.

Now, from the diagonal character of the metric tensor a_{ij} (hence, also of a^{ij} which is merely the inverse of a_{ij}), it may be easily seen that the free energy expression (17) involves quadratic forms in the strains of only the following types:

$$(\eta_{11})^2 \quad (\eta_{22})^2 \quad (\eta_{12})^2 \quad (\eta_{11}\ \eta_{22})$$

and that, moreover, these expressions are multiplied only by quantities independent of y^1 (or θ). Furthermore, the thermal loading term in F involves only products of $\alpha(T-T_0)$ and η_{11} or η_{22} together with θ-independent quantities (recalling the assumption of a constant mean value for ϵ and ν). Finally, the work integral W involves only products of pressure and u^3, together with θ-independent factors. The result of all this is a complete decoupling of distinct harmonics; i.e., associated with the m^{th} harmonic of the loading (thermal or mechanical) there correspond only the m^{th} harmonics of u^1 u^2 u^3 and of $u^1_{(o)}$ $u^2_{(o)}$ and $u^3_{(o)}$ and of the strains and stresses. This is a simple consequence of the fact that F and W involve integration with respect to θ over the interval $(0, 2\pi)$ and the fact that the sines and cosines form an orthogonal set with respect to a constant weighting function over the interval $(0, 2\pi)$. It follows from the relations

$$\int_0^{2\pi} \sin^2 m\theta \, d\theta = \int_0^{2\pi} \cos^2 m\theta \, d\theta = \pi \qquad m \neq 0$$

$$\int_0^{2\pi} \cos^2 m\theta \, d\theta = 2\pi \qquad m = 0 \tag{23}$$

that the free-energy form may be reduced to a system of two-dimensional problems independent of y^1 or θ by introducing the simple notation:

$$F_{(m)} = 2\pi\, C_m \iint dy^2\, dy^3 \; (\ldots\ldots\ldots) \tag{24}$$

Likewise, the work form W reduces to a set of one-dimensional integrals;

$$W_{(m)} = 2\pi\, C_m \int dy^2 \; (\ldots\ldots\ldots\ldots) \tag{25}$$

$$\text{with} \qquad \begin{aligned} C_m &= 1 \;:\quad m = 0 \\ &= \tfrac{1}{2} \;:\quad m > 0 \end{aligned} \tag{26}$$

wherein the m^{th} integrand involves only the m^{th} harmonic of pressure, temperature, and strain.

The problem corresponding to (19) for the m^{th} harmonic is then simply:

$$\delta\,(F_{(m)} - W_{(m)}) = 0 \tag{27}$$

The problem, originally three-dimensional, is thus effectively reduced to a set of decoupled two-dimensional problems. In practice, it will suffice to consider only $zero^{th}$ and first-order harmonics ($m = 0, 1$) unless the loading exhibits unusually severe θ-dependence associated with some sort of load or temperature concentration.

8. REDUCTION TO ONE-DIMENSIONAL PROBLEM BY INTEGRATION THROUGH SHELL THICKNESS

The work forms $W_{(m)}$ of expression (25) are already one-dimensional, and it remains to put the free-energy harmonics $F_{(m)}$ of expression (24) into similar form. This is accomplished simply by integrating with respect to y^3 through the shell thickness from -h/2 to +h/2. The integration operation involves no essential difficulty for the portions of $F_{(m)}$ quadratic in the strains, since all y^3-dependence is completely defined. The temperature contribution to $F_{(m)}$ is treated simply by defining several required weighted integrals of $\alpha(T-T_0)$ through the shell thickness. In view of the fact that the distribution of $\alpha(T-T_0)$ is input data for the thermal stress problem, any such weighted integrals will be known as required. It should be noted again that no approximations or expansions in powers of y^3 are necessary at this stage of the reduction in view of the fact that the problem is eventually to be solved numerically. The presence of variable coefficients of logarithmic character, for example, causes no difficulty in the numerical solution.

The type of result which is to be expected from this operation may be indicated as follows: Equation (14) gives $u^{\alpha}_{(1)}$ as a linear combination of $u^{\alpha}_{(o)}$ and $\frac{\partial u^3_{(o)}}{\partial y^{\alpha}}$ involving no y^3-dependence. Thus, making use of the Fourier resolution of the preceding section:

$$
\begin{aligned}
{}_m u^{\alpha} &= {}_m u^{\alpha}_{(o)}\,(y^2) + y^3\,{}_m u^{\alpha}_{(1)}\,(y^2) \\
{}_m u^3 &= {}_m u^3_{(o)}\,(y^2)
\end{aligned}
\qquad (28)
$$

Now, from the free-energy expression (17) and its two-dimensional Fourier resolution (24), it can be seen that the only y^3-dependence in $F_{(m)}$ enters through terms of the following types:

$$J\ (a^{11}\eta_{11})^2 \qquad J\ (a^{22}\eta_{22})^2 \qquad J\ (a^{11}\eta_{11}a^{22}\eta_{22})$$

$$J\ a^{11}a^{22}(\eta_{12})^2 \tag{29}$$

$$\alpha(T-T_0)\ J a^{11}\eta_{11} \qquad \text{and} \qquad \alpha(T-T_0)\ J a^{22}\eta_{22}$$

Furthermore, examination of strain expressions (15) shows that

$$a^{11}\eta_{11} = \sqrt{a^{11}}\left(\frac{\partial u^1}{\partial y^1} + \sqrt{a^{22}}\ u^2\ \frac{\partial(\sqrt{a_{11}})}{\partial y^2} + u^3\frac{\partial(\sqrt{a_{11}})}{\partial y^3}\right)$$

$$a^{22}\eta_{22} = \sqrt{a^{22}}\left(\frac{\partial u^2}{\partial y^2} + u^3\ \frac{\partial(\sqrt{a_{22}})}{\partial y^3}\right) \tag{30}$$

$$\sqrt{a^{11}\ a^{22}}\ \eta_{12} = \frac{\sqrt{a^{11}a^{22}}}{2}\left(\sqrt{a_{11}}\ \frac{\partial u^1}{\partial y^2} - \frac{u^1\partial\sqrt{a_{11}}}{\partial y^2} + \sqrt{a_{22}}\ \frac{\partial u^2}{\partial y^1}\right)$$

Moreover, J is given simply by $\sqrt{a_{11}\ a_{22}}$.

Therefore the terms (29) which are quadratic in the strains are all of the form

$$\left\{\begin{bmatrix} 1 \\ \sqrt{a^{11}} \\ \sqrt{a^{22}} \\ \sqrt{a^{11}\ a^{22}} \end{bmatrix}\right\} \left\{\begin{bmatrix} \text{multiplied by polynomials in } y^3 \\ \text{of up to 4th order} \end{bmatrix}\right\} \tag{31}$$

The temperature terms of (29) involve only the temperature, or $\alpha(T-T_0)$ multiplied by polynomials in y^3 of second order or lower.

Now terms of the types occurring in (31) are all easily integrated with respect to y^3, resulting in nothing more formidable than logarithms whose arguments may depend upon y^2. The temperature terms may be handled completely by defining the following three weighted averages of the general m^{th} harmonic of $\alpha(T-T_0)$ (recalling expression (21)).

$$\int_{-\frac{h}{2}}^{\frac{h}{2}} \begin{bmatrix} 1 \\ y^3 \\ (y^3)^2 \end{bmatrix} {}_mT(y^2, y^3)\, dy^3 = \begin{bmatrix} h \; {}_mT^{(0)}(y^2) \\ h^2 \; {}_mT^{(1)}(y^2) \\ h^3 \; {}_mT^{(2)}(y^2) \end{bmatrix} \tag{32}$$

These weighted averages are all known in terms of prescribed data for the thermal stress problem. Thus the problem (27) for the m^{th} harmonic of the displacement distribution and, correspondingly, of the stress distribution, is reduced to a one-dimensional problem with y^2, the middle-surface arclength along the meridian, serving in the role of independent variable. As a final parenthetical remark, it may be noted that the logarithmic terms resulting from the y^3-integration will all be of the form

$$L_n \left\{ \frac{1 - \frac{h/2}{R_\alpha}}{1 + \frac{h/2}{R_\alpha}} \right\} \qquad \alpha = 1 \text{ or } 2 \tag{33}$$

and hence are well-behaved as long as the local semi-thickness $\frac{h}{2}$ is smaller than the smaller of the two local principal radii of curvature, R_1, R_2.

9. BOUNDARY CONDITIONS

Only one set of conditions remains in order to complete the problem statement, and this is the prescription of boundary conditions at the forward and after edges of the radome shell. Within the framework of the energy method it is possible to prescribe in a routine manner very general boundary conditions including the presence, if necessary, of an elastic central boom.

Considering first the base of the radome ($y^2 = \ell$) the shell is assumed simply supported but with a distributed moment spring of spring constant k_3 inch-pounds per radian per inch of circumference (see Figure 3(a)). The presence of the spring k_3 corresponds to partial fixity and may be varied from zero, corresponding to simple support, to infinity (see the end of the present section) corresponding to the fully-clamped condition. The base boundary conditions are thus specified as follows:

$$\text{at} \qquad y^2 = \ell \ : \quad {}_m u^1 = {}_m u^2 = {}_m u^3 = 0 \tag{34}$$

And, to the free-energy component F_m add the base-spring energy:

$$\begin{aligned} F_m^{(3)} &= \left[\int_0^{2\pi} \frac{k_3}{2} \, R_1 \cos\beta \left(\frac{\partial \, {}_m u^3}{\partial y^2} \right)^2 dy^1 \right]_{y^2 = \ell} \cos^2(y^1 m) \\ &= 2\pi \, C_m \frac{k_3}{2} \, R_1 \cos\beta \left[\left(\frac{\partial \, {}_m u^3}{\partial y^2} \right)^2 \right]_{y^2 = \ell} \end{aligned} \tag{35}$$

Conditions (34) are specified in the conventional manner, whereas the edge moment condition, instead of requiring the usual development of an expression for macroscopic or resultant moment in terms of displacements, appears in the form of a simple addition to the free energy. These conditions complete the base boundary specification.

The nose boundary conditions are inserted in a manner similar to that illustrated by expressions (35), there being in general no nose constraint equivalent to the fixed conditions (34). Figures 3(b), (c), (d), and (e) illustrate the equivalent springs for the nose boundary conditions. Figure 3(b), with associated spring k_1, represents the resistance of a central boom (and nose attachment to the boom) against axial stretching.

The mean axial displacement at the middle surface for the nose is given by

$$\left.\frac{1}{2\pi}\int_0^{2\pi}(u^2\cos\beta + u^3\sin\beta)\,dy^1\right]_{\substack{y^3=0\\ y^2=a\ell}} = \left.{}_0u^2\cos\beta + {}_0u^3\sin\beta\right]_{\substack{y^3=0\\ y^2=a\ell}} \tag{36}$$

Thus the energy addition appropriate to axial displacement of the nose is: Add nothing to F_m for $m > 0$, and to F_o add,

$$\left.\frac{k_1}{2}({}_0u^2\cos\beta + {}_0u^3\sin\beta)^2\right]_{\substack{y^3=0\\ y^2=a\ell}} \tag{37}$$

If there is no axial restraint from a central boom, $k_1 = 0$, while nonzero k_1-values give various degrees of axial stiffness. Similarly, the mean value of nose transverse displacement, which is resisted by elastic bending of the central boom, if such a boom is present, is given by

$$\frac{1}{2\pi}\int_0^{2\pi}\left((u^2 \sin\beta - u^3 \cos\beta) \cos y^1 - u^1 \sin y^1\right) dy^1\Bigg]_{\substack{y^3=0\\ y^2=a\ell}}$$

$$= \frac{1}{2}\left({}_1u^2 \sin\beta - {}_1u^3 \cos\beta - {}_1u^1\right)_{\substack{y^3=0\\ y^2=a\ell}} \tag{38}$$

And the corresponding energy addition is (see Figure 3(c)) zero for $m \neq 1$ and

$$\frac{k_2}{2}\left(\frac{1}{2}\left[{}_1u^2 \sin\beta - {}_1u^3 \cos\beta - {}_1u^1\right]\right)^2\Bigg]_{\substack{y^3=0\\ y^2=a\ell}} \qquad \text{for } m = 1 \tag{39}$$

where k_2 is the spring constant for the boom in transverse deflection. If the boom is absent, $k_2 = 0$, while nonzero k_2-values correspond to varying degrees of boom flexural stiffness.

The central boom, if present, also resists a mean value of shell transverse slope at the nose (Figure 3(d)). This slope is given by

$$\bar{a} = \left[\frac{1}{\cos\beta} \frac{\partial}{\partial y^2} \left(\frac{1}{2} \left[{}_1u^2 \sin\beta - {}_1u^3 \cos\beta - {}_1u^1 \right] \right) \right]_{\substack{y^3 = 0 \\ y^2 = a\ell}} \tag{40}$$

the computation of which is facilitated by the fact (Figure 1) that $\frac{\partial\beta}{\partial y^2} = -\frac{1}{R_2}$. The energy addition corresponding to this is simply

$$\frac{k_4}{2} (\bar{a})^2 \qquad \text{for} \qquad m = 1 \quad \text{and zero for} \quad m \neq 1 \tag{41}$$

Again, in the absence of the boom, $k_4 = 0$.

Finally, Figure 3(e) represents the nose equivalent of the base-edge clamping. The distributed spring k_5 provides the equivalent of the degree of clamping of the nose edge to the boom or to any closing member even if the boom is absent. For purposes of computing the contribution to F from this equivalent spring distribution, it is necessary to have an expression for the y^1-component, z^1, of physical rotation. This is given by the following relation:

$$z^1 \Big|_{y^3 = 0} = \left(\frac{\partial u^3}{\partial y^2} + \frac{u^2}{R_2} \right)_{y^3 = 0} \tag{42}$$

The contribution to F due to distributed nose spring k_5 is given by the integrated square of the difference between this local rotation and the angle $(-\bar{a}\cos y^1)$ corresponding to mean rotation of the nose structure.

$$\frac{k_5}{2} \int_0^{2\pi} R_1 \cos\beta \left(\frac{\partial u^3}{\partial y^2} + \frac{u^2}{R_2} + \bar{a} \cos y^1 \right)^2 dy^1 \Bigg]_{\substack{y^3 = 0 \\ y^2 = a\ell}} \tag{43}$$

This is easily integrated to give

$$\frac{k_5}{2} R_1 \cos\beta \left\{ 2\pi \sum_{m=0}^{\infty} C_m \left(\frac{\partial_m u^3}{\partial y^2} + \frac{{}_m u^2}{R_2} \right)^2 + 2\pi(\bar{a}) \left(\frac{\partial_1 u^3}{\partial y^2} + \frac{{}_1 u^2}{R_2} \right) + \pi \bar{a}^2 \right\}_{\substack{y^2 = a\ell \\ y^3 = 0}} \tag{44}$$

where $\bar{a}$ is given by (40), and terms in (44) containing $\bar{a}$ contribute only to $F_{(1)}$ whereas the series expression contributes to F_m for all $m = 0, 1, 2, \ldots$

In the event that the nose edge is free or is simply supported at the connection to a central boom, then k_5 is simply set equal to zero, whereas a fully-clamped nose condition is achieved by letting k_5 become indefinitely large.

The approach to infinity of any of the aforementioned springs in order to simulate fully fixed conditions may be handled within a numerical difference scheme by scaling certain of the mesh-point values of displacement or differences thereof in such a way that numerical data remains bounded. This is numerically equivalent to inserting the constraints directly, as in equation (34) for the base edge displacement. If this approach is considered undesirable due to other features of the numerical solution technique, then the fully fixed condition may be placed in the direct form of equation (34). In other words, in place of letting k_3 approach infinity and including in the energy expression the contribution (35) with the consequent necessity for scaling, the condition of full fixity is equally well inserted by setting

$$\left.\frac{\partial_m u^3}{\partial y^2}\right|_{y^2 = \ell} = 0 \tag{45}$$

and imposing the corresponding constraint on the numerical difference problem.

10. FINITE-DIFFERENCE SOLUTION TECHNIQUE

The complete shell analysis is now formulated as a series of uncoupled variational problems of the form (27) in which the energy expressions $F_{(m)}$ and $W_{(m)}$ consist of one-dimensional integrals over the shell meridian plus possible boundary-condition energy additions to $F_{(m)}$ which are expressed as quadratic combinations of edge displacements and derivatives thereof. Starting from this point, a variety of solution techniques is available. One might use the Rayleigh-Ritz method of expanding unknown deflections in a series of known, fixed-boundary-condition satisfying functions and perform the variational operation directly by minimization with respect to the displacement expansion coefficients.

The existence of edge effects which exhibit strong gradients in the edge regions militates against this method as does the inaccuracy inherent in utilizing the method to obtain stresses which involve derivatives of the displacement expansion functions. Still another disadvantage of the Rayleigh-Ritz technique lies in the tremendous number of integrations which must be performed to generate the matrix of the numerical problem. Alternatively, one may perform the variational operation analytically to obtain systems of three ordinary differential equations for each harmonic (each value of m). These (Euler) equations may then be solved by finite difference techniques.

There are several disadvantages associated with this technique. First, the Euler equations must be found analytically, as must the natural boundary conditions associated with free or spring-restrained edges. Then both the equations and the boundary conditions must be placed in difference form, an operation which leaves a great deal to personal judgement. Finally, when this is complete, there is no assurance that the matrix of the system of equations will be symmetric and positive definite, and these characteristics are helpful in guaranteeing the convergence of iterative solution techniques[6]. The large-scale character expected for the system of equations indicates that iterative techniques will be needed for refinement of solutions if not for actual solution itself.

The approach followed here is, in a sense, a combination of the above two techniques. The continuous range $(a\ell, \ell)$ of y^2 is replaced by a distribution of discrete points and the values of the displacement components ${}_m u^1_{(o)}$ ${}_m u^2_{(o)}$ ${}_m u^3_{(o)}$ at these points are considered as degrees of freedom for the variational problem. The point spacing need not be uniform and, in fact, in order to describe adequately the edge-effect or "boundary-layer" effect, this spacing should be considerably smaller in the base and nose edge regions, changing to a larger value for the major internal portion of the range. The decisive point here, however, is the fact that the difference approximation is introduced directly into the energy integrals (which, in turn, become sums) and the boundary energies, thereby converting the total energy expression $(E_{(m)} - W_{(m)})$ into the sum of a quadratic form and a linear form in the point values of the displacements ${}_m u^i_{(o)}$. This serves to make the differencing more routine and less a matter of choice, but more important, it guarantees the symmetry and positive definiteness of the matrix of the equation system, since the matrix arises from the positive definite quadratic term in the free energy. Finite-difference approximation of this term should not alter its positive definite character, and will result in a symmetric system matrix. The finite difference form of the Euler equations or, what is equivalent, the equilibrium equations is then given simply by equating to zero the derivative of the total energy form with respect to each of the degrees of freedom. Thus the matrix of the quadratic energy form (multiplied by 2) becomes the matrix of the difference equations, and the vector whose inner product with the unknown displacement gives the linear form in the total energy, becomes the forcing vector for the system. Hence the above-mentioned differentiation with respect to the point-values of the deflections need not be carried out, since the results are known beforehand, and the matrix of the quadratic energy form together with the vector of the linear form serves to describe completely the system of nonhomogeneous linear equations which constitutes the difference form of the equilibrium problem. The finite-difference equivalents of all boundary conditions are automatically incorporated into the matrix of the quadratic form, and no further attention to boundary condition specification is required. This statement holds true whether the boundary conditions correspond to free-edge, partially fixed, or fully clamped situations, although in the latter case a numerical scaling transformation will be necessary if the full fixity constraint is not incorporated as an absolute constraint.

In order to illustrate in somewhat greater detail the type of difference replacement which is introduced into the energy integral, the following examples of typical terms should serve as models. Typical of the quadratic first derivative terms which appear in the energy expression is the following:

$$\int_{a\ell}^{\ell} \left(\frac{dw}{dx}\right)^2 dx \tag{46}$$

wherein w is the generic displacement variable. If the end-point ($a\ell$) is numbered n = 0 and the point ℓ by n = N, this term would be replaced by the difference approximation.

$$\sum_{n=1}^{N} \Delta_{n,\,n-1} \left[\frac{w_n - w_{n-1}}{\Delta_{n,\,n-1}}\right]^2 \tag{47}$$

where w_n is the value of w at point n, and $\Delta_{n,\,n-1}$ is the spacing between points n and n-1. Form (47) holds regardless of nonuniformities in point-spacing, i.e., regardless of relative magnitudes of the spaces $\Delta_{n,\,n-1}$.

A term of the form

$$\int_{a\ell}^{\ell} pw \quad dx \tag{48}$$

which typified the linear forms contributing to the forcing of the system would be replaced by

$$\sum_{n=0}^{N} p_n \; w_n \left(\frac{\Delta_{n,\,n-1} + \Delta_{n,\,n+1}}{2}\right) \tag{49}$$

where $\Delta_{0,-1}$ and $\Delta_{N,N+1}$ are both to be taken equal to zero. An examination of the difference forms resulting from differentiation of these expressions with respect to a point value w_n shows that proper difference fo. mulas for the second derivative of w, even for the case of an irregular mesh, result automatically. (The second derivative of w is the proper differential form associated with the variational integral (47)).

For terms such as the following:

$$\int_{a\ell}^{\ell} \left(\frac{d^2 w}{dx^2}\right)^2 dx \tag{50}$$

which typifies the highest order contributions to free energy, the difference approximation is:

$$\sum_{n=1}^{N-1} \frac{(\Delta_{n,n-1}+\Delta_{n,n+1})}{2} \cdot \left[\left(\frac{2}{\Delta_{n,n-1}+\Delta_{n,n+1}}\right)\left(\frac{1}{\Delta_{n,n-1}\ \Delta_{n,n+1}}\right) \cdot \left(\Delta_{n,n+1}\, w_{n-1} + \Delta_{n,n-1}\, w_{n+1} - (\Delta_{n,n-1}+\Delta_{n,n+1})\, w_n\right)\right]^2 \tag{51}$$

Once again, an examination of the difference form resulting from differentiation with respect to some internal w_n shows that the result is precisely the centered difference form (for a general irregular mesh) corresponding to the fourth derivative, which is the proper Euler expression corresponding to the integral (50). Furthermore, it is not difficult to establish the fact that differentiation with respect to end point values of

w_n in (47), and both end-point and next interior point values in (48) leads to backward difference formulae, for the right end of the range (and forward difference formulae for the left end of the range) corresponding to the natural boundary conditions associated with the variational expressions.

Thus the replacement of the integral expression for $(F_{(m)} - W_{(m)})$ by difference forms such as the preceding examples (with similar expressions for mixed types) and addition of difference equivalents of the boundary spring terms serves to place the entire problem in proper difference form and, at the same time, insure the symmetry and positive definiteness of the formulation. Solution for the response deformations then consists in solving the systems (one system for each harmonic, m, considered) of equations for the point values of the displacements ${}_m u^i_{(o)}$. The systems will, of course, involve a large number of simultaneous equations, but the special character of the matrix which can be achieved by proper ordering of the unknowns permits efficient solution by any one of several well-established numerical techniques.

The solution of the system of equations will be expressed in terms of the displacement components at the middle surface at the discrete number of points chosen for the difference approximation. These middle-surface values, together with the relations for the slopes $u^a_{(1)}$, in terms of these middle-surface displacements and gradients thereof, permit calculation of the displacement through the thickness of the shell at the specified mesh points.

Likewise, availability of the displacements permits calculation of the strains and stresses, with required gradients replaced by the appropriate difference approximations. Strains and stresses may be obtained by means of higher order difference formulae in order to minimize loss in accuracy due to the difference approximation of gradients.

11. CONCLUSIONS

The objective of the development reported in the foregoing sections is the construction of a digital computer program capable of generating stress and deflection solutions to the thermally and mechanically loaded axi-symmetrical radome. The technique developed stems from a general formulation of the appropriate energy expressions in terms of deflection distributions and proceeds to a difference formulation of the numerical problem by way of a direct variational method. The energy formulation is sufficiently powerful to permit inclusion of effects due to an elastic central boom with no essential additional complexity. Varying degrees of edge restraint are also capable of inclusion without difficulty. Both iterative and exact inversion techniques have been developed for solving the resulting large scale algebraic problem in a matter of a few minutes on a high-speed digital computer, and the problem is organized into a positive-definite, symmetric form which insures convergence of iterative methods.

The programming of the analysis has been carried out for the cone and ogive. The cone program has been written for the closed nose condition as well as the truncated cone with general boundary condition capable of including a central boom. The ogive is treated for the closed nose condition. Details of these programs are given in a subsequent section.

An Appendix B is included with the present report to indicate an approach based on physical considerations, to the apex boundary conditions on non-truncated shells of revolution. As noted in the appendix, the physical apex boundary conditions should be augmented with a development of mathematically proper apex conditions.

In connection with the problem of boundary conditions, however, several important points should be kept in mind. First, some of the physical apex boundary conditions, or combinations thereof, developed in Appendix B prove to be essential for boundedness of stresses, rotations, and deflections off the shell middle surface, as well as of the free-energy integral itself. Thus, these conditions must, under all circumstances, be enforced at the apex. Second, the use of direct energy methods such as is done in the present analysis, is a powerful tool in the handling of boundary conditions. Apart from direct constraints, such as fixed edges, the inclusion of the free energy of potential energies due to all sources guarantees the satisfaction of all natural boundary conditions. Thus, the incorporation of all physical apex conditions, as derived in Appendix B, which relate to the direct physical connection of the shell with itself at the apex, should give automatically all the apex boundary conditions, those not forced explicitly being implied by the variational procedure and hence appearing naturally.

APPENDIX A - LIST OF SYMBOLS

a	fraction of meridian at which truncation occurs
a_{ij}, a^{ij}	metric tensor
C_m	coefficient $=1$ for $m=0$, $=1/2$ for $m>0$
h	shell thickness
k	spring constants
ℓ	meridian length, extended to apex
p	pressure
$u^1\ u^2\ u^3$	physical deformation components
w	generic symbol for $u^1\ u^2\ u^3$
$y^1\ y^2\ y^3$	coordinates
$z^1\ z^2\ z^3$	physical rotation components
F	free energy
J	Jacobian or volume element
R_1, R_2	principal radii of curvature
T	temperature
W	virtual work
α	coefficient of linear expansion
$\bar{\alpha}$	mean rotation at shell nose
β	local meridian-curve slope
ϵ	Young's modulus
ν	Poisson's ratio
δ	first variation
Θ	longitude angle $= y^1$
λ	cone semi-angle
τ^{ij}	stress tensor
η_{ij}	strain tensor
σ^{ij}	physical components of stress
$\Delta_{n,\,n+1}$	finite difference point spacing between points n and n+1

APPENDIX B - PHYSICAL BOUNDARY CONDITIONS AT THE APEX OF A NONTRUNCATED SHELL OF REVOLUTION

Following is a discussion of the physical boundary conditions appropriate to the apex of a nontruncated shell of revolution. In a sense, the use of the term "boundary" is incorrect, since the closure of the shell at the apex implies that the apex is no longer a boundary of the shell but is an internal point. However, with respect to the coordinate system utilized (Figures 1 and 2), the apex constitutes the lower limit of the variable y^2 and hence a boundary of the y^1, y^2 domain. The term "physical" is used advisedly, since the conditions derived herein are devised on physical grounds. It is well-known in plate and shell theory that the physical boundary conditions are not always the mathematically appropriate boundary conditions. The question of mathematically appropriate boundary conditions at a free edge (not the apex of a closed shell) are resolved automatically by the use of a variational treatment; i.e., the natural boundary conditions of the variational formulation are the mathematically appropriate ones and there need be no further concern about edge physical conditions. At the apex of a closed shell, however, the natural boundary conditions cannot be expected to provide all the boundary conditions unless the apex is punctured, and this puncturing process admits solutions which should not be present for the closed shell.

The following development of physical conditions appropriate to the apex of a closed shell is, therefore, only part of the story. The degree to which these conditions coincide with the mathematically appropriate ones will require further investigation.

The types of shell shapes of practical interest fall into two categories; those having a physical singularity at the apex, such as cones and ogives, and those having no such physical singularity, such as ellipsoids and hemispheres. Within the coordinate scheme used herein, however, it must be understood that a singularity is present no matter what the shape of the shell. This is evidenced by the singular behavior of the metric element a^{11} due to the presence in this element of the factor $1/\cos^2\beta$, for the blunt-nosed shell and due to the fact that $R_1 \longrightarrow 0$ for the pointed nose shape. Now this fact leads to the preliminary conclusion that certain terms in the free-energy expression contain nonintegrable singularities. This, of course, is an impossibility since the free energy must be bounded. It will turn out that the physical boundary conditions derived herein are precisely the conditions necessary to keep F bounded. It should be emphasized that analysis of the apex region is essentially a three-dimensional problem in which the shell assumptions are invalid. Nevertheless, the apex conditions derived herein are conditions which should be approached in some sense by the shell solution as the apex is approached. It is in this context that the present appendix is to be interpreted.

The physical boundary conditions at the apex may be stated as follows: As the apex is approached, $y^2 \longrightarrow 0$, and the entire range $(0, 2\pi)$ of y^1 approaches a single common point; i.e., as $y^2 \longrightarrow 0$, all values of y^1

between 0 and 2π are physically coalescing to a common point. It follows directly from this fact that, as $y^2 \longrightarrow 0$, both the physical displacement vector $\bar{u}$ and the physical rotation vector, which will be defined as $\bar{z}$ (the rotation tensor will be denoted by ζ^i, and its physical components, by z^i), become independent of y^1 or equivalently, of θ. This, however, is precisely equivalent to the statement, following Sokolnikoff[3], that $\bar{u}$ and $\bar{z}$ become parallel vector fields with respect to latitude circles as $y^2 \longrightarrow 0$. This may be stated mathematically by prescribing the condition that the intrinsic or absolute derivatives of $\bar{z}$ and $\bar{u}$ with respect to θ must vanish as $y^2 \longrightarrow 0$. The statement then becomes:

$$\text{as} \quad y^2 \longrightarrow 0 \qquad \begin{cases} \xi^i_{,j} \dfrac{dy^j}{d\theta} \longrightarrow 0 \\[2ex] \zeta^i_{,j} \dfrac{dy^j}{d\theta} \longrightarrow 0 \end{cases} \tag{B-1}$$

but

$$\frac{dy^j}{d\theta} = 0 \qquad j = 2, 3$$
$$= 1 \qquad j = 1 \tag{B-2}$$

Thus (B-1) becomes:

$$\text{as} \quad y^2 \longrightarrow 0 \qquad \begin{cases} \xi^i_{,1} \longrightarrow 0 \\[2ex] \zeta^i_{,1} \longrightarrow 0 \end{cases} \tag{B-3}$$

Expanding the first of these (the second follows by analogy)

$$\text{as} \quad y^2 \longrightarrow 0, \quad \frac{\partial \xi^i}{\partial y^1} + \left\{ \begin{matrix} i \\ 1 \quad j \end{matrix} \right\} \xi^j \longrightarrow 0$$

or

$$\frac{\partial \xi^i}{\partial y^1} + a^{ik} \left[1j, k \right] \xi^j \longrightarrow 0 \tag{B-4}$$

Expanding still further, this becomes:

$$\text{as } y^2 \longrightarrow 0 \quad \frac{\partial \xi^1}{\partial y^1} + \frac{a^{11}}{2}\left(\frac{\partial a_{11}}{\partial y^2}\,\xi^2 + \frac{\partial a_{11}}{\partial y^3}\,\xi^3\right) \longrightarrow 0$$

$$\frac{\partial \xi^2}{\partial y^1} - \frac{a^{22}}{2}\left(\frac{\partial a_{11}}{\partial y^2}\,\xi^1\right) \longrightarrow 0 \qquad \text{(B-5)}$$

$$\frac{\partial \xi^3}{\partial y^1} - \frac{1}{2}\left(\frac{\partial a_{11}}{\partial y^3}\,\xi^1\right) \longrightarrow 0$$

Replacing the tensor quantities ξ^i by the physical displacements u^i by means of (1), the above relations become;

$$\text{as } y^2 \longrightarrow 0 \quad \sqrt{a_{11}}\,\frac{\partial u^1}{\partial y^1} + \frac{a^{11}}{2}\left(\frac{\partial a_{11}}{\partial y^2}\,u^2\sqrt{a^{22}} + \frac{\partial a_{11}}{\partial y^3}\,u^3\right) \longrightarrow 0$$

$$\sqrt{a^{22}}\,\frac{\partial u^2}{\partial y^1} - \frac{a^{22}}{2}\left(\frac{\partial a_{11}}{\partial y^2}\sqrt{a_{11}}\,u^1\right) \longrightarrow 0 \qquad \text{(B-6)}$$

$$\frac{\partial u^3}{\partial y^1} - \frac{1}{2}\left(\frac{\partial a_{11}}{\partial y^3}\sqrt{a_{11}}\,u^1\right) \longrightarrow 0$$

Now, in view of the fact, embodied in equations (14), that the displacement components u^i are calculated in a manner implying locally rigid rotation through the shell thickness, it suffices to satisfy relations (B-6) on the middle surface $y^3 = 0$. Thus, equations (B-6), specialized to the middle surface, $y^3 = 0$, constitute three of the apex physical boundary conditions. The other three conditions follow from the second of equations (B-3), by direct analogy:

as $y^2 \longrightarrow 0$

$$\left[\sqrt{a^{11}}\ \frac{\partial z^1}{\partial y^1} + \frac{a^{11}}{2}\left(\frac{\partial a_{11}}{\partial y^2}\ z^2\ \sqrt{a^{22}} + \frac{\partial a_{11}}{\partial y^3}\ z^3\right)\right]_{y^3=0} \longrightarrow 0$$

$$\left[\sqrt{a^{22}}\ \frac{\partial z^2}{\partial y^1} - \frac{a^{22}}{2}\left(\frac{\partial a_{11}}{\partial y^2}\ \sqrt{a^{11}}\ z^1\right)\right]_{y^3=0} \longrightarrow 0 \qquad \text{(B-7)}$$

$$\left[\frac{\partial z^3}{\partial y^1} - \frac{1}{2}\left(\frac{\partial a_{11}}{\partial y^3}\ \sqrt{a^{11}}\ z^1\right)\right]_{y^3=0} \longrightarrow 0$$

Equations (B-7) take on a greater significance when the actual expressions for the rotation components z^i are known in terms of the u^i. These relations are obtained as follows [3]:

$$\zeta^1 = \frac{1}{J}\left(\frac{\partial \xi_3}{\partial y^2} - \frac{\partial \xi_2}{\partial y^3}\right) = \frac{1}{J}\left(\frac{\partial u^3}{\partial y^2} - \frac{\partial (u^2\ \sqrt{a_{22}}\ )}{\partial y^3}\right)$$

$$\zeta^2 = \frac{1}{J}\left(\frac{\partial \xi_1}{\partial y^3} - \frac{\partial \xi_3}{\partial y^1}\right) = \frac{1}{J}\left(\frac{\partial (u^1\ \sqrt{a_{11}}\ )}{\partial y^3} - \frac{\partial u^3}{\partial y^1}\right) \qquad \text{(B-8)}$$

$$\zeta^3 = \frac{1}{J}\left(\frac{\partial \xi_2}{\partial y^1} - \frac{\partial \xi_1}{\partial y^2}\right) = \frac{1}{J}\left(\sqrt{a_{22}}\ \frac{\partial u^2}{\partial y^1} - \frac{\partial(\sqrt{a_{11}}\ u^1)}{\partial y^2}\right)$$

And, since the relation between the physical and tensor components of $\bar{z}$ is

$$z^i = \zeta^i\ \sqrt{a_{ii}} \qquad \text{(B-9)}$$

not summed on i

it follows that:

$$z^1 = \sqrt{a^{22}} \left(\frac{\partial u^3}{\partial y^2} - \frac{\partial}{\partial y^3} (u^2 \sqrt{a_{22}}) \right)$$

$$z^2 = \sqrt{a^{11}} \left(\frac{\partial}{\partial y^3} (u^1 \sqrt{a_{11}}) - \frac{\partial u^3}{\partial y^1} \right) \tag{B-10}$$

$$z^3 = \sqrt{a^{11} a^{22}} \left(\sqrt{a_{22}} \frac{\partial u^2}{\partial y^1} - \frac{\partial (u^1 \sqrt{a_{11}})}{\partial y^2} \right)$$

Now, from equation (14)

$$\left[\frac{\partial u^3}{\partial y^\alpha} + \sqrt{a_{\alpha\alpha}} \frac{\partial u^\alpha}{\partial y^3} - \frac{1}{2} \sqrt{a^{\alpha\alpha}} u^\alpha \frac{\partial a_{\alpha\alpha}}{\partial y^3} \right]_{y^3 = 0} = 0 \tag{B-11}$$

no sum on α

or

$$\left[\frac{\partial u^3}{\partial y^\alpha} + \frac{\partial}{\partial y^3} \left(u^\alpha \sqrt{a_{\alpha\alpha}} \right) - \sqrt{a^{\alpha\alpha}} u^\alpha \frac{\partial a_{\alpha\alpha}}{\partial y^3} \right]_{y^3 = 0} = 0 \tag{B-12}$$

Hence

$$\frac{\partial}{\partial y^3} \left(u^\alpha \sqrt{a_{\alpha\alpha}} \right) \Bigg|_{y^3 = 0} = \left[\sqrt{a^{\alpha\alpha}} u^\alpha \frac{\partial a_{\alpha\alpha}}{\partial y^3} - \frac{\partial u^3}{\partial y^\alpha} \right]_{y^3 = 0} \tag{B-13}$$

Specializing the rotations of (B-10) to the middle surface, the y^3 deflection-derivatives which occur in these expressions may be replaced using (B-13) to give the final relations for the physical rotation components on the middle surface.

$$z^1\Big|_{y^3=0} = \left[2\sqrt{a^{22}}\left(\frac{\partial u^3}{\partial y^2} - u^2\,\frac{\partial(\sqrt{a_{22}})}{\partial y^3}\right)\right]_{y^3=0}$$

$$z^2\Big|_{y^3=0} = \left[2\sqrt{a^{11}}\left(u^1\,\frac{\partial(\sqrt{a_{11}})}{\partial y^3} - \frac{\partial u^3}{\partial y^1}\right)\right]_{y^3=0} \qquad \text{(B-14)}$$

$$z^3\Big|_{y^3=0} = \left[\sqrt{a^{11}}\left(\frac{\partial u^2}{\partial y^1}\right) - \sqrt{a^{11}}\,\sqrt{a^{22}}\,\frac{\partial}{\partial y^2}\,(u^1\,\sqrt{a_{11}}\,)\right]_{y^3=0}$$

Now, the first set (B-6) of boundary conditions has an alternative interpretation: If equation (14) for $\frac{\partial u^1}{\partial y^3} = u^1_{(1)}$ is examined, it is seen that this quantity appears to diverge as $y^2 \longrightarrow 0$. For rewriting (14) in the form:

$$u^1_{(1)} = \left[\sqrt{a^{11}}\left(u^1\,\frac{\partial\sqrt{a_{11}}}{\partial y^3} - \frac{\partial u^3}{\partial y^1}\right)\right]_{y^3=0} \qquad \text{(B-15)}$$

the factor $\sqrt{a^{11}}$ implies an infinity as $y^2 \longrightarrow 0$. However the third of boundary relations (B-6) is precisely the expression needed to keep $u^1_{(1)}$ bounded at the apex. Without going into the details, it may be stated that the first two boundary relations (B-6) are precisely the requirements needed for boundedness of the physical stresses at the apex and of the free-energy expression as well. The physical stresses σ^{ij} can be shown to be related to the tensor stresses τ^{ij} by the expressions[5]:

$$\sigma^{ij} = \sqrt{\frac{a_{jj}}{a^{ii}}}\ \tau^{ij} = \sqrt{a_{ii}\, a_{jj}}\ \tau^{ij} \qquad \text{(B-16)}$$

in the present case.

(no sum on i or j)

The six general apex boundary conditions (B-6) and B-7) are next examined for the individual harmonics (values of m) under the Fourier resolution of Section VII. Considering first the axisymmetric harmonic, m = 0, it is seen that

$$\left.\begin{aligned} u^1 &\equiv 0 \\ \frac{\partial (\ \ )}{\partial y^1} &\equiv 0 \end{aligned}\right\} \qquad \text{(B-17)}$$

throughout the shell.

In consequence of these relations, it follows that

$$\left.\begin{aligned} z^2 &\equiv 0 \\ z^3 &\equiv 0 \end{aligned}\right\} \qquad \text{(B-18)}$$

throughout the shell.

Now the second and third of apex conditions (B-6) vanish identically as does the first of apex conditions (B-7). Thus, for the axisymmetric (zeroth) harmonic, the apex conditions reduce to two relations:

as $y^2 \longrightarrow 0$

$$\left[\frac{a^{11}}{2}\left(\frac{\partial a_{11}}{\partial y^2}\ {}_0u^2\ \sqrt{a^{22}} + \frac{\partial a_{11}}{\partial y^3}\ {}_0u^3\right)\right]_{y^3=0} \longrightarrow 0$$

and

$$\left.\frac{\partial \sqrt{a_{11}}}{\partial y^2}\ {}_0z^1\right]_{y^3=0} \longrightarrow 0 \qquad \text{(B-19)}$$

The second relation of (B-19) implies that as $y^2 \longrightarrow 0$

$$ {}_0z^1 \Big|_{y^3=0} \longrightarrow 0 \qquad \text{(B-20)} $$

for both pointed and blunt-nosed shapes since $\dfrac{\partial \sqrt{a_{11}}}{\partial y^2}$ is nonzero at the apex in both cases. The relation (B-20), in turn, implies as $y^2 \longrightarrow 0$

$$ \left[\frac{\partial \, {}_0u^3}{\partial y^2} - {}_0u^2 \, \frac{\partial \left(\sqrt{a_{22}} \right)}{\partial y^3} \right]_{y^3=0} \longrightarrow 0 \qquad \text{(B-21)} $$

Now the two apex conditions may be expanded to give:

as $y^2 \longrightarrow 0$

$$ \frac{\partial \, {}_0u^3}{\partial y^2} + \frac{{}_0u^2}{R_2} \longrightarrow 0 \qquad \text{(B-22)} $$

$$ \frac{1}{R_1 \cos\beta} \left[{}_0u^2 \, \frac{\partial}{\partial y^2} \left(R_1 \cos\beta \right) - {}_0u^3 \cos\beta \right]_{y^3=0} \longrightarrow 0 $$

But $\left. \dfrac{\partial \left(R_1 \cos\beta \right)}{\partial y^2} \right|_{y^2 \to 0}$ is equal to the sine of the semi-angle β at the apex.

Therefore, the second of relations (B-22) may be expressed as follows:

as $y^2 \longrightarrow 0$

$$ \frac{1}{R_1 \cos\beta} \left({}_0u^2 \sin\beta - {}_0u^3 \cos\beta \right)_{y^3=0} \longrightarrow 0 \qquad \text{(B-23)} $$

which simply states that the radial displacement at the apex is zero. The first of relat'ons (B-22) states that the slope-change must vanish at the apex. In other words, the apex angle must not change under deformation, and the apex material must not open up.

Next, the implications of (B-6) and(B-7) for the first harmonic (m = 1) are considered. Relations (B-6), give the result:

as $y^2 \longrightarrow 0$

$$\left[\sqrt{a_{11}}\left({}_1u^1 + {}_1u^2 \frac{\partial\sqrt{a_{11}}}{\partial y^2} + {}_1u^3 \frac{\partial\sqrt{a_{11}}}{\partial y^3}\right)\right]_{y^3=0} \longrightarrow 0$$

$$\left[-{}_1u^2 - \frac{\partial\sqrt{a_{11}}}{\partial y^2}\,{}_1u^1\right]_{y^3=0} \longrightarrow 0 \tag{B-24}$$

$$\left[-{}_1u^3 - \frac{\partial\sqrt{a_{11}}}{\partial y^3}\,{}_1u^1\right]_{y^3=0} \longrightarrow 0$$

Now

$$\left.\frac{\partial\sqrt{a_{11}}}{\partial y^2}\right|_{y^3=0} = \sin\beta$$

and (B-?5)

$$\left.\frac{\partial\sqrt{a_{11}}}{\partial y^3}\right|_{y^3=0} = -\cos\beta$$

So that relations (B-24) may be rewritten:

as $y^2 \longrightarrow 0$

$$\frac{1}{R_1 \cos\beta}\left[{}_1u^1 + {}_1u^2 \sin\beta - {}_1u^3 \cos\beta\right]_{y^3=0} \longrightarrow 0$$

$$\left[{}_1u^2 + {}_1u^1 \sin\beta\right]_{y^3=0} \longrightarrow 0 \qquad \text{(B-26)}$$

$$\left[{}_1u^3 - {}_1u^1 \cos\beta\right]_{y^3=0} \longrightarrow 0$$

But any one of these three relations is derivable from the other two, so that only two are independent.

Following from (B-7), (B-10), and (22), similar relations must hold for the ${}_1z^i$:

as $y^2 \longrightarrow 0$

$$\frac{1}{R_1 \cos\beta}\left[- {}_1z^1 + {}_1z^2 \sin\beta - {}_1z^3 \cos\beta\right]_{y^3=0} \longrightarrow 0$$

$$\left[{}_1z^2 - {}_1z^1 \sin\beta\right]_{y^3=0} \longrightarrow 0 \qquad \text{(B-27)}$$

$$\left[{}_1z^3 + {}_1z^1 \cos\beta\right]_{y^3=0} \longrightarrow 0$$

and again only two of the three relations are independent.

An examination of expressions (B-14) for the z^i at $y^3 = 0$ indicates that ${}_1z^2$ and ${}_1z^3$ become indeterminate as $y^2 \longrightarrow 0$. For

$$
\left. {}_1z^1 \right|_{y^3=0} = \left[2\left(\frac{\partial\, {}_1u^3}{\partial y^2} + \frac{{}_1u^2}{R^2} \right) \right]_{y^3=0}
$$

$$
\left. {}_1z^2 \right|_{y^3=0} = \left[\frac{2}{R_1 \cos\beta} \left(-\,{}_1u^1 \cos\beta + {}_1u^3 \right) \right]_{y^3=0} \qquad \text{(B-28)}
$$

$$
\left. {}_1z^3 \right|_{y^3=0} = \left[\frac{1}{R_1 \cos\beta} \left(-\,{}_1u^2 - {}_1u^1 \sin\beta \right) - \frac{\partial\, {}_1u^1}{\partial y^2} \right]_{y^3=0}
$$

However, some thought on this matter indicates that the numerators and denominators of the indeterminate forms must proceed to zero at the same rate, as $y^2 \longrightarrow 0$, so that these forms are in general finite, nonzero quantities, and two of expressions (B-26) and two of expressions (B-27) serve as the apex boundary conditions for $m = 1$.

For $m > 1$ the consequences of (B-6) and (B-7) are as follows:

as $y^2 \longrightarrow 0$

$$
\left[\frac{1}{R_1 \cos\beta} \left(m\, {}_mu^1 + {}_mu^2 \sin\beta - {}_mu^3 \cos\beta \right) \right]_{y^3=0} \longrightarrow 0
$$

$$\left[- m \; {}_m u^2 - \sin\beta \; {}_m u^1 \right]_{y^3 = 0} \longrightarrow 0$$

$$\left[- m \; {}_m u^3 + \cos\beta \; {}_m u^1 \right]_{y^3 = 0} \longrightarrow 0 \qquad \text{(B-29)}$$

with analogous expressions holding for physical rotations ${}_m z^i$.

Now if the second and third relations of (B-29) are substituted into the first, and the same operation is performed on the analogous z^i-equations, the following results are obtained:

$$\left[m \; {}_m u^1 - \left(\frac{1}{m}\right) {}_m u^1 \right]_{y^3 = 0} \longrightarrow 0$$

$$\left[m \; {}_m z^1 - \left(\frac{1}{m}\right) {}_m z^1 \right]_{y^3 = 0} \longrightarrow 0 \qquad \text{(B-30)}$$

Hence, as $y^2 \longrightarrow 0$

$${}_m u^1 \Big|_{y^3 = 0} \longrightarrow 0 \qquad \text{and} \qquad {}_m z^1 \Big|_{y^3 = 0} \longrightarrow 0 \qquad \text{(B-31)}$$

But then it must follow from the second and third relations of each of the ${}_m u^i$ conditions and the ${}_m z^i$ conditions that, as $y^2 \longrightarrow 0$

$${}_m u^i \Big|_{y^3 = 0} \longrightarrow 0 \qquad i = 1, 2, 3$$

$${}_m z^i \Big|_{y^3 = 0} \longrightarrow 0 \qquad i = 1, 2, 3 \qquad \text{(B-32)}$$

The apex physical conditions for harmonics higher than the first (for $m > 1$) are thus given by the condition that all middle surface displacements and rotations approach zero as the apex is approached.

The expressions for the ${}_m z^i$ may be obtained from (B-14)

$$
\begin{aligned}
{}_m z^1 \Big|_{y^3=0} &= 2\left(\frac{\partial\, {}_m u^3}{\partial y^2} + \frac{{}_m u^2}{R_2}\right)_{y^3=0} \\
{}_m z^2 \Big|_{y^3=0} &= \frac{2}{R_1 \cos\beta}\left(-\, {}_m u^1 \cos\beta + m\, {}_m u^3\right)_{y^3=0} \\
{}_m z^3 \Big|_{y^3=0} &= \left[\frac{1}{R_1 \cos\beta}\left(-\, m\, {}_m u^2 - {}_m u^1 \sin\beta\right) - \frac{\partial\, {}_m u^1}{\partial y^2}\right]_{y^3=0}
\end{aligned}
\qquad \text{(B-33)}
$$

Once again, the physical rotations ${}_m z^2$ and ${}_m z^3$ are indeterminate at the apex.

The questions which must be answered by considerations of mathematically proper boundary conditions are twofold. The first relates to the indeterminacy in the rotations. The second relates to the number of apex boundary conditions appropriate to each harmonic. It would appear that there should be three apex boundary conditions on the zeroth harmonic and four for all higher harmonics. The physical conditions lead formally to two apex conditions on the zeroth harmonic, four on the first harmonic, and six on higher harmonics. The six conditions, however, may overlap due to indeterminacy in the rotation components.

The determination of mathematically appropriate boundary conditions at a singular point of a differential equation, such as the apex in the present problem, is discussed formally by Friedman[7]. The mathematically proper conditions are shown by Friedman to be the specification of the conjunct (or bilinear concommitant) of the desired solution with the initials of a linearly independent set of solutions of the homogeneous differential equations. Actual implementation of such a program forms a considerable effort in itself and will not be attempted herein. The ultimate results of such an investigation should, however, agree generally with the physical apex conditions derived herein and should provide the additional information needed to explain the counting and indeterminacy questions which the physical derivation leaves unanswered.

APPENDIX C

DYNAMIC PROBLEMS

In dynamic problems such as vibrations or transient loading (pressure or thermal) it is necessary to formulate a kinetic energy integral for use in conjunction with the free-energy expression (32) or with the simpler strain energy, V. This kinetic energy expression is easily cast in the tensor form appropriate to curvilinear coordinates and takes the following form (dots denoting time-derivatives):

$$\begin{aligned} T &= \frac{1}{2}\iiint \rho \; J \; dy^1 dy^2 dy^3 \; a_{ij} \; \dot{\xi}^i \dot{\xi}^j \\ &= \frac{1}{2}\iiint \rho \; J \; dy^1 dy^2 dy^3 \; \dot{u}^i \dot{u}^i \end{aligned} \qquad \text{(C-1)}$$

in the case of orthogonal coordinates only.

wherein ρ is shell material density, $\dot{\xi}^i$ denotes tensor velocity, and $\dot{u}^i$ is physical velocity. Under vibration at a single frequency ω, the kinetic energy becomes

$$\begin{aligned} T &= \frac{1}{2}\,\omega^2 \iiint \rho \; J \; dy^1 dy^2 dy^3 \; a_{ij} \; \xi^i \xi^j \\ &= \frac{1}{2}\,\omega^2 \iiint \rho \; J \; dy^1 dy^2 dy^3 \; u^i u^i \end{aligned} \qquad \text{(C-2)}$$

The availability of the foregoing energy and work forms permits formulation of the various classes of problems to be encountered in radome applications. The underlying principle in the formulation is Hamilton's or, what is equivalent in the direct variational formulation, the Lagrange equations of motion. In the presence of thermal effects, the potential energy is to be replaced by the free energy. Following is a classification of the variational principles to be used for various cases of interest.

a. Free vibrations, without thermal effects:

$$\delta \int_{t_0}^{t_1} (T-V)\, dt = 0 \qquad \text{(C-3)}$$

where δ indicates first variation and integration with respect to time is performed between two arbitrary limits, t_0 and t_1.

b. Static pressure loading, without thermal effects:

$$\delta\ (V-W) = 0 \qquad \text{(C-4)}$$

where $$\delta W = \iint dy^1 dy^2\ J(y^1, y^2, 0)\ p_3\ \delta u^3 \qquad \text{(C-5)}$$

c. Thermal loading, without pressure loading:

$$\delta\ (F) = 0 \qquad \text{(C-6)}$$

d. Dynamic pressure loading without thermal effects:

$$\delta \int_{t_o}^{t_1} (T-V+W)\, dt = 0 \qquad \text{(C-7)}$$

where the variation operation on W takes the form:

$$\int_{t_o}^{t_1} dt \iint dy^1 dy^2\, J(y^1,y^2,0)\, p_3\, \delta u^3 \qquad \text{(C-8)}$$

e. Simultaneous thermal and pressure static loading:

$$\delta\, (F-W) = 0 \qquad \text{(C-9)}$$

where δW is as given in (38).

f. Dynamic thermal loading:

$$\delta \int_{t_o}^{t_1} (T-F)\, dt = 0 \qquad \text{(C-10)}$$

g. Simultaneous thermal and pressure dynamic loading:

$$\delta \int_{t_o}^{t_1} (T-F+W)\, dt = 0 \qquad \text{(C-11)}$$

It should be noted that case (g.) is actually all-inclusive, provided the vanishing of T in static cases and equivalence of F and V in isothermal cases is recognized.

This concludes the classification of the various problems which fall within the category of linear analysis. Within this limitation of linearity it is permissible to superimpose effects.

For example, the thermal loading which makes its appearance in the free-energy function, F, may be interpreted simply as a loading equivalent to some pressure distribution and with some associated boundary conditions. The response to this thermal loading may be calculated separately and then superimposed upon the response to other loadings such as pressure.

This linear analysis, with its consequent validity of superposition, breaks down in certain cases when one loading, be it thermal or otherwise, induces significant membrane stresses in a shell, and a second loading then acts to deform the shell in a locally normal direction. This set of circumstances is handled by an initial-stress type of analysis and is similar to situations arising in buckling problems and centrifugal stiffening effects. Its treatment requires the introduction of nonlinear strain-displacement relations and will not be handled herein.

REFERENCES

1. Hemp, W. S., Thermo-Elasticity, Aero Research Council Structure Subcommittee Report, Strut. 1683, April, 1954.
2. Miller, P. R., Free Vibrations of a Stiffened Cylindrical Shell, Aero Research Council, Report L. A. 22, May 1957.
3. Sokolnikoff, I. S., Tensor Analysis, John Wiley and Sons, Inc., 1951.
4. Novozhilov, V. V., Foundations of the Nonlinear Theory of Elasticity, Graylock Press, 1953.
5. Green, A. E. and Zerna, W., Theoretical Elasticity, Oxford University Press, 1954.
6. Crandall, S. H., Engineering Analysis, McGraw-Hill Book Company, Inc., New York, N. Y. pp. 41-46, 1956.
7. Friedman, B., Techniques of Applied Mathematics, Ordinary Differential Equations and Green's Functions, New York University, Institute of Mathematical Sciences, Division of Electromagnetic Research, Research Report No. EM-60, November 1953.

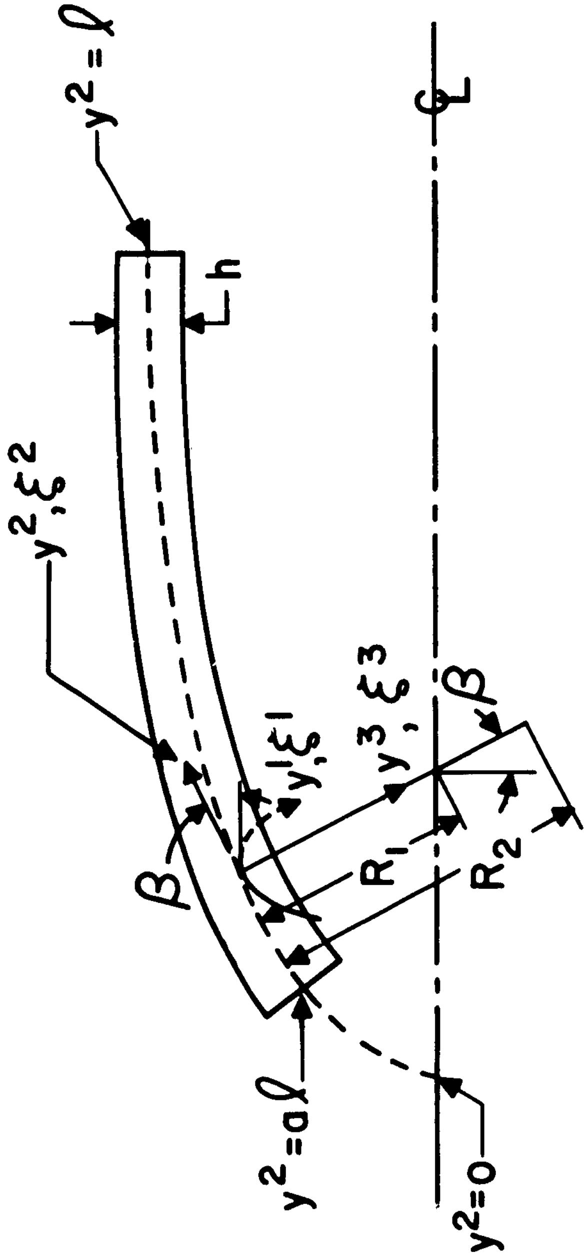

FIG. 1 GENERAL SHELL GEOMETRY

Metric Tensor for General Shell of Revolution

$$ds^2 = dy^{3^2} + \left(1 - \frac{y^3}{R_2}\right)^2 dy^{2^2} + (R_1 - y^3)^2 \cos^2\beta \; dy^{1^2}$$

$$a_{ij} = a^{ij} = 0 : \; i \neq j$$

$$a_{11} = (R_1 - y^3)^2 \cos^2\beta = 1/a^{11}$$

$$a_{22} = \left(1 - \frac{y^3}{R_2}\right)^2 = 1/a^{22}$$

$$a_{33} = 1 = 1/a^{33}$$

$$J = \sqrt{|a_{ij}|} = \sqrt{a_{11} \; a_{22} \; a_{33}} = (R_1 - y^3)\left(1 - \frac{y^3}{R_2}\right) \cos\beta$$

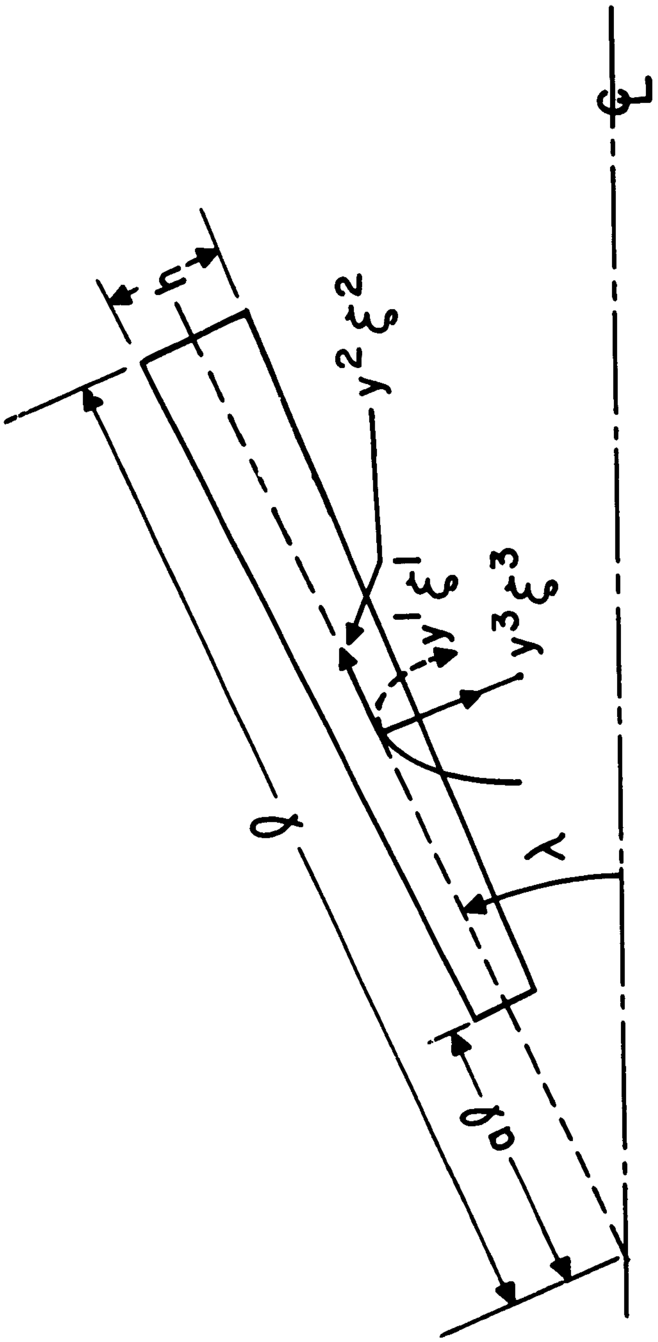

FIG. 2 CONE GEOMETRY

Metric Tensor for Cone

$R_1 = y^2 \tan\lambda$

$R_2 = \infty$

$\beta \equiv \lambda$

$a_{ij} = a^{ij} = 0 : i \neq j$

$a_{22} \equiv 1 = 1/a^{22}$

$a_{11} = (y^2 \sin\lambda - y^3 \cos\lambda)^2 = 1/a^{11}$

$a_{33} = 1 = 1/a^{33}$

$J = (y^2 \sin\lambda - y^3 \cos\lambda)$

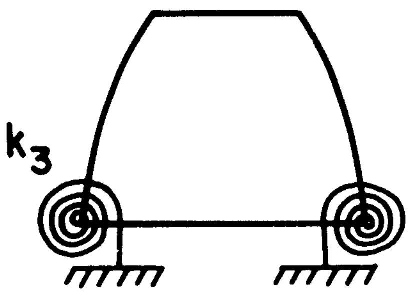

(a) BASE EDGE MOMENT DISTRIBUTED SPRING. (BASE CLAMPING ATTACHMENT)

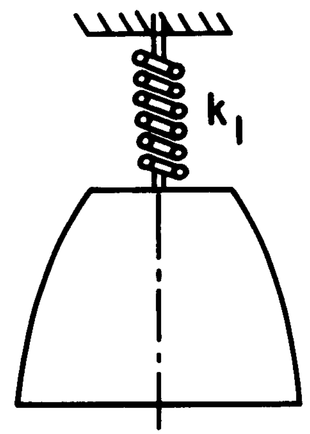

(b) NOSE AXIAL STRETCHING SPRING. (CENTRAL BOOM IN TENSION)

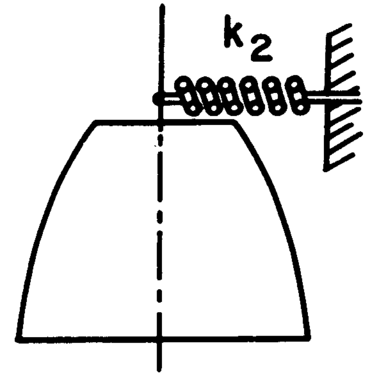

(c) NOSE TRANSVERSE DISPLACEMENT SPRING (CENTRAL BOOM IN FLEXURE)

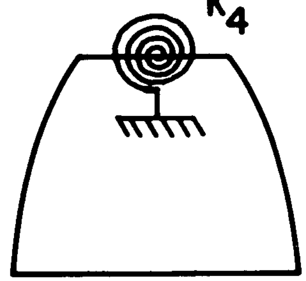

(d) NOSE BENDING SPRING CENTRAL BOOM IN FLEXURE

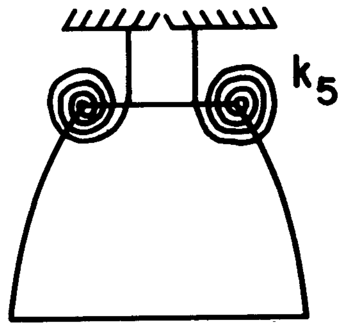

(e) NOSE EDGE MOMENT DISTRIBUTED SPRING. (NOSE CLAMPING ATTACHMENT)

FIG. 3 SPRING RESTRAINT SCHEME FOR BOUNDARY CONDITIONS

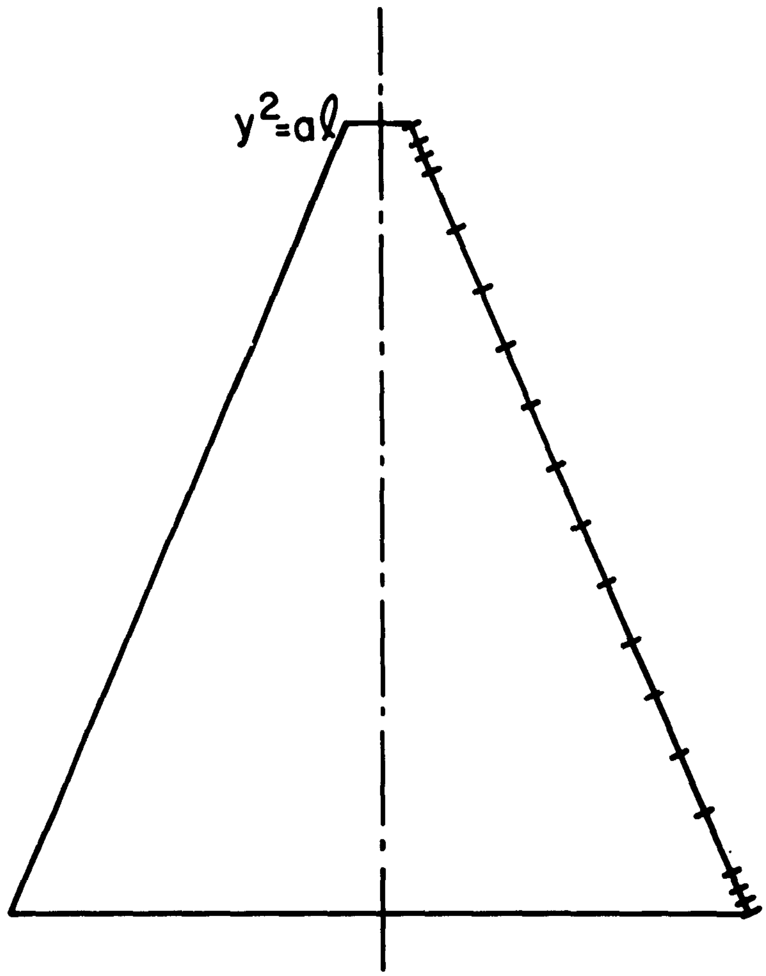

FIG. 4 TYPICAL MESH SCHEME FOR TRUNCATED CONICAL SHELL

CHAPTER IV - PART B

TRUNCATION ERROR GROWTH IN EXPLICIT DIFFERENCE SCHEMES FOR NUMERICAL SOLUTIONS OF HEAT CONDUCTION EQUATIONS

By Frank Lane

TABLE OF CONTENTS

B. TRUNCATION ERROR GROWTH IN EXPLICIT DIFFERENCE SCHEMES FOR NUMERICAL SOLUTION OF HEAT CONDUCTION EQUATIONS

SUMMARY

An analysis is made of the possible growth or accumulation of truncation error for explicit difference numerical calculations of the time-dependent temperature distribution in one-dimensional or slab configurations with constant-property materials. Two limiting cases are studied: (a) the case of homogeneous or zero initial temperature values and step heat input at one wall with the other wall insulated, and (b) the case of arbitrary nonzero initial temperature distribution and both walls insulated. For both cases, it is proven that as long as stability criteria are satisfied, the truncation error does not accumulate. Moreover, since any slab problem involving constant-property materials with variable heat flow through one wall and insulated opposite wall may be formulated as a superposition (of Duhamel type) of these two problems (a) and (b), it is apparent that truncation error will not accumulate in general providing stability criteria are satisfied.

The interpretation of these results for variable-property materials must be done somewhat intuitively, but it is expected that they hold in this case as well. One may resort, for this purpose. to the argument which replaces the variable material properties by local or instantaneous values and invokes the constant-property result in the small. Proceeding in this way, the result should hold in the large.

TRUNCATION ERROR GROWTH IN EXPLICIT DIFFERENCE SCHEMES FOR NUMERICAL SOLUTION OF HEAT CONDUCTION EQUATIONS

1. INTRODUCTION

In the finite-difference computation of temperature distributions through radome shells under the influence of aerodynamic heating, the thinness of the shell together with the values of specific heat and conductivity exhibited by ceramic materials dictate that the computations be performed using a rather course space-mesh (dividing the shell thickness into about six equal intervals) relative to shell thickness and a time step chosen relative to the space mesh such that the stability criterion for error growth is satisfied. The time step required for stability may be so small, due to shell thinness, that for a typical trajectory of, say, ten minutes duration, as many as 20,000 time-steps may be necessary to span the trajectory. (Incidentally, this requires only three minutes of IBM 704 time.) The occurrence of nonlinear phenomena, such as radiative boundary conditions depending on the fourth power of surface temperature, dictate that the explicit scheme be utilized rather than an implicit scheme which would permit larger time steps. The advantage gained by the use of fewer time steps would be more than offset by the nonlinear algebraic problems associated with the implicit scheme in the presence of nonlinear boundary data or nonlinearities imposed by temperature-dependent specific heat and/or conductivity.

The truncation error associated with the relatively coarse space mesh, and the large number of time steps required to compute a trajectory raise the question of the meaning of such a computation. Does the accumulation of truncation error render meaningless such a calculation? Following is an indication that in at least two limiting cases, the truncation error does not build up so as to render results useless after a large number of time cycles. The two cases treated are (a) the case of constant heat input at one wall with the other wall insulated and (b) the case of zero heat input or output at both walls such as would be expected after radiative equilibrium is reached during a flight trajectory calculation. In this discussion only truncation error is considered since the simple difference scheme and the small number of space intervals utilized raise the truncation-error question. Roundoff error, on the other hand, is small for the classical explicit difference scheme and, for a time step which satisfies the stability criterion, cannot be magnified by repeated time cycles. There still remains the question of accumulated roundoff error, but this is not treated herein.

2. PROBLEM A

Consider first the case of a slab at zero initial temperature subjected to a step heat input QH (t-o) at the outer wall and insulated at the inner wall. The exact solution to this problem is the following:

$$T = \frac{Q}{c}\left(\frac{t}{h} + \frac{c\,x^2}{2\,kh} - \frac{ch}{6k} \quad \frac{-2\,ch}{\pi^2\,k}\sum_{1}^{\infty}\frac{(-1)^n}{n^2}\, e^{-n^2\pi^2 kt/ch^2} \cos\frac{n\pi x}{h}\right) \qquad (1)$$

where h = wall thickness

c = (specific heat) multiplied by density

k = conductivity

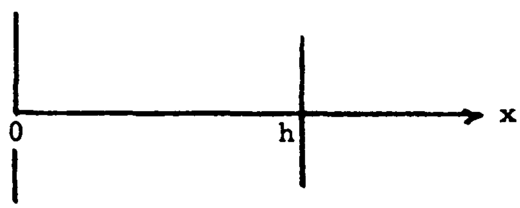

(The assumption of zero initial temperature is not restrictive since case (b) will treat the problem of nonzero initial temperature with zero heat flow at the two walls.)

Now as an indication of the degree to which the exponential terms in the above series (1) decay with time, it should be noted that, in the difference method, the ratio β given by

$$\beta = \frac{k\ \Delta t}{c\ \Delta x^2} \qquad (2)$$

where Δt is time step

Δx is space interval

is of the order of 0.5. Thus the largest exponential term

$$e^{-\pi^2 kt/ch^2}$$

may be estimated after N time steps if the space mesh is $\frac{1}{M}$ times the wall thickness.

$$e^{-\pi^2 kt/ch^2}\Bigg|_{\substack{\text{N time}\\ \text{steps}}} = e^{-\frac{\pi^2 Nk\Delta t}{M^2\, c(\Delta h)^2}} \approx e^{-\frac{\pi^2 N}{M^2} \times \frac{1}{2}} \tag{3}$$

With a space mesh of $\frac{1}{6}$ times the thickness of the wall, M = 6 and after 100 time steps

$$e^{-\pi^2 kt/ch^2}\Bigg|_{\substack{\text{100 time steps}\\ M = 6}} \approx e^{-\frac{\pi^2 \times 100}{72}} = e^{-13.7} \tag{4}$$

This term, as is seen from (1), is to be compared with terms of the order of unity. Thus after a time equivalent to 100 time steps in the difference method, the exponential terms in the series are insignificant. Hence for times greater than this, the difference in temperature distributions between two times t_1 and t_2 (both greater than 100 Δ t) is given very closely by

$$T\Big|_{t_2} - T\Big|_{t_1} \doteq \frac{Q}{ch}(t_2 - t_1) \tag{5}$$

This is obviously independent of x.

Next the difference approximation is scrutinized. The difference scheme appropriate to the present problem is, in terms of the sketch,

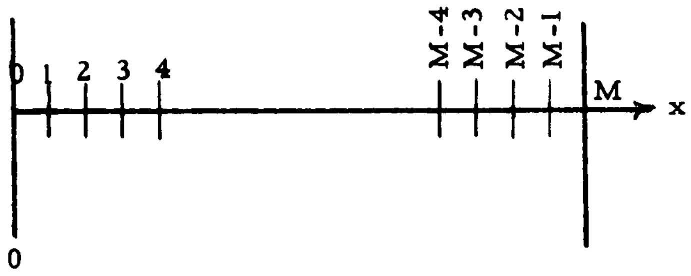

$$T_o^{n+1} = T_o^n + 2\beta\ (T_1^n - T_o^n)$$

$$T_m^{n+1} = T_m^n + \beta\ (T_{m-1}^n + T_{m+1}^n - 2\,T_m^n) \qquad m = 1,\ 2\ .....\ M\text{-}1 \tag{6}$$

$$T_M^{n+1} = T_M^n + 2\beta\,(T_{M-1}^n - T_M^n) + 2\ \frac{\beta\Delta x}{k}\ Q$$

$$T_m^o = 0 \qquad m = 0,\ 1,\ 2\ ......\ M$$

where $\beta = \dfrac{k\ \Delta t}{c(\Delta x)^2}$ as noted earlier .

This may be expressed in matrix form

$$T^{n+1} = A\ T^n + b \tag{7}$$

$$
\text{where} \quad A = \begin{bmatrix} (1-2\beta) & 2\beta & 0 & 0 & \cdot & \cdot & 0 & 0 \\ \beta & (1-2\beta) & \beta & 0 & 0 & \cdot & \cdot & 0 \\ 0 & \beta & (1-2\beta) & \beta & 0 & \cdot & \cdot & 0 \\ \cdots & \cdots & \cdots & \cdots & \cdots & \cdots & \cdots & \cdots \\ 0 & 0 & \cdot & \cdot & 0 & \beta & (1-2\beta) & \beta \\ 0 & 0 & \cdot & \cdot & 0 & 0 & 2\beta & (1-2\beta) \end{bmatrix} \tag{8}
$$

$$
\text{and where} \quad b = \begin{bmatrix} 0 \\ 0 \\ 0 \\ \cdot \\ \cdot \\ \cdot \\ 0 \\ \left(\dfrac{2\beta\,\Delta x Q}{k}\right) \end{bmatrix}, \quad T^n = \begin{bmatrix} T_o^n \\ T_1^n \\ T_2^n \\ \cdot \\ \cdot \\ \cdot \\ \cdot \\ T_M^n \end{bmatrix} \tag{9}
$$

$$
\text{and where} \quad T^o = \begin{bmatrix} 0 \\ 0 \\ 0 \\ \cdot \\ \cdot \\ \cdot \\ 0 \\ 0 \end{bmatrix} \tag{10}
$$

Now $$T^1 = AT^0 + b = b$$
$$T^2 = AT^1 + b = Ab + b = (A + I)\, b \qquad (11)$$
$$T^3 = AT^2 + b = (A^2 + A + I)\, b$$
etc.

Thus, the vector T^n at the n^{th} time step is simply:

$$T^n = (A^{n-1} + A^{n-2} + \ldots\ldots\ldots + A + I)\, b \qquad (12)$$

Likewise the difference vector between the temperatures at two times $n_1 \Delta t$ and $n_2 \Delta t$ is given by

$$T^{n_2} - T^{n_1} = \underbrace{(A^{n_2-1} + A^{n_2-2} + \ldots\ldots + A^{n_1+1} + A^{n_1}}_{(n_2 - n_1)\ \text{terms}}\,)\, b \qquad (13)$$

Next, it is necessary to examine the eigenvalues λ and eigen vectors of the matrix A. This is best performed by considering the difference equation

$$\beta\, q^{m-1} + (1-2\beta-\lambda)\, q^m + \beta\, q^{m+1} = 0 \qquad (14)$$
$$m = 1, 2 \ldots\ldots M-1$$

with initial and final conditions

$$(1-2\beta-\lambda)\, q^0 + 2\beta q^1 = 0$$
$$2\beta\, q^{M-1} + (1-2\beta-\lambda)\, q^M = 0 \qquad (15)$$

Now let

$$\frac{1-2\beta-\lambda}{\beta} = -2\cos\theta \qquad (16)$$

where it might turn out that θ is imaginary, but this possibility is accepted for the present. Then the general solution of (14) is

$$q^m = a \cos m\theta + b \sin m\theta \tag{17}$$

Introducing (17) into initial and final conditions (15), there results:

$$\begin{aligned} &- a \cos\theta + a \cos\theta + b \sin\theta = 0 \\ &- \cos\theta \ (a \cos M\theta + b \sin M\theta) + a \cos (M-1)\theta + b \sin (M-1)\theta = 0 \end{aligned} \tag{18}$$

From the first of (18) there results:

$$b = 0 \tag{19}$$

since $\theta = 0$ leads to a result which will be included in those which follow from the vanishing of b. The second of equations (18) then becomes

$$- \cos\theta \, (\cos M\theta) + \cos (M-1)\theta = 0 \tag{20}$$

Or, expanding out the $\cos (M-1)\theta$ term,

$$- \cos\theta \cos M\theta + \cos M\theta \cos\theta + \sin M\theta \sin\theta = 0 \tag{21}$$

so that $$\sin M\theta \sin\theta = 0 \tag{22}$$

The proper eigen vectors are then given by

$$\theta_n = \frac{n\pi}{M} \qquad n = 0 \quad 1, 2, 3 \ldots . \; M \tag{23}$$

where it can be shown that $n > M$ leads to eigenvalue results which overlap those of (23); e.g.

$$\cos\left(\frac{M+\nu}{M}\right)\pi = \cos (M-\nu) \frac{\pi}{M} \tag{24}$$

$$\nu = 1, 2, 3 \ldots . .$$

Now the eigenvalues λ_n corresponding to the θ_n of (23) are

$$\lambda_n = -2\beta + 1 + 2\beta\cos\theta_n = 1 + 2\beta(\cos\theta_n - 1)$$
$$= 1 + 2\beta\left(\cos\frac{n\pi}{M} - 1\right) \tag{25}$$

Thus, finally, the M + 1 eigenvalues, together with their corresponding eigenvectors are

$$\begin{array}{llllll}
n = & 0 & 1 & 2 & 3 & \ldots\ldots M \\
\lambda_n = & 1 & \left[1+2\beta\left(\cos\frac{\pi}{M}-1\right)\right] & \left[1+2\beta\left(\cos\frac{2\pi}{M}-1\right)\right] & \left[1+2\beta\left(\cos\frac{3\pi}{M}-1\right)\right] & \ldots\ldots\ldots \\
q^n = & \begin{bmatrix} 1 \\ 1 \\ 1 \\ 1 \\ 1 \\ 1 \\ 1 \\ \vdots \\ 1 \end{bmatrix} & \begin{bmatrix} 1 \\ \cos\frac{\pi}{M} \\ \cos\frac{2\pi}{M} \\ \cos\frac{3\pi}{M} \\ \cdot \\ \cdot \\ \cdot \\ \cdot \\ \cdot \\ \cos M\frac{\pi}{M} \end{bmatrix} & \begin{bmatrix} 1 \\ \cos\frac{2\pi}{M} \\ \cos\frac{4\pi}{M} \\ \cos\frac{6\pi}{M} \\ \cdot \\ \cdot \\ \cdot \\ \cdot \\ \cdot \\ \cos 2\pi \end{bmatrix} & \begin{bmatrix} 1 \\ \cos\frac{3\pi}{M} \\ \cos\frac{6\pi}{M} \\ \cos\frac{9\pi}{M} \\ \cdot \\ \cdot \\ \cdot \\ \cdot \\ \cdot \\ \cos 3\pi \end{bmatrix} & \ldots\ldots\ldots\ldots
\end{array} \tag{26}$$

Now any vector, such as b of equation (7), is expressible in the form

$$b = \sum_{m=0}^{M} b_{(m)}\, q^m \tag{27}$$

where the $b_{(m)}$ are given by

$$b_{(m)} = \frac{(b,\ p^m)}{(p^m,\ q^m)} \qquad \text{no sum on } m \tag{28}$$

where the p^m are the <u>row</u> eigenvectors corresponding to λ_m (the q^m are the column eigenvectors) and the symbol $(b,\ p^m)$ indicates inner product.

Now the eigenrow p^o corresponding to $\lambda_o = 1$ is seen to be given by

$$p^o = \begin{bmatrix} \frac{1}{2} & 1 & 1 & 1 & 1 & 1 & \ldots\ldots\ldots & 1 & 1 & \frac{1}{2} \end{bmatrix} \tag{29}$$

and the normalization factor $(p^o,\ q^o)$ is

$$(p^o,\ q^o) = \frac{1}{2} + 1 + 1 \ \ldots\ldots + 1 + 1 + \frac{1}{2} = M \tag{30}$$

Thus, the vector b is expressible as

$$\begin{aligned} b &= \begin{bmatrix} 1 \\ 1 \\ 1 \\ 1 \\ 1 \\ \cdot \\ \cdot \\ 1 \\ 1 \end{bmatrix} \frac{1}{M}\left(\frac{2\beta\Delta x Q}{k}\right)\left(\frac{1}{2}\ 1\ 1\ 1 \ldots 1\ 1\ \frac{1}{2}\right)\begin{bmatrix} 0 \\ 0 \\ 0 \\ 0 \\ \cdot \\ \cdot \\ 0 \\ 0 \\ 1 \end{bmatrix} + \sum_{m=1}^{M} \frac{(b, p^m)\ q^m}{(p^m,\ q^m)} \\ &= \frac{\beta\Delta x Q}{M\,k}\begin{bmatrix} 1 \\ 1 \\ 1 \\ \cdot \\ \cdot \\ 1 \end{bmatrix} + \sum_{m=1}^{M} b_m\, q^m \end{aligned} \tag{31}$$

Now it is easily seen from (26) that for m > 0 the eigenvalues λ_m are less than unity

$$\lambda_m < 1 \qquad \text{for} \qquad m > 0 \tag{32}$$

Moreover, for $\beta \leq \frac{1}{2}$ which is necessitated by the stability criterion,

$$\lambda_m \geq -1 \tag{33}$$

When $\beta < \frac{1}{2}$ the inequality holds in (33).

Thus,

$$\begin{aligned} &\text{for} \quad \beta < \tfrac{1}{2} \\ &\left|\lambda_m\right| < 1 \qquad \text{for} \quad m > 0 \end{aligned} \tag{34}$$

For example, when $M = 6$, $\beta = 0.4$

$$\begin{aligned} \lambda_0 &= 1 \\ \lambda_1 &= 1 + 0.8\,(\cos\tfrac{\pi}{6} - 1) = .894 \\ \lambda_2 &= 1 + 0.8\,(\cos\tfrac{2\pi}{6} - 1) = 0.60 \\ \lambda_3 &= 1 + 0.8\,(\cos\tfrac{3\pi}{6} - 1) = 0.200 \\ \lambda_4 &= 1 + 0.8\,(\cos\tfrac{4\pi}{6} - 1) = -.200 \\ \lambda_5 &= 1 + 0.8\,(\cos\tfrac{5\pi}{6} - 1) = -.492 \\ \lambda_6 &= 1 + 0.8\,(\cos\pi - 1) = -0.6 \end{aligned} \tag{35}$$

Now, consider the quantity

$$A^n \; b$$

which is typical of terms occurring in (13).

$$A^n b = \sum_{m=0}^{M} A^n b_m q^m$$

$$= \sum_{m=0}^{M} (\lambda_m)^n b_m q^m \tag{36}$$

Now $(.894)^{100}$ is less than $\frac{1}{30,000}$ so that for the case cited in (35), when $n > 100$, recalling that $\lambda_o = 1$,

$$A^n b \doteq (\lambda_o)^n b_o q^o = b_o q^o$$

$$= \frac{\beta \Delta x Q}{M k} \begin{bmatrix} 1 \\ 1 \\ 1 \\ 1 \\ \cdot \\ \cdot \\ \cdot \\ 1 \\ 1 \end{bmatrix} \tag{37}$$

by reference to (31).

Finally, referring back to (13), for n_1, n_2 both greater than 100,

$$T^{n_2} - T^{n_1} = \left(A^{n_2-1} + A^{n_2-2} + \ldots\ldots + A^{n_1+1} + A^{n_1}\right) b$$

$$\doteq (n_2 - n_1) \frac{\beta \Delta x Q}{M k} \begin{bmatrix} 1 \\ 1 \\ 1 \\ 1 \\ \cdot \\ \cdot \\ \cdot \\ \cdot \\ 1 \\ 1 \end{bmatrix} \tag{38}$$

but

$$\frac{\beta\,\Delta x\,Q}{M\,k} = \frac{k\Delta t}{c(\Delta x)^2}\,\frac{\Delta x\,Q}{M\,k}$$

$$= \frac{Q\,\Delta t}{h\,c} \tag{39}$$

so that, for n_2 , n_1 both > 100

$$T^{n_2} - T^{n_1} \doteq (t_2 - t_1)\,\frac{Q}{h\,c}\begin{bmatrix}1\\1\\1\\1\\ \cdot\\ \cdot\\ \cdot\\1\\1\end{bmatrix} \tag{40}$$

which is seen to correspond exactly to the analytical result of equation (5).

Thus it has been shown that the difference between the temperature distributions calculated by the explicit difference technique at any two time steps agrees with the analytical result after a certain time (say corresponding to 100 steps) has elapsed. This shows that there is no accumulation of truncation error despite the coarse space mesh regardless of the number of time steps computed.

3. PROBLEM B

Consider next the case where no heat flows through either wall but where there is a nonzero temperature distribution at some time t_o.

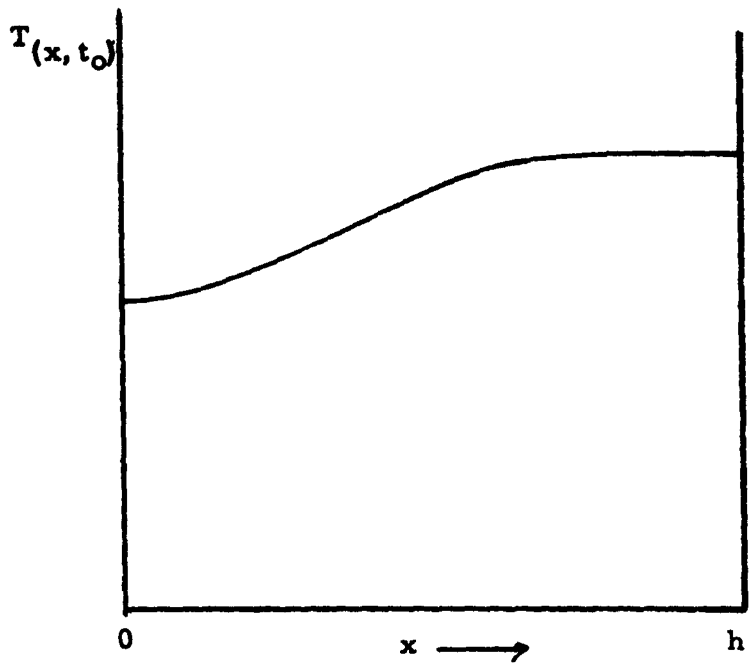

The argument used in this case to prove that truncation error does not accumulate after a large number of time steps is based simply on energy conservation. First, it is known that the solution to the difference scheme (which is simply system (6) with no Q term) approaches the flat or constant temperature condition with increasing time and that this uniform distribution is the correct one for large time. The only question remaining is therefore that of a possible constant vertical displacement between the exact and the difference solutions. Once again round-off error is not considered.

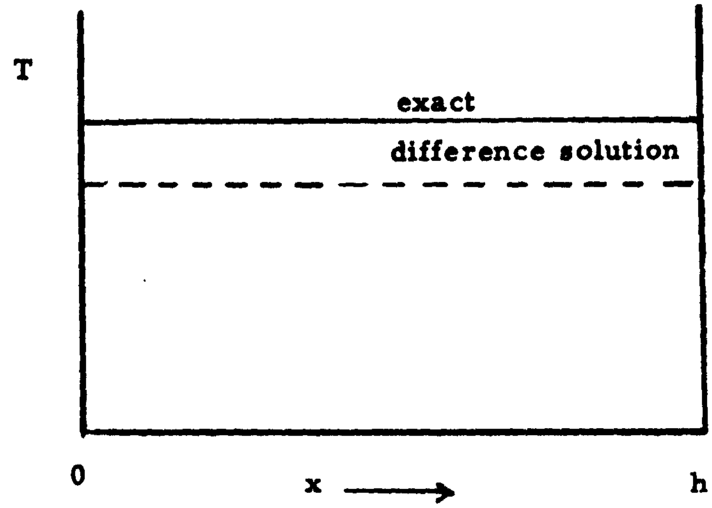

It is this shift which can be shown <u>not</u> to accumulate by virtue of accumulated truncation error.

Consider the energy content or simply the integrated temperature for the initial distribution.

$$\int_0^h T(x, t_o)\, dx \tag{41}$$

This is approximated by the trapezoidal-rule quadrature

$$\int_0^h T(x, t_o)\, dx \cong \frac{T_o^{n_o}}{2} + \frac{T_M^{n_o}}{2} + \left(T_1^{n_o} + T_2^{n_o} + \ldots\ldots + T_{M-1}^{n_o}\right) \tag{42}$$

where $n_o \Delta t = t_o$.

Define the scalar quantity I^n by

$$I^n = \frac{T_o^n}{2} + \frac{T_M^n}{2} + \left(T_1^n + T_2^n + \ldots + T_{M-1}^n\right) \tag{43}$$

Now consider the expression for I^{n+1} utilizing the homogeneous form of system (6).

$$I^{n+1} = \frac{T_o^{n+1}}{2} + \frac{T_M^{n+1}}{2} + \left(T_1^{n+1} + T_2^{n+1} + \ldots\ldots + T_{M-1}^{n+1}\right)$$

$$= \frac{1}{2}\left(T_o^n + 2\beta(T_1^n - T_o^n)\right) + \frac{1}{2}\left(T_M^n + 2\beta(T_{M-1}^n - T_M^n)\right) \tag{44}$$

$$+ \sum_{m=1}^{M-1}\left(T_m^n + \beta(T_{m-1}^n + T_{m+1}^n - 2T_m^n)\right) .$$

Expanding and collecting, this becomes

$$\begin{aligned} I^{n+1} &= \frac{1}{2}(T_o^n + 2\beta(T_1^n - T_o^n)) + \frac{1}{2}(T_M^n + 2\beta(T_{M-1}^n - T_M^n)) \\ &+ T_1^n + \beta\left(T_o^n + T_2^n - 2T_1^n\right) \\ &+ T_2^n + \beta\left(T_1^n + T_3^n - 2T_2^n\right) \\ &+ \\ &\cdot \\ &\cdot \\ &\cdot \\ &+ T_{M-2}^n + \beta\left(T_{M-3}^n + T_{M-1}^n - 2T_{M-2}^n\right) \\ &+ T_{M-1}^n + \beta\left(T_{M-2}^n + T_M^n - 2T_{M-1}^n\right) \\ &= \frac{1}{2}T_o^n + \frac{1}{2}T_M^n + \left(T_1^n + T_2^n + \ldots\ldots + T_{M-1}^n\right) \\ &= I^n \end{aligned} \tag{45}$$

Thus, neglecting round-off, the trapezoidal-rule quadrature is "conserved". That is, the value of I^n is the same as the value of I^{n_o} for all n greater than n_o. Any error (aside from round-off) in the trapezoidal-rule approximation to $\int_0^h T\,dx$ appears directly as a quadrature error at initial time t_o, and never changes. This rules out the possibility of an increasing displacement between true and difference-calculated temperatures due to accumulated truncation errors for large times.

Stated differently; the analytical or exact solution conserves the integral $\int_0^h T(x, \theta)\,dx$ for all time after Q vanishes. The difference solution conserves I^n which is the trapezoidal approximation to this integral. Neglecting round-off, if $T(x, t)$ is the exact solution with initial values $T(x, t_o)$ and if

$$I^{n_o} = \int_0^h T(x, t_o)\,dx + \epsilon_o \tag{46a}$$

where ϵ_o is quadrature error at time t_o

Then $$I^n = \int_0^h T(x, t)\,dx + \epsilon_o \qquad \text{for all } n > n_o \tag{46b}$$

since the two integrals are equal and $I^n = I^{n_o}$.

Thus the accumulated truncation error cannot cause the increasing divergence of the exact and difference solutions; i.e., I^n differs from the integral $\int_0^h T\,dx$ at time t by exactly the same amount that I^{n_o} differs from $\int_0^h T\,dx$ at time t_o.

APPENDIX

EXACT SOLUTION OF PROBLEM (A)

Now it can be shown that the general n^{th} eigenrow $\left(\text{corresponding to } \lambda_n = 1 + 2\beta\left(\cos\frac{n\pi}{M} - 1\right)\right)$ is given by

$$P_{(n)} = \left[\frac{1}{2},\ \cos\theta_n,\ \cos 2\theta_n,\ \cos 3\theta_n,\ \cos 4\theta_n, \ldots, \cos(M-1)\theta_n, \overbrace{\frac{1}{2}\cos M\theta_n}^{\frac{1}{2}(-1)^n}\right] \tag{47}$$

where it should be recalled that $\theta_n = n\pi/M$.

The expression (29) for p^o is obviously a special case of this for $(n = 0,\ \theta_n = 0,\ \lambda_n = 1)$. With some trigonometric effort it can be shown that the n^{th} norm $N_{(n)}$ is given by

$$\begin{aligned} N_{(n)} = \left(P_{(n)},\ q_{(n)}\right) &= M \qquad \text{for } n = 0,\ M \\ &= M/2 \qquad \text{for } 0 < n < M \end{aligned} \tag{48}$$

Having this data, it is now possible to write down a complete solution to problem (a).

From expressions (12) and (27)

$$\begin{aligned} T^n &= (A^{n-1} + A^{n-2} + \ldots\ldots + A^2 + A + I)\, b \\ &= (A^{n-1} + A^{n-2} + \ldots\ldots + A^2 + A + I) \sum_{m=0}^{M} b_{(m)}\, q^{(m)} \\ &= \sum_{m=0}^{M} b_{(m)} \left(A^{n-1} + \ldots\ldots + 1\right) q^{(m)} \end{aligned} \tag{49}$$

But

$$A^r q^{(m)} = \left(\lambda_{(m)}\right)^r q^{(m)} \tag{50}$$

so that

$$T^n = \sum_{m=0}^{M} b_{(m)} \left(\lambda_{(m)}^{n-1} + \lambda_{(m)}^{(n-2)} + \ldots\ldots + 1\right) q^{(m)} \tag{51}$$

Now

$$\begin{aligned} b_{(m)} &= \frac{1}{N_{(m)}} \left(P_{(m)}, b\right) \\ &= \frac{1}{N_{(m)}} \left(\frac{2\beta\Delta x Q}{k}\right) \underbrace{\left(\frac{1}{2} \cos M\theta_m\right)}_{\frac{1}{2}(-1)^m} \\ &= \frac{M}{N_{(m)}} \quad \frac{Q\Delta t}{h c} \quad (-1)^m \end{aligned} \tag{52}$$

using equation (39)

Therefore

$$\begin{aligned} b_o &= \frac{Q\Delta t}{h\ c} \\ b_M &= \frac{Q\ \Delta t}{h\ c} \ (-1)^M \\ b_m &= \frac{2\ Q\ \Delta t}{h\ c} \ (-1)^m \qquad 0 < m < M \end{aligned} \tag{53}$$

And, we have finally for T^n the result:

$$T^n = \frac{Q\Delta t}{h\,c}\left\{ n \begin{bmatrix} 1 \\ 1 \\ 1 \\ 1 \\ 1 \\ 1 \\ 1 \\ 1 \\ 1 \end{bmatrix} - 2\,(\lambda_1^{n-1} + \lambda_1^{n-2} + \lambda_1^{n-3} + \ldots + 1) \begin{bmatrix} 1 \\ \cos \pi/M \\ \cos 2\pi/M \\ \cos 3\pi/M \\ \cdot \\ \cdot \\ \cdot \\ \cos M\pi/M \end{bmatrix} \right.$$

$$+ 2\left(\lambda_2^{n-1} + \lambda_2^{n-2} + \ldots + 1\right) \begin{bmatrix} 1 \\ \cos 2\pi/M \\ \cos 4\pi/M \\ \cdot \\ \cdot \\ \cdot \\ \cdot \\ \cdot \\ \cos 2M\pi/M \end{bmatrix} - 2\left(\lambda_3^{n-1} + \lambda_3^{n-2} + \ldots + 1\right) \begin{bmatrix} 1 \\ \cos 3\pi/M \\ \cos 6\pi/M \\ \cdot \\ \cdot \\ \cdot \\ \cdot \\ \cdot \\ \cos 3\pi/M \end{bmatrix} + \ldots$$

$$+ (-1)^M \left(\lambda_M^{n-1} + \lambda_M^{n-2} + \ldots\ldots + 1\right) \begin{bmatrix} 1 \\ -1 \\ 1 \\ -1 \\ 1 \\ \cdot \\ \cdot \\ (-1)^M \end{bmatrix} \qquad (54)$$

Now

$$\lambda_m = 1 + 2\,\beta\left(\cos \frac{m\,\pi}{M} - 1\right) \qquad \text{from (26)}$$

$$\lambda_o = 1$$

and $$\left(\lambda_m^{n-1} + \lambda_m^{n-2} + \ldots\ldots + 1\right) = \frac{1 - \lambda_m^n}{1 - \lambda_m} \qquad m \neq 0 \qquad (55)$$

Thus (54) may be rewritten in the form

$$T^n = \frac{Q\Delta t}{h\,c}\left\{ n\begin{bmatrix}1\\1\\1\\1\\1\\1\\1\end{bmatrix} - \frac{2(1-\lambda_1^n)}{(1-\lambda_1)}\begin{bmatrix}1\\ \cos\pi/M\\ \cos 2\pi/M\\ \cdot\\ \cdot\\ \cdot\\ \cdot\\ \cos M\pi/M\end{bmatrix} + \frac{2(1-\lambda_2^n)}{1-\lambda_2}\begin{bmatrix}1\\ \cos 2\pi/M\\ \cos 4\pi/M\\ \cdot\\ \cdot\\ \cdot\\ \cdot\\ \cos 2M\pi/M\end{bmatrix} - \frac{2(1-\lambda_3^n)}{1-\lambda_3}\begin{bmatrix}1\\ \cos 3\pi/M\\ \cos 6\pi/M\\ \cdot\\ \cdot\\ \cdot\\ \cdot\\ \cos 3M\pi/M\end{bmatrix}\right.$$

$$+ \cdots\cdots + (-1)^M \frac{(1-\lambda_M^n)}{1-\lambda_M}\begin{bmatrix}1\\-1\\1\\-1\\ \cdot\\ \cdot\\ \cdot\\ (-1)^M\end{bmatrix} \tag{56}$$

Recalling that, for $\beta < \frac{1}{2}$; $\left|\lambda_m\right| < 1$ for $m > 0$, expression (56) may be simplified for a time sufficiently large that λ_1^n and hence λ_m^n, $m > 1$, are negligible.

$$T^n\Big|_{\substack{\text{n large enough so}\\ \text{that } \lambda_1^n \ll 1}} = \frac{Q\,\Delta t}{h\,c}\left\{ n\begin{bmatrix}1\\1\\1\\1\\1\\1\end{bmatrix} - \frac{1}{\beta(1-\cos\frac{\pi}{M})}\begin{bmatrix}1\\ \cos\pi/M\\ \cos 2\pi/M\\ \cdot\\ \cdot\\ \cdot\\ \cos\ \pi\end{bmatrix} + \frac{1}{\beta(1-\cos\frac{2\pi}{M})}\begin{bmatrix}1\\ \cos 2\pi/M\\ \cos 4\pi/M\\ \cdot\\ \cdot\\ \cdot\\ \cos 2\pi\end{bmatrix}\right.$$

$$- \frac{1}{\beta(1-\cos\frac{3\pi}{M})}\begin{bmatrix}1\\ \cos 3\pi/M\\ \cos 6\pi/M\\ \cdot\\ \cdot\\ \cdot\\ \cos 3\pi\end{bmatrix} + \cdots\cdots + \frac{(-1)^M}{2\beta(1-\cos\frac{M\pi}{M})}\begin{bmatrix}1\\-1\\1\\-1\\ \cdot\\ \cdot\\ \cdot\\ (-1)^M\end{bmatrix} \tag{57}$$

In the above expression, only the first term is time-dependent. This corresponds to (and agrees with) the first term in (1). The remaining terms must correspond to the second and third terms in (1). A numerical check indicates that this is very closely satisfied for the particular case where $M = 6$. In fact, the error can be shown to be given by the difference between exact integrals or weighted integrals of these terms and seven-point trapezoidal-rule quadrature approximations thereto.

CHAPTER IV - PART C

THERMAL STRESSES IN SPHERICAL SHELLS OF ARBITRARY THICKNESS UNDER ARBITRARY AXISYMMETRIC TEMPERATURE DISTRIBUTIONS

By Dennis Eisen and Frank Lane

TABLE OF CONTENTS

C. THERMAL STRESSES IN SPHERICAL SHELLS OF ARBITRARY THICKNESS UNDER ARBITRARY AXISYMMETRIC TEMPERATURE DISTRIBUTIONS

1. INTRODUCTION

The present report describes an analytical method for determining the elastic stresses developed in a complete spherical shell of arbitrary but uniform thickness under axisymmetrical thermal loading. A related problem has been solved by McDowell and Sternberg (Ref. 1) with the restriction that the thermal loading be entirely steady (i.e., the temperature satisfies Laplace's equation). It is the purpose of the present report to extend their analysis to the case where the impressed axisymmetric thermal loading is an arbitrary one and may have come from transient, unsteady conditions. In other words, the temperature distribution is not restricted to be harmonic in the present analysis.

The results should be useful in two respects. First, they provide estimates of thermal stresses in the nose region of blunt-nosed radomes under transient thermal loading. Second, they should serve as numerical checks on the solutions to radome thermal stress problems obtained by thin shell theory in the nose region.

2. ANALYSIS

In the absence of body forces, the general equations of thermoelasticity are given (Refs. 1, 3 and 4) as

$$\text{Equilibrium:} \quad \frac{\partial \tau_{ij}}{\partial x_j} = 0 \,, \tag{1}$$

$$\text{Stress-Strain:} \quad \tau_{ij} = 2\mu \left[e_{ij} + \left(\frac{\nu}{1-2\nu} e_{kk} + \frac{1+\nu}{1-2\nu} \alpha T \right) \delta_{ij} \right] , \tag{2}$$

$$\text{Strain-Displacement:} \quad 2 e_{ij} = \frac{\partial u_i}{\partial x_j} + \frac{\partial u_j}{\partial x_i} \,, \tag{3}$$

where μ is the first Lamé constant, ν is Poisson's ratio, α the coefficient of linear expansion, and x_i a rectangular cartesian coordinate system. In the absence of surface tractions, the boundary conditions are given as

$$\tau_{ij} \ell_j = 0 \qquad \text{on B} \,, \tag{4}$$

where ℓ_j are the scalar components of the outer unit normal to the boundary surfaces B.

The solution to (1), (2), (3) will be obtained in the following manner: The complete solution $[S]$ will be subdivided into two solutions, $[S^o]$ and $[S^*]$ such that

$$[S] = [S^o] + [S^*] \,, \tag{5}$$

where $[S^o]$ represents any particular solution to the general equations (1), (2), (3), and $[S^*]$ is the solution to the so-called "residual problem" which satisfies (1), (2), (3) with $T = 0$ and annuls the surface tractions which $[S^o]$ gives rise to on the boundary B.

It may be noted that a particular solution to (1), (2), (3) may be found immediately by setting

$$u_i = \frac{\partial \phi}{\partial x_i}, \tag{6}$$

with
$$\nabla^2 \phi = \frac{a(1+\nu)}{1-\nu} T = k_o T. \tag{7}$$

The temperature field T in this problem need not be steady-state (i.e. $\nabla^2 T \neq 0$) and therefore ϕ need not be biharmonic.

This known axisymmetric temperature distribution $T(r, \cos\theta)$ may be put in the form

$$T(r, \cos\theta) = \sum_{n=0}^{\infty} F_n(r) P_n(\cos\theta), \tag{8}$$

where r, θ are the radial distance from the origin and latitude measured from the x_3 axis, respectively. (The cyclic longitude coordinate may be denoted by γ.) The functions $F_n(r)$ are given by

$$F_n(r) = \frac{2n+1}{2} \int_{-1}^{1} T(r, \cos\theta) P_n(\cos\theta) \, d(\cos\theta). \tag{9}$$

The particular solution to the Poisson equation (7) may be obtained by first substituting functions of the type

$$\phi_n(r, \cos\theta) = f_n(r) \cdot P_n(\cos\theta) \tag{10}$$

into (6) where ∇^2 in spherical coordinates becomes, for axisymmetry,

$$\nabla^2 = \frac{\partial^2}{\partial r^2} + \frac{2}{r}\frac{\partial}{\partial r} + \frac{\cot\theta}{r^2}\frac{\partial}{\partial\theta} + \frac{1}{r^2}\frac{\partial^2}{\partial\theta^2}. \tag{11}$$

There results a differential equation on $f_n(r)$,

$$f_n''(r) + \frac{2}{r} f_n'(r) - \frac{n(n+1)}{r^2} f_n(r) = k_o F_n(r) , \tag{12}$$

for which a particular solution may be given in terms of a Green's function as

$$f_n(r) = \frac{k_o}{2n+1} \int_r^{r_1} \left[r^{-n-1} \zeta^{n+2} - r^n \zeta^{-n+1} \right] F_n(\zeta)\, d\zeta , \tag{13}$$

where r_1 is the radius of the outer shell. (The radius of the inner shell will subsequently be denoted by r_o .) And hence,

$$\sum_{n=0}^{\infty} \phi_n(r, \cos\theta) = \sum_{n=0}^{\infty} \frac{k_o}{2n+1} \int_r^{r_1} \left[r^{-n-1} \zeta^{n+2} - r^n \zeta^{-n+1} \right] F_n(\zeta)\, d\zeta \cdot P_n(\cos\theta) \tag{14}$$

is the particular solution to (6) that is sought.

For notational purposes define

$$G_n(r) = \frac{k_o}{2n+1} \int_r^{r_1} r^{-n-3} \zeta^{n+2} F_n(\zeta)\, d\zeta , \tag{15}$$

$$H_n(r) = \frac{k_o}{2n+1} \int_r^{r_1} r^{n-2} \zeta^{-n+1} F_n(\zeta)\, d\zeta , \tag{16}$$

and denote $\cos\theta$ by p and $\sin\theta$ by $\hat{p}$. Then $\left[S_n^o\right]$ may be written as

$$\phi_n^o(r, p) = r^2 \left(G_n(r) - H_n(r) \right) P_n(p) , \tag{17}$$

radial deformation: $u_n^o = \dfrac{\partial \phi_n^o}{\partial r} = -r \left[(n+1)\, G_n(r) + n\, H_n(r) \right] P_n(p)$, (18)

meridional deformation: $w_n^o = \dfrac{1}{r} \dfrac{\partial \phi_n^o}{\partial \theta} = -\hat{p}\, r \left[G_n(r) - H_n(r) \right] P_n'(p)$, (19)

$$e^{o}_{rr_n} = \frac{\partial u^{o}_n}{\partial r} = \left[(n+1)\ (n+2)\ G_n(r) - n(n-1)\ H_n(r) + k_o\ F_n(r)\right] P_n(p), \quad (20)$$

$$e^{o}_{\gamma\gamma_n} = \frac{u^{o}_n}{r} + \frac{w^{o}_n}{r}\ \frac{p}{\hat{p}} = -\left[(n+1)\ G_n(r) + n\,H_n(r)\right] P_n(p) - p\left[G_n(r) - H_n(r)\right] P_n'(p) \quad (21)$$

$$e^{o}_{\theta\theta_n} = \frac{u^{o}_n}{r} + \frac{1}{r}\ \frac{\partial w^{o}_n}{\partial\theta} = -\left[(n+1)\ G_n(r) + n\,H_n(r)\right] P_n(p) - p\left[G_n(r) - H_n(r)\right] P_n'(p)$$

$$+ (1-p^2)\left[G_n(r) - H_n(r)\right] P_n''(p), \quad (22)$$

$$e^{o}_{r\theta_n} = \frac{1}{2}\left(\frac{1}{r}\ \frac{\partial u^{o}_n}{\partial\theta} - \frac{w^{o}_n}{r} + \frac{\partial w_n}{\partial r}\right) = \hat{p}\left[(n+2)\ G_n(r) + (n-1)\ H_n(r)\right] P_n'(p), \quad (23)$$

$$T^{o}_{rr_n} = 2\mu\left[(n+1)\ (n+2)\ G_n(r) - n(n-1)\ H_n(r)\right] P_n(p)\ , \quad (24)$$

$$T^{o}_{\gamma\gamma_n} = -\,2\,\mu\left\{\left[(n+1)\ G_n(r) + n\,H_n(r) + k_oF_n(r)\right] P_n(p) + p\left[G_n(r) - H_n(r)\right] P_n'(p)\right\}, \quad (25)$$

$$T^{o}_{\theta\theta_n} = -2\,\mu\left\{\left[(n+1)\ G_n(r) + n\,H_n(r) + k_oF_n(r)\right] P_n(p) + p\left[G_n(r) - H_n(r)\right] P_n'(p)\right.$$

$$\left. - (1-p^2)\left[G_n(r) - H_n(r)\right] P_n''(p)\right\}, \quad (26)$$

$$T^{o}_{r\theta_n} = 2\ \mu\ \hat{p}\left[(n+2)\ G_n(r) + (n-1)\ H_n(r)\right] P_n'(p)\ , \quad (27)$$

where the primes denote differentiation with respect to p.

The next step is to obtain the solution to the "residual problem" (where T * 0) and whose boundary conditions are

$$T^{*}_{rr_n}(r_k, p) = -\ 2\,\mu\left[(n+1)\ (n+2)\ G_n(r_k) - n(n-1)\ H_n(r_k)\right] P_n(p)\ , \quad (28)$$

$$T^{*}_{r\theta_n}(r_k, p) = -\ 2\,\mu\ \hat{p}\left[(n+2)\ G_n(r_k) + (n-1)\ H_n(r_k)\right] P_n'(p)\ , \quad (29)$$

where $k = 0, 1$. In view of (15) and (16), on the outer surface

$$\tau^*_{rr_n}(r_1, p) = 0, \tag{30}$$

$$\tau^*_{r\theta_n}(r_1, p) = 0, \tag{31}$$

while on the inner surface,

$$\tau^*_{rr_n}(r_0, p) = -2\mu\left[(n+1)(n+2)\, G_n(r_0) - n(n-1)\, H_n(r_0)\right] P_n(p), \tag{32}$$

$$\tau^*_{r\theta_n}(r_0, p) = -2\mu\, \hat{p}\left[(n+2)\, G_n(r_0) + (n-1)\, H_n(r_0)\right] P_n'(p). \tag{33}$$

The solution of the residual problem of Elasticity Theory can be traced through Refs. 6, 5, 7, 2, and finally 1, where McDowell and Sternberg have presented an explicit solution in the form of a linear combination of four separate solution fields. That is,

$$\left[S^*_n\right] = a_n\left[A_n\right] + b_n\left[B_n\right] + c_n\left[A_{-n-1}\right] + d_n\left[B_{-n-1}\right], \tag{34}$$

where for $\left[A_n\right]$:

$$2\mu u = \frac{n r_1^2}{r}\left(\frac{r}{r_1}\right)^n P_n(p), \tag{35}$$

$$2\mu w = -\hat{p}\,\frac{r_1^2}{r}\left(\frac{r}{r_1}\right)^n P_n'(p), \tag{36}$$

$$\tau_{rr} = n(n-1)\left(\frac{r_1}{r}\right)^2\left(\frac{r}{r_1}\right)^n P_n(p), \tag{37}$$

$$\tau_{\gamma\gamma} = \left(\frac{r_1}{r}\right)^2\left[n\left(\frac{r}{r_1}\right)^n P_n(p) - p\left(\frac{r}{r_1}\right)^n P_n'(p)\right], \tag{38}$$

$$\tau_{\theta\theta} = -\left(\frac{r_1}{r}\right)^2 \left[n^2 \left(\frac{r}{r_1}\right)^n P_n(p) - p\left(\frac{r}{r_1}\right)^n \dot{P}_n'(p) \right], \tag{39}$$

$$\tau_{r\theta} = -(n-1)\left(\frac{r_1}{r}\right)^2 \hat{p}\left(\frac{r}{r_1}\right)^n P_n'(p), \tag{40}$$

and for $\left[B_n\right]$:

$$2\mu u = -(n+1)(n-2+4\nu)\, r\left(\frac{r}{r_1}\right)^n P_n(p), \tag{41}$$

$$2\mu w = (n+5-4\nu)\, r\,\hat{p}\left(\frac{r}{r_1}\right)^n P_n'(p), \tag{42}$$

$$\tau_{rr} = -(n+1)\left[(n+1)(n-2) - 2\nu\right]\left(\frac{r}{r_1}\right)^n P_n(p), \tag{43}$$

$$\tau_{\gamma\gamma} = -(n+1)\left[n-2-2(2n+1)\nu\right]\left(\frac{r}{r_1}\right)^n P_n(p) + (n+5-4\nu)\, p\left(\frac{r}{r_1}\right)^n P_n'(p), \tag{44}$$

$$\tau_{\theta\theta} = (n+1)(n^2+4n+2+2\nu)\left(\frac{r}{r_1}\right)^n P_n(p) - (n+5-4\nu)\, p\left(\frac{r}{r_1}\right)^n P_n'(p) \tag{45}$$

$$\tau_{r\theta} = (n^2+2n-1+2\nu)\,\hat{p}\left(\frac{r}{r_1}\right)^n P_n'(p). \tag{46}$$

The solutions for $\left[A_{-n-1}\right]$ and $\left[B_{-n-1}\right]$ are obtained by replacing n by -n-1 wherever it appears in equations (35) through (46). Hence for $\left[A_{-n-1}\right]$ (and noting that $P_{-n-1}(p) = P_n(p)$):

$$2\mu u = -(n+1)\frac{r_1^2}{r}\left(\frac{r_1}{r}\right)^{n+1} P_n(p), \tag{47}$$

$$2\mu w = -\hat{p}\,\frac{r_1^2}{r}\left(\frac{r_1}{r}\right)^{n+1} P_n'(p), \tag{48}$$

$$\tau_{rr} = (n+1)(n+2)\left(\frac{r_1}{r}\right)^2\left(\frac{r_1}{r}\right)^{n+1} P_n(p), \tag{49}$$

$$T_{\gamma\gamma} = -\left(\frac{r_1}{r}\right)^2 \left[(n+1)\left(\frac{r_1}{r}\right)^{n+1} P_n(p) + p\left(\frac{r_1}{r}\right)^{n+1} P_n'(p)\right] , \tag{50}$$

$$T_{\theta\theta} = -\left(\frac{r_1}{r}\right)^2 \left[(n^2 + 2n+1)\left(\frac{r_1}{r}\right)^{n+1} P_n(p) - p\left(\frac{r_1}{r}\right)^{n+1} P_n'(p)\right] , \tag{51}$$

$$T_{r\theta} = (n+2)\left(\frac{r_1}{r}\right)^2 \hat{p} \left(\frac{r_1}{r}\right)^{n+1} P_n'(p) , \tag{52}$$

and for $\left[B_{-n-1}\right]$:

$$2\mu u = -n(n+3-4\nu)\, r\left(\frac{r_1}{r}\right)^{n+1} P_n(p) , \tag{53}$$

$$2\mu w = -(n-4+4\nu)\, r\,\hat{p}\left(\frac{r_1}{r}\right)^{n+1} P_n'(p) , \tag{54}$$

$$T_{rr} = n\left[n(n+3) - 2\nu\right]\left(\frac{r_1}{r}\right)^{n+1} P_n(p) , \tag{55}$$

$$T_{\gamma\gamma} = -n\left[n+3-2(2n+1)\nu\right]\left(\frac{r_1}{r}\right)^{n+1} P_n(p) - (n-4+4\nu)\, p\left(\frac{r_1}{r}\right)^{n+1} P_n'(p), \tag{56}$$

$$T_{\theta\theta} = -n\left[n^2 - 2n - 1 + 2\nu\right]\left(\frac{r_1}{r}\right)^{n+1} P_n(p) + (n-4+4\nu)\, p\left(\frac{r_1}{r}\right)^{n+1} P_n'(p) , \tag{57}$$

$$T_{r\theta} = (n^2 - 2 + 2\nu)\,\hat{p}\left(\frac{r_1}{r}\right)^{n+1} P_n'(p) . \tag{58}$$

The coefficients a_n, b_n, c_n, d_n are determined from the boundary conditions on T_{rr}^* and $T_{r\theta}^*$. Combining (37), (43), (49), (55) and equating to (30) and then (32); and then combining (40), (46), (52), (58) and similarly equating to (31) and then (33) will yield n sets of four simultaneous equations for the determination of a_n, b_n, c_n, d_n.

These equations are

$$n(n-1)\ a_n - (n+1)\left[(n+1)\ (n-2) - 2\nu\right] b_n + (n+1)(n+2)\ c_n + n\left[n^2+3n-2\nu\right] d_n = 0\ , \tag{59}$$

$$-(n-1)\ a_n + (n^2 + 2n - 1 + 2\nu)\ b_n + (n+2)\ c_n + (n^2 - 2 + 2\nu)\ d_n = 0\ , \tag{60}$$

$$\begin{aligned} n(n-1)\ \rho^{n-2} a_n - (n+1)\left[(n+1)\ (n-2) - 2\nu\right] \rho^n b_n + (n+1)(n+2)\ \rho^{-n-3} c_n \\ + n\left[n^2 + 3n - 2\nu\right] \rho^{-n-1} d_n = -2\mu\left[(n+1)(n+2)\ G_n(r_o) - n(n-1)\ H_n(r_o)\right]\ , \end{aligned} \tag{61}$$

$$\begin{aligned} -(n-1)\ \rho^{n-2} a_n + (n^2+2n-1+2\nu)\ \rho^n b_n + (n+2)\ \rho^{-n-3} c_n + (n^2 - 2 + 2\nu)\ \rho^{-n-1} d_n \\ = -2\mu\left[(n+2)\ G_n(r_o) + (n-1)\ H_n(r_o)\right]\ , \end{aligned} \tag{62}$$

where $\rho \equiv \dfrac{r_o}{r_1} < 1$. Note that the terms in $\left[S_n^*\right]$ containing a_o, a_1, d_o will not contribute to the stresses and therefore represent rigid body motions and will be indeterminate.

APPENDIX I

SIMPLIFICATION OF $e^{o}_{\theta\theta}$ AND $\tau^{o}_{\theta\theta}$

The dependence of $e^{o}_{\theta\theta_n}$ (Eq. 22) and $\tau^{o}_{\theta\theta_n}$ (Eq. 26) upon $P''_n(p)$ may be removed in the following manner:

The differential equation satisfied by $P_n(p)$ is well known to be:

$$(1 - p^2)\, P''_n = -(n^2 + n)\, P_n + 2p\, P'_n \,. \qquad \text{(A-1)}$$

And therefore the original expressions can just as well be written as

$$e^{o}_{\theta\theta_n} = - \left[(n+1)^2\, G_n - n^2\, H_n\right] P_n(p) + p \left[G_n - H_n\right] P'_n(p)\,, \qquad \text{(A-2)}$$

$$\tau^{o}_{\theta\theta_n} = -2\mu \left\{ \left[(n+1)^2\, G_n - n^2 H_n + k_o F_n\right] P_n(p) - p\left[G_n - H_n\right] P'_n(p) \right\} \qquad \text{(A-3)}$$

APPENDIX II - TEST CASES

Case 1: $T(r, p) = T_o$ (constant throughout shell)

This case should give a trivial stress distribution.

By inspection $F_o(r) = T_o$; $F_n(r) = 0$, $n \neq 0$.

$$G_o(r) = k_o \int_r^{r_1} r^{-3} \zeta^2 T_o \, d\zeta = \frac{1}{3} k_o T_o \left[\left(\frac{r_1}{r}\right)^3 - 1 \right]$$

$$H_o(r) = k_o \int_r^{r_1} r^{-2} \zeta T_o \, d\zeta = \frac{1}{2} k_o T_o \left[\left(\frac{r_1}{r}\right)^2 - 1 \right]$$

The particular solution gives $T^o_{rr} = 2\mu \left[2 G_o(r) \right] = \frac{4}{3} \mu \, k_o T_o \left[\left(\frac{r_1}{r}\right)^3 - 1 \right]$

and $T^o_{\theta\theta} = -2\mu \left[G_o(r) + k_o F_o(r) \right] = -\frac{2\mu}{3} \left[\left(\frac{r_1}{r}\right)^3 + 2 \right] = T^o_{\gamma\gamma}$

$T^o_{r\theta} = 0$

For the residual problem the simultaneous equations reduce to

$$2(1+\nu) b_o + 2c_o = 0$$

$$2(1+\nu) b_o + 2 c_o \rho^{-3} = -2\mu \left[2 G_o(r_o) \right]$$

which yield

$$c_o = -\frac{2}{3} \mu \, k_o T_o \quad ; \quad b_o = \frac{2}{3} \frac{\mu \, k_o T_o}{(1+\nu)}$$

and $T^*_{rr} = 2(1+\nu) b_o + 2 \left(\frac{r_1}{r}\right)^3 c_o = \frac{4\mu}{3} k_o T_o \left[1 - \left(\frac{r_1}{r}\right)^3 \right]$

$$T^*_{\theta\theta} = 2(1+\nu) b_o - \left(\frac{r_1}{r}\right)^3 c_o = \frac{2\mu}{3} k_o T_o \left[2 + \left(\frac{r_1}{r}\right)^3 \right] = T^*_{\gamma\gamma}$$

$$T^*_{r\theta} = 0$$

and hence $\tau_{rr} = \tau^{o}_{rr} + \tau^{*}_{rr} = 0$

$$\tau_{\theta\theta} = \tau^{o}_{\theta\theta} + \tau^{*}_{\theta\theta} = 0$$

$$\tau_{\gamma\gamma} = \tau_{\theta\theta} = 0$$

$$\tau_{r\theta} = 0$$

which is the correct result.

<u>Case 2</u> . $T(r, p) = T_o \left(\frac{r}{r_1}\right) \cos\theta = T_o \left(\frac{r}{r_1}\right) P_1(p)$

This (linear temperature distribution) case should also give trivial stresses

By inspection $F_1(r) = T_o\left(\frac{r}{r_1}\right)$; $F_n(r) = 0 \; (n \neq 1)$

$$G_1(r) = \frac{k_o}{3} \int_r^{r_1} \frac{r^{-4}}{r_1} \zeta^4 \, T_o \, d\zeta = \frac{k_o T_o}{15} \left[\left(\frac{r_1}{r}\right)^4 - \left(\frac{r}{r_1}\right)\right]$$

$$H_1(r) = \frac{k_o}{3} \int_r^{r_1} \frac{r^{-1}}{r_1} \zeta \, T_o \, d\zeta = \frac{k_o T_o}{6} \left[\left(\frac{r_1}{r}\right) - \left(\frac{r}{r_1}\right)\right]$$

The particular solutions are

$$\tau^{o}_{rr} = 2\mu \cdot 6\, G_1(r) \cos\theta = \frac{4\mu}{5} k_o T_o \left[\left(\frac{r_1}{r}\right)^4 - \left(\frac{r}{r_1}\right)\right] \cos\theta$$

$$\tau^{o}_{r\theta} = 6\mu\, G_1(r) \sin\theta = \frac{2}{5} \mu k_o T_o \left[\left(\frac{r_1}{r}\right)^4 - \left(\frac{r}{r_1}\right)\right] \sin\theta$$

$$\tau^{o}_{\theta\theta} = -2\mu \left[3\, G_1(r) - k_o F_1(r)\right] \cos\theta = -\frac{2\mu}{5} k_o T_o \left[\left(\frac{r_1}{r}\right)^4 + 4\left(\frac{r}{r_1}\right)\right] \cos\theta$$

$$\tau^{o}_{\gamma\gamma} = \tau^{o}_{\theta\theta}$$

The simultaneous equations become

$$2(2+2\nu)\, b_1 + 6\, c_1 + (4-2\nu)\, d_1 = 0$$

$$(2+2\nu)\, b_1 + 3\, c_1 + (-1+2\nu)\, d_1 = 0$$

$$2(2+2\nu)\, \rho\, b_1 + 6\rho^{-4}\, c_1 + (4-2\nu)\, \rho^{-2}\, d_1 = -2\,\mu \cdot 6\, G_1(r_o)$$

$$(2+2\nu)\, \rho\, b_1 + 3\rho^{-4}\, c_1 + (-1+2\nu)\, \rho^{-2}\, d_1 = -2\,\mu \cdot 3\, G_1(r_o)$$

from which $d_1 = 0$; $c_1 = -\dfrac{2\mu}{15}\, k_o T_o$; $G_1 = \dfrac{\mu k_o T_o}{5(1+\nu)}$

and $$T^*_{rr} = \left[4(1+\nu)\left(\frac{r}{r_1}\right) b_1 + 6\left(\frac{r_1}{r}\right)^4 c_1\right]\cos\theta = \frac{4}{5}\,\mu k_o T_o\left[\left(\frac{r}{r_1}\right) - \left(\frac{r_1}{r}\right)^4\right]\cos\theta$$

$$T^*_{r\theta} = \left[2(1+\nu)\left(\frac{r}{r_1}\right) b_1 + 3\left(\frac{r_1}{r}\right)^4 c_1\right]\sin\theta = \frac{2}{5}\,\mu k_o T_o\left[\left(\frac{r}{r_1}\right) - \left(\frac{r_1}{r}\right)^4\right]\sin\theta$$

$$T^*_{\theta\theta} = T^*_{\gamma\gamma} = \left[8(1+\nu)\left(\frac{r}{r_1}\right) b_1 - 3\left(\frac{r_1}{r}\right)^4 c_1\right]\cos\theta = \frac{2}{5}\,\mu k_o T_o\left[4\left(\frac{r}{r_1}\right) + \left(\frac{r_1}{r}\right)^4\right]\cos\theta$$

Hence $$T_{rr} = T^o_{rr} + T^*_{rr} = 0$$

$$T_{r\theta} = T^o_{r\theta} + T^*_{r\theta} = 0$$

$$T_{\theta\theta} = T_{\gamma\gamma} = T^o_{\theta\theta} + T^*_{\theta\theta} = 0$$

which is the correct result.

<u>Case 3</u> . $T(r, \varphi) = \frac{T_o r_o}{r_1 - r_o}\left(\frac{r_1}{r} - 1\right)$ (Surfaces at different uniform temp.)

This is a purely radial temperature distribution for which the stress distributions are easily calculable (References 3 and 4).

By inspection $F_o(r) = \frac{T_o r_o}{r_1 - r_o}\left(\frac{r_1}{r} - 1\right)$; $F_n(r) = 0 \quad n \neq 0$

$$G_o(r) = k_o \int_r^{r_1} r^{-3} \frac{T_o r_o}{r_1 - r_o}\left(\frac{r_1}{\zeta} - 1\right)\zeta^2 \, d\zeta = \frac{k_o T_o r_o}{r_1 - r_o}\left[\frac{1}{6}\left(\frac{r_1}{r}\right)^3 - \frac{1}{2}\left(\frac{r_1}{r}\right) + \frac{1}{3}\right]$$

$$H_o(r) = k_o \int_r^{r_1} r^{-2} \frac{T_o r_o}{r_1 - r_o}\left(\frac{r_1}{\zeta} - 1\right)\zeta \, d\zeta = \frac{k_o T_o r_o}{r_1 - r_o}\left[\frac{1}{2}\left(\frac{r_1}{r}\right)^2 - \left(\frac{r_1}{r}\right) + \frac{1}{2}\right]$$

The particular solution gives $\tau^o_{rr} = 2\mu\left[2G_o(r)\right] = \frac{2\mu k_o T_o r_o}{r_1 - r_o}\left[\frac{1}{3}\left(\frac{r_1}{r}\right)^3 - \left(\frac{r_1}{r}\right) + \frac{2}{3}\right]$

$$\tau^o_{r\theta} = 0$$

$$\tau^o_{\gamma\gamma} = \tau^o_{\theta\theta} = -2\mu\left[G_o(r) + k_o F_o(r)\right] = \frac{-2\mu k_o T_o r_o}{r_1 - r_o}\left[\frac{1}{6}\left(\frac{r_1}{r}\right)^3 + \frac{1}{2}\left(\frac{r_1}{r}\right) - \frac{2}{3}\right]$$

For the residual problem the simultaneous equations become

$$2(1+\nu)\, b_o + 2\, c_o = 0 \qquad (1)$$

$$a_o + (-1+2\nu)\, b_o + 2\, c_o + 2(-1+\nu)\, d_o = 0 \qquad (2)$$

$$2(1+\nu)\, b_o + 2\rho^{-3}\, c_o = -2\mu\left[2\, G_o(r_o)\right] \qquad (3)$$

$$a_o \rho^{-2} + (-1+2\nu)\, b_o + 2\rho^{-3}\, c_o + 2(-1+\nu)\, \rho^{-1} d_o = -2\mu\left[2\, G_o(r_o) - H_o(r_o)\right] \qquad (4)$$

Only (1) and (3) need be considered; they yield

$$c_o = \frac{\mu k_o T_o r_o}{(1-\rho^{-3})(r_1 - r_o)}\left[\frac{1}{3}\rho^{-3} - \rho^{-1} + \frac{2}{3}\right] \; ; \quad b_o = \frac{-c_o}{1+\nu}$$

Hence $\tau^*_{rr} = 2(1+\nu)\, b_o + 2\left(\frac{r_1}{r}\right)^3 c_o = \frac{2\mu k_o T_o r_o}{(1-\rho^{-3})(r_1-r_o)}\left[\frac{1}{3}\rho^{-3} - \rho^{-1} + \frac{2}{3}\right]\left[\left(\frac{r_1}{r}\right)^3 - 1\right]$

$$\tau^*_{r\theta} = 0$$

$$\tau^*_{\theta\theta} = \tau^*_{\gamma\gamma} = 2(1+\nu)\, b_o - \left(\frac{r_1}{r}\right)^3 c_o = \frac{-\mu k_o T_o r_o}{(1-\rho^{-3})(r_1-r_o)}\left[\frac{1}{3}\rho^{-3} - \rho^{-1} + \frac{2}{3}\right]\left[2 + \left(\frac{r_1}{r}\right)^3\right]$$

And adding and simplifying:

$\tau_{r\theta} = 0$ and,

$$\tau_{rr} = \frac{\alpha E T_o}{1-\nu}\,\frac{r_o r_1}{r_1^3 - r_o^3}\left\{ r_1 + r_o - \frac{1}{r}\left(r_1^2 + r_1 r_o + r_o^2\right) + \frac{r_1^2 r_o^2}{r^3}\right\} \quad ;$$

$$\tau_{\theta\theta} = \frac{\alpha E T_o}{1-\nu}\,\frac{r_o r_1}{r_1^3 - r_o^3}\left\{ r_o + r_1 - \frac{1}{2r}\left(r_1^2 + r_1 r_o + r_o^2\right) - \frac{r_1^2 r_o^2}{2r^3}\right\}$$

This solution checks with the stress distribution calculated using the simple schemes available (Ref. 3 and 4) for purely radial temperature distributions.

REFERENCES

1. McDowell, E. T. and Sternberg, E., Axisymmetric Thermal Stresses in a Spherical Shell of Arbitrary Thickness, Journal of Applied Mechanics, Vol. 24, No. 3, p. 376, 1957.
2. Sternberg, E., Eubanks, R. A., Sadowsky, M. A., On the Axisymmetric Problem of Elasticity Theory for a Region Bounded by Two Concentric Spheres, Proc. First U. S. National Congress Applied Mechanics, A.S.M.E., New York, 1952.
3. Timoshenko, S. and Goodier, J. N., Theory of Elasticity, McGraw-Hill Co., New York, New York, Second Edition, 1951.
4. Sokolnikoff, I. S., Mathematical Theory of Elasticity, McGraw-Hill Book Co., New York, N. Y., Second Edition, 1956.
5. Sadowsky, M. A. and Sternberg, E., Stress Concentration Around a Triaxial Ellipsoidal Cavity, Journal of Applied Mechanics, Vol. 16, No. 2., p. 149, 1949.
6. Papkovich, P. F., Solution générale des équations differentielles fondamentales d' élasticité exprimee par trois fonctions harmoniques, Comptes rendus hebdomadaires des séances de l'académie des sciences, Paris, Vol. 195, p. 513, 1932.
7. Eubanks, R. A. and Sternberg, E., On the Completeness of the Boussinesq-Papkovich Stress Functions, Journal of Rational Mechanics and Analysis, Vol. 5, No. 5., p. 735, 1956.

8. Jeffereys and Jeffereys, Methods of Mathematical Physics, Cambridge University Press, Cambridge, Great Britain, Third Edition, Ch. 24, 1956.

9. Goodier, J. N. and Hodge, Jr., P. G., Elasticity and Plasticity, John Wiley and Sons, Inc., New York, New York, 1958.

10. Hoff, N. J., Editor, High Temperature Effects in Aircraft Structures, Pergamon Press, New York, New York, Ch. 10, 1958.

CHAPTER IV - PART D

DIGITAL PROGRAMS FOR THE STRUCTURAL ANALYSES OF HOMOGENEOUS CONICAL AND OGIVAL SHELLS UNDER MECHANICAL AND THERMAL LOADING

By Daniel E. Magnus
and Dennis Eisen

TABLE OF CONTENTS

SYMBOLS

a	fraction of meridian at which truncation occurs
a_{ij}, a^{ij}	metric tensor
d_m	coefficient $= 0$ for $m = 0$; $= 1$ for $m > 0$
h	shell thickness
k_i	spring constants $i = 1, 7$
ℓ	meridian length, extended to apex (L)
m	harmonic number
n	number of spaces along generator
p	pressure (lb./L^2)
w, v, u	physical deformation components (See Figure 1)
y^1, y^2, y^3	coordinates (See Figure 1)
y, z	equivalent to y^2 and y^3, respectively
A	matrix associated with quadratic form
C_m	coefficient $= 1$ for $m = 0$, $= 1/2$ for $m > 0$
F	free energy
J	Jacobian or volume element
K_1	edge moment spring constant at base; $k_1/\epsilon\,\ell^2$
K_2	edge shear spring constant at base; k_2/ϵ
K_3	transverse displacement spring constant at truncation; $k_3/\epsilon\,\ell$
K_4	bending spring constant at truncation; $k_4/\epsilon\,\ell^3$
K_5	edge moment spring constant at truncation; $k_5/\epsilon\,\ell^2$
K_6	edge shear spring constant at truncation; k_6/ϵ
K_7	axial stretching spring constant at truncation; $k_7/\epsilon\ell$

R_1, R_2	principal radii of curvature; also $R \equiv R_2$
T	temperature; T_o reference temperature
W	virtual work
α	coefficient of linear expansion
β	local meridian - curve slope
β_o	β at apex
ϵ	Young's modulus; $\epsilon_o \equiv$ reference modulus
ν	Poisson's ratio
θ	longitude angle = y^1
λ	cone semi-angle
τ^{ij}	stress tensor
η_{ij}	strain tensor
σ_k^{11}	physical stress in θ direction; $k = 1, 2, 3$ for $z = -h/2, 0, h/2$
σ_k^{22}	physical stress in y^2 direction; $k = 1, 2, 3$ for $z = -h/2, 0, h/2$
σ_k^{12}	physical shear stress; $k = 1, 2, 3$ for $z = -h/2, 0, h/2$

D. DIGITAL PROGRAMS FOR THE STRUCTURAL ANALYSES OF HOMOGENEOUS CONICAL AND OGIVAL SHELLS UNDER MECHANICAL AND THERMAL LOADING

1. INTRODUCTION

In this part, the digital programs for the structural analysis of the homogeneous conical and ogival shell under mechanical and thermal loading are described. Both programs are based upon the same analytical approach, but as will be seen, the two programs use different numerical procedures in formulating the energy integrals. In general, the numerical techniques used in the cone program will be explained in detail and then supplemented by any variations used in the ogive program.

The cone program is designed for the structural analysis of conic shells with closed or truncated nose conditions. By merely changing the problem inputs and machine setting, the analysis can be changed from one condition to another. In this regard, it should be emphasized that the closed cone is not analyzed as a specialization of the boundary condition used for the truncated cone. Rather, independent requirements are imposed for the closed cone; a factor which adds considerably to the internal complexity of the program. The ogive program is for the closed nose shell only.

Both programs are designed for the analysis of any general loading where temperature and/or pressure are involved. In order to analyze a shell with a generic loading, the load must first be expressed as a Fourier series in the θ direction. (See Figure 1 for nomenclature.) Each of the Fourier harmonics must be separately analyzed by the digital program, and since the analysis is based upon linear theory, the final deflections and stresses can be found by superimposing the results from each harmonic. Taking account of the lack of precision of most aerodynamic and thermal input data derived from unsymmetric loading conditions, it is probable that no more than two harmonics will be required to adequately describe a realistic loading.

The analysis of the shell geometries is based upon a variational principle involving the "free energy", F, of the system and the external work, W, of the mechanical loading. The concepts and analytical details of the analysis appear in Part A. It is found that the nth harmonic component of the free energy can be written in the following form, which is suitable for both the cone and ogive geometries:

$$(F-W)_m = 2\pi C_m \epsilon_0 \ell^3 \left\{ \iint \frac{J}{2}\, dy^3\, dy^2 \left[\left(\frac{\epsilon}{\epsilon_0}\right) \frac{1}{1+\nu}\, \eta_{\alpha\beta} T^{\alpha\beta\gamma\delta}\, \eta_{\gamma\delta} - \left(\frac{\epsilon}{\epsilon_0}\right) \frac{2\alpha(T-T_0)}{1-\nu}\, a^{\alpha\beta}\, \eta_{\alpha\beta} \right] - \int J\, dy^2 \left(\frac{p}{\epsilon_0}\right) w_m \right\} \tag{1}$$

where

$$T^{\alpha\beta\gamma\delta} = \left(a^{\alpha\delta}\, a^{\beta\gamma} + \frac{\nu}{1-\nu}\, a^{\alpha\beta} a^{\gamma\delta} \right).$$

As will be shown in Section 2, the numerical method of evaluating the energy of the cone is not the same as the method for the ogive. For the cone, the integration through the thickness (y^3) is carried out analytically, and the integration along the generator is done numerically. For the ogive both the integration through the thickness and along the generator are done by numerical methods; the integration through the thickness being carried out using a Gauss quadrature. In both programs the integral along the generator is expressed in finite difference form as a function of the w, v, and u displacements of the mesh points. Then, by taking the variation of the energy expression, a set of linearly simultaneous equations for w, v, and u are obtained for the n stations along the generator. The system of equations have the very important property of being symmetric positive definite, which is a direct consequence of the energy formulation. As will be shown in Section 4, a positive definite matrix is a sufficient condition for the block tri-diagonal method of solution of the equations.

By way of contrast, an alternate method of obtaining the simultaneous equations will be described, and the inherent disadvantage noted. The variation of the energy expression, equation (1), could be taken in analytical form thus resulting in the Euler equations and the associated boundary conditions. These differential equations would then have to be expressed in finite difference form. Unfortunately, the final simultaneous algebraic equations would not necessarily be symmetric, and the coefficient matrix could appear as either positive definite or indefinite depending on the method of differencing. Furthermore, the solution of the equations would be considerably more involved. This disadvantage is particularly significant since the matrix under consideration can be of the order 450.

As yet, no mention has been made of the boundary conditions to be imposed. In general, the boundary conditions are expressed in terms of springs, which vary in magnitude from zero to infinity. A zero spring implies the shell is free of a particular constraint. For finite values of the springs, the energy contribution is computed and added directly to the energy matrix. An infinite spring represents a rigid constraint, and in order to avoid numerical difficulties in the limit, special procedures are employed.

In Figure 2 , the various types of spring configurations are shown. The base conditions for the cone or ogive are described by springs K_1 and K_2. The other 5 springs shown in Figure 2 are applicable only to the truncated cone. With these springs, it is possible to impose any boundary condition at the truncation including the conditions of the unified radome with a nose boom. Regarding the closed-nose cone or ogive, independent closure conditions are imposed depending on the harmonic number. The methods of introducing the spring and closure conditions are described in Section 3.

Upon solving the system of simultaneous equations, the displacements w, v, and u are found for n points along the generator of the shell. These displacements and the first and second derivatives with respect to y^2 are the necessary variables for determining the state of stress, which is discussed in Section 5 below.

The programs have been written for the IBM 704 digital computer with a core capacity of 8K and at least 2 magnetic tapes for the cone program and 3 magnetic tapes for the ogive program. In addition, the ogive program requires 2 physical drums. The programs can be read into the computer using either binary cards or binary magnetic tape. The latter method of operation is, of course, desirable for economy reasons.

When using the maximum number of spaces (n = 72) along the generator of the cone, the total running time for the zeroth harmonic is less than 3 minutes; for the first harmonic with 216 simultaneous equations, the program requires approximately 5 minutes. Approximately 75 seconds of this time are required to solve the 216 simultaneous equations.

In the ogive program, the maximum number of points along the generator was increased to 151, thereby requiring the solution of 453 simultaneous equations for the first harmonic. As yet, a complete problem has not been run using the ogive program, because part of the stress calculation is still being modified. Hence, an accurate timing of the program is not available, but it is estimated that the total running time will be 10 minutes.

Numerous test problems have been analyzed using the cone program, and 5 of these problems are discussed in Section 6 of this report. Most of the problems are for the zeroth harmonic since these problems are more amenable to theoretical analysis, but some discussion is included for a cone with a first harmonic thermal loading. The ogive program has been used to compute the displacements w and v for the zeroth harmonic with constant pressure loading. These results are presented in graphical form and are compared with theoretical results based upon membrane theory.

2. FORMULATION OF THE ENERGY MATRIX AND LOADING VECTOR

For the cone and ogive, which are axisymmetric shells with $a^{ij} = a_{ij} = 0$ for $i \neq j$, the free energy part of equation (1) can be written in the following form:

$$F_m = 2\pi \frac{C_m \epsilon_o \ell^3}{2} \iint \frac{J}{1-\nu^2} \left(\frac{\epsilon}{\epsilon_o}\right) dy^2 dy^3 \left\{ \left[\eta_{11}, \ \eta_{12}, \ \eta_{22} \right] \begin{bmatrix} a^{11}a^{11} & 0 & \nu a^{11}a^{22} \\ 0 & 2a^{11}a^{22} & 0 \\ \nu a^{22}a^{11} & 0 & a^{22}a^{22} \end{bmatrix} \begin{Bmatrix} \eta_{11} \\ \eta_{12} \\ \eta_{22} \end{Bmatrix} - 2\alpha(1+\nu)(T-T_o) \left[a^{11}, 0, a^{22} \right] \begin{Bmatrix} \eta_{11} \\ \eta_{12} \\ \eta_{22} \end{Bmatrix} \right\} \quad (2)$$

Equation (2) is in dimensionless form with all physical dimensions scaled by the length of the generator from the apex of the shell to the base mounting.

The above energy integral can be numerically evaluated in finite difference form using two different methods. One approach is to expand analytically the η_{ij} in terms of the displacements w, v and u and perform the indicated matrix multiplications with the metrics. The integrand of the energy becomes a complicated expression involving various powers of the displacements and their derivatives. These must be integrated in the y^2 and y^3 directions. The integration through the thickness can be carried out by analytic procedures leaving only a single integral in the y^2 direction. The integrand of the final expression is expressed in finite difference form and the integration replaced by a summation. This approach for the evaluation of the free energy expression is used in the cone program where the final analytical expressions before introducing the rummation procedure are not too complicated.

For the ogive, the expression to be integrated in the y^2 direction was found to be complicated and would require extensive programming effort. By using a slightly different approach, a simpler programming procedure was found. This method consists of expressing the η_{ij} in finite difference form and introducing them directly into equation (2) thereby eliminating the analytic steps of the procedure used on the cone. The matrix multiplication is done numerically and using a Gauss quadrature, the matrix is numerically integrated through the thickness. Finally, the matrix is integrated in the y^2 direction. This procedure is specifically applied to the quadratic form in equation (2); the linear form involving the temperature terms is not complicated and can be integrated analytically through the thickness as was done with the cone.

After the numerical integration by either of the above methods, the free energy and external work term can be written as:

$$1/2\ X' AX = (W-T)X \tag{3}$$

where X is the displacement vector with components w, v, and u at the various mesh points along the generator, X'AX is the quadratic form of the energy expression and (W-T)X is the linear form of the work term W combined with the linear form of the temperature terms T appearing in the free energy expression. By taking the variation of equation (3), the following equation is obtained for the displacements:

$$AX = W - T \tag{4}$$

where the matrix A is of symmetric positive definite form. For simplicity in solving the simultaneous equations, the rows and columns of matrix A are arranged so that all non-zero elements are contained in 15 diagonal rows. With this arrangement of the matrix, the order of the components of the displacement vector is:

$$X = \begin{Bmatrix} w_1 \\ v_1 \\ u_1 \\ \cdot \\ \cdot \\ \cdot \\ w_i \\ v_i \\ u_i \\ \cdot \\ \cdot \\ \cdot \\ w_{n+1} \\ v_{n+1} \\ u_{n+1} \end{Bmatrix} \tag{5}$$

where n+1 is the total number of points along the generator. The arrangement of the X vector is the same in the cone and ogive program except for fictitious elements which are placed before w_1 and after u_{n+1} in the ogive program. These elements will be discussed in the latter part of this section.

a. <u>Energy Expression and Grid Spacing for the Cone</u>

Omitting the rather lengthy algebraic details, the free energy for the cone can be written:

$$F_m = \frac{\pi C_m \epsilon \ell^3}{1-\nu^2} \int_a^1 \int_{-h/2}^{h/2} dydz \Bigg\{ \Bigg[\frac{1}{\Delta} \Bigg(mu + v \sin\lambda - w \cos\lambda$$

$$+ z \left[\frac{m(mw - u \cos\lambda)}{y \sin\lambda} - \sin\lambda \frac{dw}{dy} \right] \Bigg)^2 + \Delta \left(\frac{dv}{dy} - z \frac{d^2w}{dy^2} \right)^2$$

$$+ 2\nu \left(\frac{dv}{dy} - z \frac{d^2w}{dy^2} \right) \left(mu + v \sin\lambda - w \cos\lambda + z \left[\frac{m(mw - u\cos\lambda)}{y \sin\lambda} - \sin\lambda \frac{dw}{dy} \right] \right)$$

$$+ \frac{d_m(1-\nu)}{2\Delta} \Bigg(\Delta \frac{du}{dy} - u \sin\lambda - mv + z \Bigg[\Delta \frac{d}{dy} \left(\frac{mw - u \cos\lambda}{y \sin\lambda} \right)$$

$$- \sin\lambda \left(\frac{mw - u\cos\lambda}{y \sin\lambda} \right) + m \frac{dw}{dy} \Bigg] \Bigg)^2$$

$$- 2(1+\nu) \left[\alpha (T - T_o) \right]_m \Bigg(\Delta \frac{dv}{dy} + mu + v \sin\lambda - w \cos\lambda + z \Bigg[\frac{m(mw - u\cos\lambda)}{y \sin\lambda}$$

$$- \sin\lambda \frac{dw}{dy} - \Delta \frac{d^2w}{dy^2} \Bigg] \Bigg) \Bigg] \Bigg\} \qquad (6)$$

where $\Delta = y \sin\lambda - z \cos\lambda = \sqrt{a_{11}}$

and $C_m = \left\{ \begin{array}{l} 1;\ m = o \\ 1/2;\ m > o \end{array} \right\}$; $d_m = \left\{ \begin{array}{l} o;\ m = o \\ 1;\ m > o \end{array} \right\}$

In many shell investigations, various approximations are introduced into equation (6) to reduce the equation to a simpler form. For example, Love's first approximation (see Reference 1) drops the z in the Δ terms.

Still other methods expand the Δ^{-1} terms as an infinite power series and from order of magnitude studies, only certain terms in the series are retained. For the digital program, however, there are no reasons for introducing approximations into equation (6). As will be seen, the Δ^{-1} terms at worst introduce logarithmic terms upon integration through the thickness, and these terms are certainly not difficult to evaluate in the digital program. Hence, equation (6) is integrated assuming a uniform wall thickness and upon rearrangement becomes:

$$F_m = \frac{\pi C_m \epsilon \ell^3}{1-\nu^2} \int_a^1 dy \Bigg\{\Bigg[h\Bigg\{\left(\frac{dv}{dy}\right)^2 y \sin\lambda + 2\nu \frac{dv}{dy}(mu + v\sin\lambda - w\cos\lambda) +$$

$$\frac{d_m(1-\nu)}{2}\left[\left(\frac{du}{dy}\right)^2 y \sin\lambda - 2\frac{du}{dy}(u\sin\lambda + m v)\right]\Bigg\} +$$

$$e\left\{(mu + v\sin\lambda - w\cos\lambda)^2 + \frac{d_m}{2}(1-\nu)(u\sin\lambda + m v)^2\right\} +$$

$$\frac{h^3}{12}\Bigg\{2\left(\frac{dv}{dy}\right)\left(\frac{d^2w}{dy^2}\right)\cos\lambda + \left(\frac{d^2w}{dy^2}\right)^2 y\sin\lambda - 2\nu\frac{d^2w}{dy^2}\left[\frac{m(mw-u\cos\lambda)}{y\sin\lambda} - \sin\lambda\frac{dw}{dy}\right]$$

$$+\frac{d_m}{2}(1-\nu)\left[\left[\frac{d}{dy}\left(\frac{mw-u\cos\lambda}{y\sin\lambda}\right)\right]^2 y\sin\lambda - 2\left(\frac{du}{dy}\right)\frac{d}{dy}\left(\frac{mw-u\cos\lambda}{y\sin\lambda}\right)\cos\lambda +\right.$$

$$2\left(-\frac{mw-u\cos\lambda}{y}+m\frac{dw}{dy}\right)\frac{d}{dy}\left(\frac{mw-u\cos\lambda}{y\sin\lambda}\right)\Bigg]\Bigg\}+$$

$$f\left\{\left[\frac{m(mw-u\cos\lambda)}{y\sin\lambda}-\sin\lambda\frac{dw}{dy}\right]^2 y\tan\lambda+2\left[\frac{m(mw-u\cos\lambda)}{y\sin\lambda}-\sin\lambda\frac{dw}{dy}\right](mu+v\sin\lambda-w\cos\lambda)+\right.$$

$$\left.\frac{d_m}{2}(1-\nu)\left[\left(-\frac{mw-u\cos\lambda}{y}+m\frac{dw}{dy}\right)^2 y\tan\lambda+2(u\sin\lambda+mv)\left(\frac{mw-u\cos\lambda}{y}-m\frac{dw}{dy}\right)\right]\right\}$$

$$-h\left\{\left[2(1+\nu)\left(\frac{dv}{dy}\,y\sin\lambda+mu+v\sin\lambda-w\cos\lambda\right)\tau^{(0)}\right]\right\}+$$

$$-h^2\left\{\left[2(1+\nu)\left(-\frac{dv}{dy}\cos\lambda+\frac{m(mw-u\cos\lambda)}{y\sin\lambda}-\sin\lambda\frac{dw}{dy}-y\sin\lambda\frac{d^2w}{dy^2}\right)\tau^{(1)}\right]\right\}$$

$$-h^3\left\{\left[2(1+\nu)\left(\cos\lambda\frac{d^2w}{dy^2}\right)\tau^{(2)}\right]\right\}\Bigg]\Bigg\} \qquad (7)$$

where the logarithmic terms are

$$e=\frac{1}{\cos\lambda}\,\ell n\,\frac{1+\frac{h}{2y}\cot\lambda}{1-\frac{h}{2y}\cot\lambda}$$

$$(8)$$

$$f=-\frac{h}{\cos\lambda}+e\,y\tan\lambda$$

and the temperature terms are in the integral form

$$\begin{bmatrix} T^{(0)} \\ T^{(1)} \\ T^{(2)} \end{bmatrix} = \frac{1}{h} \int_{-h/2}^{h/2} \alpha(T-T_o) \begin{bmatrix} 1 \\ z/h \\ z^2/h^2 \end{bmatrix} dz . \qquad (9)$$

The quantities $T^{(0)}$, $T^{(1)}$, and $T^{(2)}$, which can be the results of a heat condition analysis, are the necessary thermal inputs to the digital program and must be specified at the mesh points along the generator. Since the coefficient of linear expansion α appears under the integral sign in equation (9), the cone program can be used for constant or temperature dependent α. Regarding the elastic material properties, Young's modulus ϵ has been assumed constant and factored out of the integral in equation (7); it is not a required input to the program but is used to scale the pressure inputs as shown in equation (1). Poisson's ratio ν, which is assumed constant, appears in equation (7) and is a required input to the program. The other program inputs are: a, the distance from the apex to the location at the truncation; λ, the semi-angle; h, the thickness; and n, the number of spaces along the generator between a and the base mounting. The number of mesh spaces n can be varied from 12 to 72 in increments of 12.

As shown in Figure 3, the program does not assign a uniform mesh to the cone; rather, a uniformly fine mesh is used near the edges, and a coarse mesh is used in the middle. The two edge areas with closely spaced points will be called the boundary region while the area between the boundary region is called the membrane region. The program assigns n/3 spaces to the membrane region and the remaining 2n/3 spaces are divided equally between the two boundary regions. Further, the program assumes the distance, δ, between stations in the membrane region is 4 times as large as the spacing in the boundary region. This is sufficient information to completely establish the mesh points along the generator.

To express equation (7) in finite difference form, the formulas shown in Appendix A were used. Note that special formulas were required at the junction points between the membrane and boundary regions. For the matrix of the quadratic form, the difference formulas are applied to the terms multiplied by $h^3/12$ in equation (7) and integrated over the mesh. This results in an n x n matrix, which is added to a null matrix A_1. Then the terms multiplied by f, e, and h are evaluated in the same manner and are added directly to the matrix A_1 as the computation proceeds.

b. Energy Expression and Grid Spacing for the Ogive.

For the ogive, the quadratic portion of the free energy expression (equation 2) is numerically integrated in both the y^2 and y^3 directions. To avoid some of the differencing problems which were manifest in the cone, the η_{ij} terms in the positive definite symmetric matrix $\left\{\eta' T \eta\right\}$ are differenced by first using a two-point forward first derivative and a three-point central second derivative. The expression is then reformulated by replacing all first derivatives by a two - point backward first derivative. For the uniform mesh the resulting quadratic forms are then combined in the following manner:

$$\left\{\eta' T \eta\right\} = \frac{1}{2}\left\{\eta' T\eta\right\}_{forward} + \frac{1}{2}\left\{\eta' T\eta\right\}_{backward} \qquad \text{(b-1)}$$

where $T \equiv T^{\alpha\beta\gamma\delta}$.

The energy term is then numerically integrated in the y^3 direction by using a five-point Gauss quadrature; that is, at any given station y_i^2,

$$\int_{y^3=-\frac{h}{2}}^{y^3=\frac{h}{2}} \frac{J(y^3)}{2(1-\nu^2(y^3))} \frac{\epsilon(y^3)}{\epsilon_o}\left\{\eta' T\eta\right\} d(y^3) \Rightarrow \sum_{i=1}^{i=5} \frac{a_i\, J(q_i)}{2(1-\nu^2(q_i))} \frac{\epsilon(q_i)}{\epsilon_o}\left\{\eta' T\eta\right\}_{q_i} \qquad \text{(b-2)}$$

where the q_i are h/2 times the normalized five-point Gauss quadrature coordinates, and the a_i are h/2 times the normalized five-point Gauss quadrature weighting factors. The grid spacing through the thickness of the shell consists of the five mesh points whose positions are dictated by the Gauss quadrature (see Appendix B). Note that since the normalized Young's modulus and Poisson's ratio appear under the integral sign of equation (b-2), the program will permit the analysis of non-homogeneous but isotropic materials. Specifically, the program has been written for ν and ϵ/ϵ_o varying through the thickness (y^3) but uniform in the y^2 direction.

Integration in the y^2 direction is then achieved by summing over all stations along the generator. The mesh spacing along the y^2 can be chosen by the operator to be either a uniform mesh of n + 1 points along the entire length of the shell or a non-uniform mesh representing a membrane region for the first two-thirds of the shell, and a boundary layer region for the remaining one-third of the shell near the base. For the latter case the spacing of the boundary layer region is taken to be one-fourth that of the membrane region and the total number of spaces n must be divisible by three. Special differencing formula must be used when at the juncture point and note, in particular, that equation (b-1) will be replaced by

$$\left\{\eta' T \eta\right\}_{\text{juncture}} = a \left\{\eta' T \eta\right\}_{\text{forward}} + b \left\{\eta' T \eta\right\}_{\text{backward}} \qquad \text{(b-3)}$$

where a and b are appropriate weighting factors.

In order that the forward and backward difference schemes may be applied to all stations along the generator including the first and last point, it has been necessary to create two fictitious points, number zero and n + 2. These points are subsequently eliminated by defining their contributions as

$$w_0 = 2w_1 - w_2, \quad w_{n+2} = 2w_{n+1} - w_n$$

$$v_0 = 2v_1 - v_2, \quad v_{n+2} = 2v_{n+1} - v_n$$

$$u_0 = 2u_1 - u_2, \quad u_{n+2} = 2u_{n+1} - u_n,$$

when no other boundary or closure conditions take precedence.

As has been already discussed, the program for the radome ogive is in some respects more general than the program for the cone in that the shell material need not be restricted to a homogeneous one, and the operator may select either a completely uniform mesh or one representing the membrane and boundary layer regions of the shell.

In addition to these options, the operator may also select, by proper choice of sense switches, Love's first approximation to the ogive analysis.

This approximation eliminates all z/R_1 and z/R terms in the formulation of the problem (see Reference 1). Another option available to the operator permits the solution of a non-truncated cone problem.

3. BOUNDARY CONDITIONS

The energy formulation of the previous section results in a set of simultaneous equations, and for n + 1 grid points along the generator, there are 3(n + 1) equations for the w, v and u displacements. A special case is the zeroth harmonic where by symmetry all the u displacements are zero. The number of equations is then reduced to 2(n + 1). In the following discussion, the general case will always be assumed.

The matrix A of the simultaneous equations is singular and the rank is 3 n + 1. By physical reasoning, it can be seen that such must be the case because the cone is free in space and an arbitrary rigid-body motion can be added to the displacement vector. Hence, the displacement vector is not unique. This condition is easily changed by specifying the base as a plane of reference for the v and u displacements. Hence, the v_{n+1} and u_{n+1} rows and columns of the A matrix are eliminated. The displacement vector of equation (5), which is specifically written for the cone, then becomes:

$$X = \begin{Bmatrix} w_1 \\ v_1 \\ u_1 \\ \cdot \\ \cdot \\ \cdot \\ w_i \\ v_i \\ u_i \\ \cdot \\ \cdot \\ \cdot \\ w_{n+1} \end{Bmatrix} . \qquad (5a)$$

For both the cone and ogive, the boundary constraints are imposed using an energy technique; that is, the various boundary conditions are represented by springs loading the edges and the strain energy of the springs is added into the energy matrix for the shell. The various springs are shown in Figure 2 and the method of applying these springs will be demonstrated for the base spring k_1. Specifically, the cone geometry will be considered in this discussion unless indicated otherwise.

The numerical value of each spring constant determines the method of modifying the A-matrix. If the spring constant is zero, the digital program makes no modification to the A-matrix. For finite values of the spring, the energy contribution is computed and added to the A-matrix. For example, the energy contribution for k_1 is

$$F^{(1)} = \int_0^{2\pi} \frac{k_1}{2}\ y \sin\lambda \left(\frac{dw}{dy}\right)^2 dy^1 \Bigg]_{y^2=1} \cos^2(m\theta)$$

$$= 2\pi C_m \frac{k_1}{2}\ y \sin\lambda \left(\frac{dw}{dy}\right)^2 \Bigg]_{y^2=1} . \qquad (10)$$

Or in finite difference form equation (10) becomes:

$$F_m^{(1)} = \frac{16K_1 C_m \epsilon \ell^3 \pi}{\delta^2} (w_{n+1} - w_n)^2$$

$$= \frac{16K_1 C_m \epsilon \ell^3 \pi}{\delta^2} \left\{w_n, v_n, u_n, w_{n+1}\right\} \begin{bmatrix} 1 & 0 & 0 & -1 \\ 0 & 0 & 0 & 0 \\ 0 & 0 & 0 & 0 \\ -1 & 0 & 0 & 1 \end{bmatrix} \begin{Bmatrix} w_n \\ v_n \\ u_n \\ w_{n+1} \end{Bmatrix} \qquad (11)$$

where $K_1 = k_1/\epsilon \ell^2$ and δ is the spacing of stations in the membrane region. Hence, the matrix in equation (11) is added directly to the $w_n, v_n, \cdots, w_{n+1}$ elements of the A-matrix. If γ is defined as the 4 x 4 matrix in equation (11), the spring energy $F^{(1)}$ can be written as a partitioned matrix in terms of the displacement vector X:

$$F^{(1)} = \frac{16 K_1 \pi C_m \epsilon \ell^3}{\delta^2} \quad X' \begin{bmatrix} 0 & 0 \\ 0 & \gamma \end{bmatrix} X \quad . \tag{12}$$

Of course, before making an energy addition, any constants factored out of matrix A must likewise be factored from the matrix $F^{(i)}$. In the cone program, the factored constant is $\frac{\pi C_m \epsilon \ell^3}{1-\nu^2}$.

The above procedure applies to the other base spring constant K_2 and all the spring constants which are finite at the location of the cone truncation. In Table I of Appendix C, the γ matrices are given for each spring constant K_i. Also given in this table are the definitions of the dimensionless K_i and the assumed form of the displacement vector.

In theory, the procedure of adding the energies $F^{(i)}$ to the A-matrix still applies, when the constraint becomes infinitely rigid; that is, $K_i \rightarrow \infty$. However, numerical difficulties occur when very large values of K_i are used. In order to avoid the difficulties, special consideration is given to the infinitely rigid constraints by using connection procedures. For example, when K_1 is to be considered infinitely rigid equation (10) implies:

$$\left. \frac{dw}{dy} \right|_{y = 1.0} = 0 \quad . \tag{13}$$

Or in finite difference form equation (13) becomes

$$w_{n+1} = w_n \tag{14}$$

To impose the condition of equation (14), a connection matrix C which is a rectangular matrix of size n+1 by n is defined as follows:

$$X = C\bar{X} \tag{15}$$

where

$$C\bar{X} = \begin{bmatrix} I & 0 \\ 0 & \gamma_c \\ & \\ & \end{bmatrix} \begin{Bmatrix} w_1 \\ v_1 \\ u_1 \\ \cdot \\ \cdot \\ \cdot \\ \cdot \\ w_n \\ v_n \\ u_n \end{Bmatrix} \tag{15a}$$

and

$$\gamma_c = \begin{bmatrix} 1 & 0 & 0 \\ 0 & 1 & 0 \\ 0 & 0 & 1 \\ 1 & 0 & 0 \end{bmatrix} . \tag{15b}$$

The connection matrix C is used to eliminate from equation (3) the displacement w_{n+1} in terms of w_n in the following manner:

$$\frac{1}{2} X' AX = (W-T)X \tag{3}$$

Now by equation (15)

$$\frac{1}{2} \bar{X}' (C' AC)\bar{X} = (W-T)C\bar{X} \tag{16}$$

and after taking the variation of equation (16)

$$(C' AC)\bar{X} = WC-TC . \tag{17}$$

Equation (17) expresses a set of simultaneous equations for w, v and u with the required boundary constraint of equation (14) imposed. The set of simultaneous equations can be solved for $\overline{X}$, and the desired displacement vector X obtained from equation (15).

In Table II of Appendix C, the submatrices γ_c of the connection matrices are given for the various combinations of the infinite constraints K_i. As shown in the table, only certain spring constants are associated with a specified value of the harmonic number m. If m = 1, only K_3 and/or K_4 are pertinent to the connection conditions at the truncation, and the program ignores the springs K_j; j = 5, 7. For certain combinations of rigid constraints, the implied connection conditions are trivial such as $u_1 = u_2 = 0$ for $K_3 = K_4 = \infty$. Under such circumstances, a connection matrix is not defined and the conditions are imposed upon the matrix and forcing vector by eliminating the required rows and columns.

As yet, no mention has been made of the closed cone boundary conditions, and how they are imposed. The base springs K_1 and K_2 are handled in the usual manner. For the nose of the cone, special boundary conditions were derived in Part A. These conditions are expressed as connection matrices for the digital program and used in the manner already described. The connection matrices are different for different harmonic numbers and are summarized in Table III. As a passing parenthetical remark, notice that for m = 0, the connection matrix for the closed cone in Table III is identical with the connection matrix of Table II for $K_5 = K_6 = \infty$. This implies that the cone with a clamped boundary and a very small truncation behaves like the closed cone.

This is a coincidence, since the method of deriving the closed cone condition was independent of the spring conditions. As shown in the tables for $m > 0$, the closure condition does not correspond to any of the spring constraints.

In the cone program, all of the springs shown in Figure 2 , are applicable to the analysis. However, the cone program requires K_2 always to be infinite. For the ogive program, only springs K_1 and K_2 at the base are applicable, since the shell is assumed to be closed at the nose. In Appendix C, Tables IV and V summarize the energy matrices γ and connection matrices γ_c for the spring constants K_1 and K_2, and Table VI shows the closure matrices. Particular note should be taken of the closure matrices which must not only impose the closure conditions on the elements of the first few mesh points but also remove the fictitious elements w_o, v_o, and u_o. As mentioned in the previous section, the fictitious mesh points at the nose and base were used as a convenience in differencing the energy expression. To remove these points, the following relation is used:

$$f_o = 2f_1 - f_2 \tag{18}$$

where f can be w, v, or u. Equation (18) has been included in the closure matrices. Likewise at the base, the fictitious point n+2 is removed by

$$f_{n+2} = 2f_{n+1} - f_n \ . \tag{19}$$

Equation (19) has been included in the constraint matrices for K_1 and K_2.

4. SOLUTION OF THE LINEAR SIMULTANEOUS EQUATIONS

For the cone, the maximum number of simultaneous equations is 216, while for the ogive the number of equations increases to 453. With systems of this size, the method of solution must be selected with care, if the computational time and costs are to be within reason. Standard methods of elimination for the solution of the simultaneous equations require approximately $i^3/3$ operations where i is the number of equations and an operation is considered to be a multiplication or division. Indeed, the computational time would be prohibitive despite the high speed computers of today. For $i=450$, approximately 5 hours would be required to carry out just the required multiplications and divisions on the IBM 704. Obviously, solutions must be made using methods which take advantage of the convenient form of the equations.

In Section 2, it was indicated that by properly arranging the rows and columns of the A-matrix all non-zero elements can be located in 15 diagonal rows. Such a matrix is in a convenient form for solution by the block tri-diagonal method which permits skipping the operations on the zero elements. The operation count for the solution is then approximately $\frac{13}{3}\, ij^2$ where j is the size of square submatrices to be defined subsequently. By taking the ratio of the operation count of the block tri-diagonal method and the standard elimination method, we find:

$$r = 13 \frac{j^2}{i^2}$$

In the digital programs j=6 and for i=450, the number of operations is reduced by a factor of roughly 430. Hence, to perform the required number of multiplications and divisions, the time is reduced from 5 hours to roughly 40 seconds. Besides the tremendous saving in computing time, the block tri-diagonal method is very economical with regard to data storage, because only the non-zero elements of the matrix must be stored.

The block tri-diagonal method is defined by the A-matrix subdivided in the following manner:

$$A = \begin{bmatrix} A_1 & C_1 & & \\ B_2 & A_2 & C_2 & \\ & \ddots & \ddots & C_{k-1} \\ & & B_k & A_k \end{bmatrix} \tag{20}$$

where the A_k, B_k, and C_k are jxj submatrices which are sized to include all non-zero elements of the A-matrix. There will be i/j rows or columns of such blocks. The matrix is then factored in upper and lower triangular form:

$$A = LU$$

where

$$L = \begin{bmatrix} \alpha_1 & & & \\ B_2 & \alpha_2 & & \\ & B_3 & \alpha_3 & \\ & & \ddots & \ddots \\ & & B_k & \alpha_k \end{bmatrix} \text{ and } U = \begin{bmatrix} I & \gamma_1 & & \\ & I & \gamma_2 & \\ & & \ddots & \gamma_{k-1} \\ & & & I \end{bmatrix} . \tag{21}$$

Note that for the lower triangular matrix the first diagonal row below the main diagonal is the same as in A. The other submatrices in L and U are readily obtained.

$$\alpha_1 = A_1$$

$$\alpha_i = A_i - B_i \; \gamma_{i-1} \qquad i = 2, k \tag{22}$$

$$\gamma_i = \alpha_i^{-1} \; C_i \qquad i = 1, k-1$$

The system is then solved by defining:

$$LY = P \tag{23}$$

where P is the original loading vector associated with A. Equation (23) is solved by:

$$Y_1 = \alpha_1^{-1} P_1$$

$$Y_i = \alpha_i^{-1} (P_i - B_i Y_{i-1}) \qquad i = 2, \ldots k\,. \tag{24}$$

Recognizing that

$$UX = Y$$

the final deflection vector X is obtained from the equations:

$$X_k = Y_k$$

$$X_i = Y_i - \gamma_{i+1} \, Y_{i+1} \qquad i = k-1,\, k-2,\, \ldots 1\,. \tag{25}$$

As with all numerical methods, certain conditions or properties of the system must be satisfied if the block tri-diagonal method is to be used. The critical operation in the block tri-diagonal method is the computation of α_i^{-1}. The computation will fail if

$$\left| \alpha_i \right| = 0\,.$$

As mentioned earlier, the A-matrix is symmetric positive definite and as will be shown, this is a sufficient condition to assure that α_i is non-singular. The proof follows from the fact that all diagonal minors of a positive definite matrix are non-singular, or if

$$A^{(\ell)} = \begin{bmatrix} A_1 & C_1 & & & \\ B_2 & A_2 & C_2 & & \\ & \ddots & \ddots & \ddots & \\ & & \ddots & \ddots & C_{\ell-1} \\ & & & B_\ell & A_\ell \end{bmatrix}$$

then $\qquad A^{(\ell)} \neq 0 \quad \text{for } \ell = 1, 2, \cdots k$

But

$$\alpha_1 = A_1$$

$$\therefore \left|\alpha_1\right| \neq 0 \quad .$$

Now, proceeding by induction assuming $\alpha_j (j=1, \cdots i-1)$ exists, we compute $\left|\alpha_i\right|$:

$$A^{(i)} = LU = \begin{bmatrix} \alpha_1 & & \\ B_2 & \ddots & \\ & \ddots & \ddots \\ & & B_i \quad \alpha_i \end{bmatrix} \begin{bmatrix} I & \gamma_i & & \\ & \ddots & \ddots & \\ & & \ddots & \gamma_{i-1} \\ & & & I \end{bmatrix} .$$

Obviously $\quad \left|U\right| \neq 0 \qquad$ and

$$\frac{\left|A^{(i)}\right|}{\left|U\right|} = \left|\alpha_1\right| \left|\alpha_2\right| \quad \cdots \quad \left|\alpha_{i-1}\right| \left|\alpha_i\right| .$$

Therefore

$$|\alpha_i| = \frac{|A^{(i)}|}{|U| \sum_{1}^{i-1} |\alpha_j|} \neq 0$$

and α_i is non-singular for all i.

When solving a large system of equations, the growth of round-off error and inherent errors is a familiar difficulty and has provided the field on numerical analysis with a bottomless problem which has absorbed tremendous amounts of human effort. This error difficulty persists and has not been resolved by large computers; rather, it has been reduced to a lower order of magnitude by the use of double or triple precision operations. However, the numerical analyst must always concern himself with the fact that some matrix will be encountered that will cause unpermissible error in the result. Being aware of these facts, a method of improving the solution was devised for the digital program. The method consists of computing the first solution X_o and using this to compute a residual R_i, which in turn is used to obtain a correction to the original solution. The procedure is repeated until a specified number of significant figures is achieved in each component of the i-dimensional solution. Symbolically the method is as follows:

$$X_o = A^{-1}b$$

$$R_o = b - AX_o$$

$$\Delta X_o = A^{-1}R_o$$

$$X_1 = X_o + \Delta X_o$$

or

$$R_i = b - AX_i$$

$$\Delta X_i = A^{-1}R_i$$

$$X_{i+1} = X_i + \Delta X_i$$

5. EVALUATION OF STRESSES

The physical stresses are derived from the tensorial stresses by the relation

$$\sigma^{\alpha\beta} = \tau^{\alpha\beta}\sqrt{a_{\alpha\alpha}}\;\sqrt{a_{\beta\beta}} \tag{26}$$

where the a's are metrics and

$$\tau^{\alpha\beta} = \frac{\epsilon}{1+\nu}\, T^{\alpha\beta\gamma\delta}\,\eta_{\gamma\delta} - \frac{\epsilon\, a}{1-\nu}\, a^{\alpha\beta}\,(T-T_o)\,.$$

For the physical stresses of the cone, the following expressions are derived from equation (26)

$$\frac{\sigma^{11}}{\epsilon} = \frac{\cos m\theta}{1-\nu^2}\left\{\frac{1}{y\sin\lambda}\left[mu + v\sin\lambda - w\cos\lambda + z\left(\frac{m(mw-u\cos\lambda)}{y\sin\lambda} - \sin\lambda\frac{dw}{dy}\right)\right] + \nu\left(\frac{dv}{dy} - z\frac{d^2w}{dy^2}\right) - a(1+\nu)\,(T-T_o)\right\}$$

$$\frac{\sigma^{12}}{\epsilon} = \frac{\sin m\theta}{2(1+\nu)}\left\{\frac{du}{dy} - \frac{u}{y} - \frac{mv}{y\sin\lambda} + z\left[\frac{d}{dy}\left(\frac{mw-u\cos\lambda}{y\sin\lambda}\right) + \frac{m}{y\sin\lambda}\frac{dw}{dy} - \frac{1}{y}\left(\frac{mw-u\cos\lambda}{y\sin\lambda}\right)\right]\right\}$$

$$\frac{\sigma^{22}}{\epsilon} = \frac{\cos m\theta}{1-\nu^2}\left\{\frac{dv}{dy} - z\frac{d^2w}{dy^2} + \frac{\nu}{y\sin\lambda}\left[mu + v\sin\lambda - w\cos\lambda + z\left(\frac{m(mw-u\cos\lambda)}{y\sin\lambda} - \sin\lambda\frac{dw}{dy}\right)\right] - a(1+\nu)\,(T-T_o)\right\}. \tag{27}$$

At each mesh point along the generator, the stresses of equation (27) are evaluated at the outside surface, the mid-plane, and the inside surface ($z = -h/2, 0, h/2$). In order to evaluate the stress at a particular point, the product of the temperature difference and α must be provided as an input. An exception for which the program does not require any temperature inputs is the isothermal case with pressure loading. The stresses are also functions of the displacements, which are obtained from the solution of the simultaneous equations, and the derivatives of the displacements which are computed by finite difference techniques. It should be recalled that the cone has two boundary regions and membrane region. The computation of the derivatives at junction points between these regions requires special consideration.

For the first derivatives, a standard 3-point centered difference formula is used for all internal points removed from the boundaries and the junction points. At the edges of the cone, a 3-point backward or forward differencing formula is used to compute the first derivative. The forward difference would be used at the left edge, and the backward difference at the right edge or base. To compute the first derivatives at the junction points of the two regions, a 3-point forward or backward difference formula is again used and the computation is always based upon data in the fine mesh region.

The second derivatives are computed in a manner similar to the first derivatives. A 3-point centered difference formula for the second derivative is used at all points removed from the edges or junction points. A 4-point forward or backward differencing formula is used at the edges and junctions with the computation based on data from the fine mesh region.

The physical stresses for the ogive are given by:

$$\frac{\sigma^{11}}{\epsilon_o} = \frac{\epsilon}{\epsilon_o}\frac{\cos m\theta}{1-\nu^2}\left\{\frac{1}{R_1\cos\beta}\left[\left(1-\frac{z}{R_1}\right)mu + \sin\beta\left(1-\frac{z}{R}\right)v - \left(\cos\beta - \frac{m^2 z}{R_1\cos\beta}\right)w - \sin\beta\, z\,\frac{\partial w}{\partial y}\right]\right.$$

$$\left. + \nu\left[-\frac{w}{R} + \left(1-\frac{z}{R}\right)\frac{\partial v}{\partial y} - z\frac{\partial^2 w}{\partial y^2}\right] - \alpha\,(1+\nu)\,(T-T_o)\right\}$$

$$\frac{\sigma^{22}}{\epsilon_o} = \frac{\epsilon}{\epsilon_o}\frac{\cos m\theta}{1-\nu^2}\left\{\frac{\nu}{R_1\cos\beta}\left[\left(1-\frac{z}{R_1}\right)mu + \sin\beta\left(1-\frac{z}{R}\right)v - \left(\cos\beta - \frac{m^2 z}{R_1\cos\beta}\right)w - \sin\beta\, z\,\frac{\partial w}{\partial y}\right]\right.$$

$$\left. + \left[-\frac{w}{R} + \left(1-\frac{z}{R}\right)\frac{\partial v}{\partial y} - z\frac{\partial^2 w}{\partial y^2}\right] - \alpha\,(1+\nu)\,(T-T_o)\right\}$$

$$\frac{\sigma^{12}}{\epsilon_o} = \frac{\epsilon}{\epsilon_o}\frac{\sin m\theta}{2(1+\nu)}\left\{\frac{\cos\beta_o\sin\beta}{\cos^2\beta\, R_1^2}\,zu - \frac{m\sin\beta}{R_1^2\cos^2\beta}\,zw + \left(1-\frac{z}{R_1}\right)\frac{\partial u}{\partial y} + \frac{mz}{R_1\cos\beta}\frac{\partial w}{\partial y}\right.$$

$$\left. + \frac{1}{R_1\cos\beta}\left[\left(1-\frac{z}{R_1}\right)\sin\beta\, u - m\left(1-\frac{z}{R}\right)v + \frac{m\sin\beta}{R_1\cos\beta}\,zw + mz\frac{\partial w}{\partial y}\right]\right\}. \tag{28}$$

The finite difference formulas for the derivatives in the above expressions are the same as for the cone program. The stresses themselves are calculated at the mid-plane and outer and inner surfaces and require values of Poisson's ratio and a normalized Young's modulus at these points.

6. NUMERICAL RESULTS

Numerous problems have been analyzed using the digital programs, and for problems which have a theoretical solution the analytical and numerical results have been compared. Theoretical results are available for comparison with several interesting cases for the zeroth harmonic with pressure or thermal loading. Five of these cases are discussed in this section. For harmonic numbers greater than zero, the number of theoretical solutions are limited and in this report only one problem with m = 1 is discussed.

For the cone, the following problems are discussed:

Problem No.	m	λ	a	Loading
1	0	.1489	-	Closed cone - constant temperature increase
2	0	.1489	.1	Truncated cone - constant pressure
3	0	.1489	.1	Truncated cone - constant temperature increase
4	0	.4636	.1	Truncated cone - Linear temperature along ℄
5	1	.6435	.1	Truncated cone - Linear temperature along diameter

In all of the above problems, the (non-dimensional) wall thickness and Poisson's ratio are assumed constant and equal to 0.00206 and 0.25, respectively. Furthermore, only the results with 72 spaces along the generator are considered.

Problem 1 is the analysis of a closed cone uniformly heated with a temperature change of 1000°F. The base is assumed to have no edge moment but edge shear prevents any radial growth. This is equivalent to K_1 = 0 and

$K_2 = \infty$. As shown in Figure 4, the deflections w and v are smoothly varying curves over the 73 mesh points. The abscissa has been labled with two scales. The upper scale indicates the y distance along the generator while the lower scale indicates the mesh point number. The first mesh point is located at $y = .0069$ which is slightly larger than the distance to the inside apex. The first boundary region ends at station 25 and the second boundary region starts at station 49. The membrane region between stations 25 and 49 has a mesh spacing of δ, where $\delta = .0276$. As mentioned in Section 2, the points in the boundary regions have a uniform spacing of $\delta/4$.

If the base of the cone is completely unrestrained, the closed cone with uniform heating is theoretically in a zero-stress state. Further, the displacements are found to be:

$$\begin{aligned} w &= -\alpha T \tan\lambda = -.15001024 \times 10^{-2} \\ v &= -\alpha T (1-y) = -10 \times 10^{-3} (1-y) \end{aligned} \qquad (29)$$

where $\alpha = 10^{-5}$, the value used in the digital program. The numerical results from the program agree well with the theoretical values from equation (29), for all values of y away from the base region. The maximum error was found to be 3 parts in 1500 or 0.2%. In the vicinity of the base mounting, the theoretical solution is not applicable because the base is assumed to be free whereas in problem 1 the base has some constraint. The numerical solution with the damped oscillations in w is typical of the edge phenomenon of shells.

Also shown in Figure 4 is the stress σ_2^{22} along the generator. The stress is in dimensionless form and must be multiplied by Young's modulus ϵ to obtain the physical stress. The stress, like the w displacement, has a damped oscillatory character in the vicinity of the base, and away from the base the stress varies from 30 to 300 psi for $\epsilon = 30 \times 10^6$. In theory, the stress should become zero away from the base. In the immediate proximity of the nose, the stress has not been plotted because the structure violates the shell assumptions and behaves like a 3-dimensional body.

The mid-plane stress σ_2^{11} and the stresses off the mid-plane are similar in nature to σ_2^{22}; that is, the stresses are large in the vicinity of the base and become small in the membrane region. These stresses are found to be in good agreement with theory.

For problem 2, the cone has a 10% truncation and a uniform pressure loading. The base boundary conditions are $K_1 = 0$ and $K_2 = \infty$, while at the location of the truncation no constraint is imposed; that is, $K_5 = K_6 = K_7 = 0$. The deflections w and v for problem 2 are plotted in Figure 5 as the solid curves. The circled points represent the theoretical solution to the same problem based upon the following equations from membrane theory:

$$\begin{aligned} w &= \frac{p}{\epsilon}\,\frac{\tan^2\lambda}{2h}\left[\frac{3}{2}\,y^2 + \nu\,(a^2 - 1) + \frac{1}{2} + a^2 \ln y\right] \\ v &= \frac{p}{\epsilon}\,\frac{\tan\lambda}{2h}\left[\left(\nu - \frac{1}{2}\right)(y^2 - 1) + a^2 \ln y\right]. \end{aligned} \tag{30}$$

For the same problem, the mid-plane stresses σ_2^{11} and σ_2^{22} are plotted in Figure 6, and the stresses σ_1^{11} and σ_1^{22} ($z = -h/2$) are plotted in Figure 7. Again the circled points are the results of analytical calculations for selected points along the generator. The agreement is seen to be good. For the stresses σ_3^{11} and σ_3^{22} which have not been plotted, the numerical and analytical results were found to be in good agreement.

In Appendix D, the complete set of inputs and outputs is shown for problem 2. Also included in Appendix D is the program outputs for problem 3. Both these problems have the same cone geometry but different loads and boundary conditions.

In problem 3, the truncated cone is analyzed for a uniform increase of temperature. At the base $K_1 = 0$ and $K_2 = \infty$, while at the truncation the edge is assumed to have no radial growth or change of slope. This corresponds to $K_5 = K_6 = \infty$. In Figure 8, the displacements w and v are shown, and the edge phenomenon is again noted. In the membrane region, the theoretical displacements are computed using equation (29) and the error in w found to be roughly 3 parts in 1500. Theoretically, the stresses should be zero in the membrane region and, as shown by the tabulation in Appendix D, the computed stresses are small, varying from 30 to 300 psi for $\epsilon = 30 \times 10^6$. The agreement is considered satisfactory.

In problem 4, a truncated cone is thermally loaded with a temperature distribution which is linear along the axis of the cone. If the edges of the cone are free from constraints, the theoretical displacements are found to be:

$$\begin{aligned} w &= - \alpha T \frac{\tan \lambda}{2} (1 - y^2) \\ v &= - \alpha T (y - 1)^2/2 \quad . \end{aligned} \tag{31}$$

Furthermore, the cone is found to be in a zero state of stress.

The displacements w and v from the digital program are shown in Figure 9. The circled points are obtained from equation (31), and are seen to agree well with the numerical results from the program. The stresses at the mid-plane and off the mid-plane were found to be small and in satisfactory agreement with the theoretical zero state of stress.

The last example to be considered for the cone is problem 5 where the first harmonic of the loading is used. The loading is a linear temperature distribution along a diameter of the cone. The cone is free at the truncation and constrained from radial growth at the base ($K_2 = \infty$). Because of these boundary conditions, it is not possible to obtain an analytical solution which can be compared with the w, v and u displacements shown in Figure 10. However, the stresses in the membrane region should be zero or at least small. The stresses from the digital program varied from 30 to 300 psi ($\epsilon = 30 \times 10^6$) in the membrane region and are considered to be in satisfactory agreement with theory.

One of the first problems analyzed with the ogive program was that of a uniform pressure loading on a shell with free edge constraints. A uniform mesh having 73 points was selected. The following table summarizes the inputs to the problem; note that all lengths have been scaled by the length of the generator:

β_o = .25 radian $\qquad \nu(z)$ = .25 for all z

R = 4.0 $\qquad \epsilon(z)/\epsilon_o$ = 1.0 for all z

h = .00125 $\qquad p/\epsilon_o = .25 \times 10^{-5}$

m = 0 $\qquad K_1 = K_2 = 0$

The resulting deflections are shown in Figure 11. As a comparison the membrane solution

$$v = -\frac{(p/\epsilon_o)R^2}{4h}\left\{\cot\phi - \frac{3}{2}\sin\phi_o\left[\cot\phi\csc\phi + \ln(\cot\phi/2)\right]\right.$$

$$\left. + \frac{2}{3}\sin^2\phi_o\left[\cot\phi\csc^2\phi + 2\cot\phi\right]\right\} \cdot \sin\phi\sin\phi_o$$

$$w = v\cot\phi - \frac{(p/\epsilon_o)R^2}{h}\quad \Phi\left\{\frac{1}{2}\Phi - \frac{7}{8}\right\}$$

$$\Phi = \frac{\sin\phi - \sin\phi_o}{\sin\phi}, \qquad \phi = \frac{\pi}{2} - \beta_o$$

has been calculated for several values of ϕ and as seen in the graph, the agreement is good. It is to be particularly noted that the maximum v and minimum w do not occur at the extremity of the nose, but are located at about station number 4. This phenomenon is predicted by theory. The ogive program has not been used to compute stresses since that part of the program is undergoing modification. Stress results will be described in subsequent scientific reports.

7. CONCLUSIONS

The digital programs enable the design engineer to make detailed investigations of the structural requirements for ogival and conical radomes under thermal and/or pressure loading. The programs can be used to analyze the radome for any flight mission, provided the required thermal and pressure loading is known. For a defined load, the program provides the design engineer with (1) the displacements w, v, and u at the mid-surface of the shell, and (2) the normal and shear stress at $z = -h/2$, 0, and $h/2$. This information is given for $n + 1$ points along the generator.

Besides investigating various loading conditions, the programs can be used to investigate different methods of mounting the radome. In the cone program, no radial growth at the base is allowed, but any degree of edge moment constraint can be specified ($K_1 = 0$, finite or ∞ and $K_2 = \infty$). At the truncation of the cone, any arbitrary constraint can be imposed by specifying the proper combination of spring constants. In all, there are 5 springs at the truncation, each of which can be specified as zero, finite or infinite. Hence, a conical radome with a nose boom can be investigated for various amounts of flexibility in the boom. In addition, the cone program can be used for the analysis of the closed nose structure. The ogive program has been constructed for the closed nose condition only. At the base of the ogive, completely general constraints are permitted; that is, both K_1 and K_2 can be zero, finite or infinite.

All of the numerical results discussed in Section 6 are for the spring constants zero or infinite. Problems with finite springs at the edges are omitted since suitable analytical solutions are not available for comparison purposes. However, the programs have been used to analyze systems with finite springs, and as the value of the spring constants was varied from zero to larger and larger values, the results were observed to change in a consistent manner from the zero constraint case to the infinitely rigid case.

The numerical results indicate that the digital program for the cone accurately computes the displacements and stresses for pressure and/or thermal loading. Any discrepancies between the numerical and theoretical results are indeed small and well within the requirements of the design engineer. Similar remarks are applicable to the ogive program regarding the displacements.

It is concluded that the combination of the above cone and ogive programs make possible a detailed examination of any conical or ogival radome for all nose and base boundary conditions, material properties and load distributions of practical interest.

APPENDIX A

FINITE DIFFERENCE FORMULAS FOR THE CONE PROGRAM

The free energy expression as shown by equation (7) involves zeroth, first, and second derivatives of the displacements and products thereof. For all of the terms not involving a second derivative, the following difference approximations are used:

$$\int r^2 dy = \sum_1^N \frac{r_i^2 + r_{i+1}^2}{2} \delta_i$$

$$\int (r')^2 dy = \sum_1^N (r_{i+1} - r_i)^2 \cdot \frac{1}{\delta_i}$$

$$\int r's'dy = \sum_1^N (r_{i+1} - r_i)(s_{i+1} - s_i) \cdot \frac{1}{\delta_i}$$

$$\int rs'\,dy = \frac{1}{2}\sum_1^N (r_{i+1} + r_i)(s_{i+1} - s_i)$$

where δ_i is the spacing of the stations at the ith mesh point, r and s are any of the displacement w, v, or u, and N is the number of spaces along the generator. The above formulas apply without any modification to a uniform or variable mesh size.

For terms involving the second derivative of a displacement, special consideration must be given to the junction points between the membrane and boundary regions. Let the junction points be called N1 and N2 for the left and right boundary regions, respectively. The finite difference forms are then written as:

$$\int r(s'')^2 \, dy = \sum_a^b r_i \frac{(s_{i+1} - 2s_i + s_{i-1})^2}{\delta_i^3} + \frac{8}{5}\frac{1}{\delta^3} r_{N1} (4s_{N1-1} - 5s_{N1} + s_{N1+1})^2$$

$$+ \frac{8}{5}\frac{1}{\delta^3} r_{N2} (s_{N2-1} - 5s_{N2} + 4s_{N2+1})^2$$

$$\int r's''dy = \sum_a^b \frac{(r_{i+1} - r_{i-1})(s_{i+1} - 2s_i + s_{i-1})}{2\,\delta_i^2} + \frac{1}{2\delta^2}(r_{N1+1} + 3r_{N1} - 4r_{N1-1})(4s_{N1-1} - 5s_{N1} + s_{N1+1})$$

$$+ \frac{1}{2\delta^2} (4r_{N2+1} - 3r_{N2} + r_{N1-1})(s_{N2-1} - 5s_{N2} + 4s_{N2+1})$$

where a and b have the following values for the various regions

left boundary region	$a = 2$; $b = N1-1$
membrane region	$a = N1+1$; $b = N2-1$
right boundary region	$a = N2+1$; $b = N$.

APPENDIX B

FIVE-POINT GAUSS QUADRATURE COORDINATES AND WEIGHTS

$q_1 = -.906179846$	$a_1 = .236926885$
$q_2 = -.538469310$	$a_2 = .478628670$
$q_3 = 0$	$a_3 = .568888889$
$q_4 = .538469310$	$a_4 = .478628670$
$q_5 = .906179846$	$a_5 = .236926885$

APPENDIX C

TABLE I

Energy Contribution from the Boundaries of the Cone

K_i	a_i	$\gamma_i\ (m \lessgtr 1)$	$\gamma_i\ (m = 1)$
$K_1 = \frac{k_1}{\epsilon \ell^2}$	$\frac{16(1-\nu^2)\sin\lambda}{\delta^2}$	$\begin{bmatrix} 1 & 0 & 0 & -1 \\ 0 & 0 & 0 & 0 \\ 0 & 0 & 0 & 0 \\ -1 & 0 & 0 & 0 \end{bmatrix} \begin{Bmatrix} w_n \\ v_n \\ u_n \\ w_{n+1} \end{Bmatrix}$	same as $m \lessgtr 1$
$K_2 = \frac{k_2}{\epsilon}$	$(1-\nu^2)\sin\lambda$	$\left[\cos^2\lambda\right] \left\{w_n\right\}$	same as $m \gtrless 1$
$K_3 = \frac{k_3}{\epsilon \ell}$	$(1-\nu^2)/\pi$	none	$\left[1\right] \left\{u_1\right\}$
$K_4 = \frac{k_4}{\epsilon \ell^3}$	$\frac{16(1-\nu^2)}{\pi\delta^2\cos^2\lambda}$	none	$\begin{bmatrix} 0 & 0 & 0 & 0 & 0 & 0 \\ 0 & 0 & 0 & 0 & 0 & 0 \\ 0 & 0 & 1 & 0 & 0 & -1 \\ 0 & 0 & 0 & 0 & 0 & 0 \\ 0 & 0 & 0 & 0 & 0 & 0 \\ 0 & 0 & -1 & 0 & 0 & 1 \end{bmatrix} \begin{Bmatrix} w_1 \\ v_1 \\ u_1 \\ w_2 \\ v_2 \\ u_2 \end{Bmatrix}$
$K_5 = \frac{k_5}{\epsilon \ell^2}$	$\frac{16(1-\nu^2)a}{\delta^2\csc\lambda}$	$\begin{bmatrix} 1 & 0 & 0 & -1 & 0 & 0 \\ 0 & 0 & 0 & 0 & 0 & 0 \\ 0 & 0 & 0 & 0 & 0 & 0 \\ -1 & 0 & 0 & 0 & 0 & 0 \\ 0 & 0 & 0 & 0 & 0 & 0 \\ 0 & 0 & 0 & 0 & 0 & 0 \end{bmatrix} \begin{Bmatrix} w_1 \\ v_1 \\ u_1 \\ w_2 \\ v_2 \\ u_2 \end{Bmatrix}$	none
$K_6 = \frac{k_6}{\epsilon}$	$(1-\nu^2)a\sin\lambda$	$\begin{bmatrix} \cos^2\lambda & -\sin\lambda\cos\lambda \\ -\sin\lambda\cos\lambda & \sin^2\lambda \end{bmatrix} \begin{Bmatrix} w_1 \\ v_1 \end{Bmatrix}$	none
$K_7 = \frac{k_7}{\epsilon \ell}$	$\frac{(1-\nu^2)}{2\pi}$	$\begin{bmatrix} \sin^2\lambda & \sin\lambda\cos\lambda \\ \sin\lambda\cos\lambda & \cos^2\lambda \end{bmatrix} \begin{Bmatrix} w_1 \\ v_1 \end{Bmatrix}$	none

Note: $F^{(i)} = \left(\frac{\pi C_m \ell^3 \epsilon}{1-\nu^2}\right) a_i K_i \gamma_i$

TABLE II

Connection Conditions γ_c for Various Combinations of Infinite Spring Constants for the Cone

Spring Combination	γ_c^i ($m \lessgtr 1$)	γ_c^i ($m = 1$)
K_1	$\begin{bmatrix} 1 & 0 & 0 \\ 0 & 1 & 0 \\ 0 & 0 & 1 \\ 1 & 0 & 0 \end{bmatrix} \begin{Bmatrix} u_{n-1} \\ w_n \\ v_n \\ u_n \end{Bmatrix}$	same as $m \lessgtr 1$
K_2	$w_{n+1} = 0$	$w_{n+1} = 0$
K_1 and K_2	$w_n = w_{n+1} = 0$	$w_n = w_{n+1} = 0$
K_3	none	$u_1 = 0$
K_4	none	$\begin{bmatrix} 1 & 0 & 0 & 0 & 0 \\ 0 & 1 & 0 & 0 & 0 \\ 0 & 0 & 0 & 0 & 1 \\ 0 & 0 & 1 & 0 & 0 \\ 0 & 0 & 0 & 1 & 0 \\ 0 & 0 & 0 & 0 & 1 \end{bmatrix} \begin{Bmatrix} w_1 \\ v_1 \\ w_2 \\ v_2 \\ u_2 \\ \vdots \end{Bmatrix}$
K_3 and K_4	none	$u_1 = u_2 = 0$
K_5	$\begin{bmatrix} 0 & 0 & 1 \\ 1 & 0 & 0 \\ 0 & 1 & 0 \\ 0 & 0 & 1 \end{bmatrix} \begin{Bmatrix} v_1 \\ u_1 \\ w_2 \\ v_2 \\ \vdots \end{Bmatrix}$	none
K_6	$\begin{bmatrix} \tan\lambda & 0 \\ 1 & 0 \\ 0 & 1 \end{bmatrix} \begin{Bmatrix} v_1 \\ u_1 \\ w_2 \\ \vdots \end{Bmatrix}$	none
K_5 and K_6	$\begin{bmatrix} 0 & 1 \\ 0 & \cot\lambda \\ 1 & 0 \\ 0 & 1 \end{bmatrix} \begin{Bmatrix} u_1 \\ w_2 \\ v_2 \\ u_2 \\ \vdots \end{Bmatrix}$	none

TABLE II (Continued)

Spring Combination	$\gamma_c^i \quad (m \lessgtr 1)$	$\gamma_c^i \quad (m = 1)$
K_7	$\begin{bmatrix} -\cot\lambda \\ 1 \\ \ \end{bmatrix} \begin{Bmatrix} v_1 \\ u_1 \\ w_2 \\ v_2 \\ \vdots \end{Bmatrix}$	none
K_5 and K_7	$\begin{bmatrix} 0 & 1 \\ 0 & \tan\lambda \\ 1 & 0 \\ 0 & 1 \end{bmatrix} \begin{Bmatrix} u_1 \\ w_2 \\ v_2 \\ u_2 \\ \vdots \end{Bmatrix}$	none
K_6 and K_7	$w_1 = v_1 = 0$	none
K_5, K_6 and K_7	$w_1 = v_1 = w_2 = 0$	none

TABLE III

Nose Closure Matrices for Cone

γ_c (m = 0)	γ_c (m = 1)	γ_c (m > 1)
$\begin{bmatrix} 0 & 1 \\ 0 & \cot\lambda \\ 1 & 0 \\ 0 & 1 \end{bmatrix} \begin{Bmatrix} u_1 \\ w_2 \\ v_2 \\ u_2 \\ \vdots \end{Bmatrix}$	$\begin{bmatrix} (1-q) & 0 & q\cos\lambda \\ \tan\lambda & 0 & -\csc\lambda \\ q\cos\lambda & 0 & (1+q\cos^2\lambda) \\ 1 & 0 & 0 \\ 0 & 1 & 0 \\ 0 & 0 & 1 \end{bmatrix} \begin{Bmatrix} w_2 \\ v_2 \\ u_2 \\ w_3 \\ \vdots \end{Bmatrix}$	$w_1 = v_1 = u_1 = 0$ $w_2 = v_2 = u_2 = 0$

where $q = \dfrac{\delta}{4\, y_2 \sin^2\lambda}$ and y_2 = y at station 2.

TABLE IV

Energy Matrices for the Base Connection Springs

Moment Spring, modulus K_1

$$2\pi C_m(\epsilon/\epsilon_o)R_1\cos\beta_{n+1}\frac{K_1}{2}\begin{bmatrix} \frac{1}{2\delta^2} & 0 & 0 & -\frac{1}{2\delta^2} & \frac{1}{2R\delta} & 0 & 0 & 0 & 0 \\ 0 & 0 & 0 & 0 & 0 & 0 & 0 & 0 & 0 \\ 0 & 0 & 0 & 0 & 0 & 0 & 0 & 0 & 0 \\ -\frac{1}{2\delta^2} & 0 & 0 & \frac{1}{\delta^2} & 0 & 0 & -\frac{1}{2\delta^2} & 0 & 0 \\ -\frac{1}{2R\delta} & 0 & 0 & 0 & \frac{1}{R^2} & 0 & \frac{1}{2R\delta} & 0 & 0 \\ 0 & 0 & 0 & 0 & 0 & 0 & 0 & 0 & 0 \\ 0 & 0 & 0 & -\frac{1}{2\delta^2} & \frac{1}{2R\delta} & 0 & \frac{1}{2\delta^2} & 0 & 0 \\ 0 & 0 & 0 & 0 & 0 & 0 & 0 & 0 & 0 \\ 0 & 0 & 0 & 0 & 0 & 0 & 0 & 0 & 0 \end{bmatrix}\begin{Bmatrix} w_n \\ v_n \\ u_n \\ w_{n+1} \\ v_{n+1} \\ u_{n+1} \\ w_{n+2} \\ v_{n+2} \\ u_{n+2} \end{Bmatrix}$$

Radial Growth Spring, modulus K_2

$$2\pi C_m(\epsilon/\epsilon_o)R_1\cos\beta_{n+1}\frac{K_2}{2}\begin{bmatrix} \cos^2\beta_{n+1} & -\sin\beta_{n+1}\cos\beta_{n+1} & 0 & 0 & 0 & 0 \\ -\sin\beta_{n+1}\cos\beta_{n+1} & \sin^2\beta_{n+1} & 0 & 0 & 0 & 0 \\ 0 & 0 & 0 & 0 & 0 & 0 \\ 0 & 0 & 0 & 0 & 0 & 0 \\ 0 & 0 & 0 & 0 & 0 & 0 \\ 0 & 0 & 0 & 0 & 0 & 0 \end{bmatrix}\begin{Bmatrix} w_{n+1} \\ v_{n+1} \\ u_{n+1} \\ w_{n+2} \\ v_{n+2} \\ u_{n+2} \end{Bmatrix}$$

These are for $m \geq 1$. When $m = 0$ delete rows and columns numbered 3, 6, 9 in the first matrix and rows and columns numbered 3 and 6 in the second matrix.

TABLE V

Base Connection for the Radome Ogive

Spring Combination	(m = 0)	(m ≥ 1)
K_1 Finite, K_2 Finite	$\begin{bmatrix} 1 & 0 & 0 \\ 0 & 1 & 0 \\ 0 & 0 & 1 \\ 0 & 0 & 0 \\ 1 & 0 & 2 \\ 0 & -1 & 0 \end{bmatrix} \begin{Bmatrix} w_n \\ v_n \\ w_{n+1} \end{Bmatrix}$	$\begin{bmatrix} 1 & 0 & 0 & 0 \\ 0 & 1 & 0 & 0 \\ 0 & 0 & 1 & 0 \\ 0 & 0 & 0 & 1 \\ 0 & 0 & 0 & 0 \\ 0 & 0 & 0 & 0 \\ 1 & 0 & 0 & 2 \\ 0 & -1 & 0 & 0 \\ 0 & 0 & -1 & 0 \end{bmatrix} \begin{Bmatrix} w_n \\ v_n \\ u_n \\ w_{n+1} \end{Bmatrix}$
K_1 Infinite, K_2 Finite	$\begin{bmatrix} 1 & 0 & 0 \\ 0 & 1 & 0 \\ 0 & 0 & 1 \\ 0 & 0 & 0 \\ 1 & 0 & 0 \\ 0 & -1 & 0 \end{bmatrix} \begin{Bmatrix} w_n \\ v_n \\ w_{n+1} \end{Bmatrix}$	$\begin{bmatrix} 1 & 0 & 0 & 0 \\ 0 & 1 & 0 & 0 \\ 0 & 0 & 1 & 0 \\ 0 & 0 & 0 & 1 \\ 0 & 0 & 0 & 0 \\ 0 & 0 & 0 & 0 \\ 1 & 0 & 0 & 0 \\ 0 & -1 & 0 & 0 \\ 0 & 0 & -1 & 0 \end{bmatrix} \begin{Bmatrix} w_n \\ v_n \\ u_n \\ w_{n+1} \end{Bmatrix}$
K_1 Finite, K_2 Infinite	$\begin{bmatrix} 1 & 0 \\ 0 & 1 \\ 0 & 0 \\ 0 & 0 \\ -1 & 0 \\ 0 & -1 \end{bmatrix} \begin{Bmatrix} w_n \\ v_n \end{Bmatrix}$	$\begin{bmatrix} 1 & 0 & 0 \\ 0 & 1 & 0 \\ 0 & 0 & 1 \\ 0 & 0 & 0 \\ 0 & 0 & 0 \\ 0 & 0 & 0 \\ -1 & 0 & 0 \\ 0 & -1 & 0 \\ 0 & 0 & -1 \end{bmatrix} \begin{Bmatrix} w_n \\ v_n \\ u_n \end{Bmatrix}$
K_1 Infinite, K_2 Infinite	$\begin{bmatrix} 1 & 0 \\ 0 & 1 \\ 0 & 0 \\ 0 & 0 \\ 1 & 0 \\ 0 & -1 \end{bmatrix} \begin{Bmatrix} w_n \\ v_n \end{Bmatrix}$	$\begin{bmatrix} 1 & 0 & 0 \\ 0 & 1 & 0 \\ 0 & 0 & 1 \\ 0 & 0 & 0 \\ 0 & 0 & 0 \\ 0 & 0 & 0 \\ 1 & 0 & 0 \\ 0 & -1 & 0 \\ 0 & 0 & -1 \end{bmatrix} \begin{Bmatrix} w_n \\ v_n \\ u_n \end{Bmatrix}$

TABLE VI

Nose Closure for the Radome Ogive

For m = 0:

$$\begin{bmatrix} \frac{2\delta}{R} & 1 & 0 \\ 2 & 0 & -1 \\ \tan\beta_1 & 0 & 0 \\ 1 & 0 & 0 \\ 0 & 1 & 0 \\ 0 & 0 & 1 \end{bmatrix} \left\{ \begin{matrix} v_1 \\ w_2 \\ v_2 \\ \vdots \end{matrix} \right\}$$

For m > 1:

$$\begin{bmatrix} 1 & 0 & 0 \\ 0 & 1 & 0 \\ 0 & 0 & 1 \\ 0 & 0 & 0 \\ 0 & 0 & 0 \\ 0 & 0 & 0 \\ 1 & 0 & 0 \\ 0 & 1 & 0 \\ 0 & 0 & 1 \end{bmatrix} \left\{ \begin{matrix} w_2 \\ v_2 \\ u_2 \\ \vdots \end{matrix} \right\}$$

For m = 1:

$$\begin{bmatrix} \frac{2\delta}{R} - \frac{2\delta}{(R_1\cos^2\beta)_1} & \frac{-2\delta\sin\beta_1}{(R_1\cos^2\beta)_1} & 1 & 0 & 0 \\ 2 & 0 & 0 & -1 & 0 \\ \frac{-2\delta}{(R_1\cos\beta)_1} & \frac{-2\delta\sin\beta_1}{(R_1\cos\beta)_1} & 0 & 0 & 1 \\ \tan\beta_1 & \sec\beta_1 & 0 & 0 & 0 \\ 1 & 0 & 0 & 0 & 0 \\ 0 & 1 & 0 & 0 & 0 \\ 0 & 0 & 1 & 0 & 0 \\ 0 & 0 & 0 & 1 & 0 \\ 0 & 0 & 0 & 0 & 1 \end{bmatrix} \left\{ \begin{matrix} v_1 \\ u_1 \\ w_2 \\ v_2 \\ u_2 \\ \vdots \end{matrix} \right\}$$

APPENDIX D
DIGITAL PROGRAM OUTPUTS FOR PROBLEMS 2 AND 3

```
GASL          0026-3000   PROB 2           9/24/59
1 7


INPUT

CLASS  8     N#72     HARMONIC#  0.     ANG# 0.1489E-00     A# 1.0000E-01     THICK.# 0.2060E-02     NU# 0.2500E-00

SPRING CONS

    0.          0.          0.          0.          0.          0.          0.90E 04

PRESSURE

   0.2500E-05
```

OUTPUTS   MISSILE AT LOCATION 0.   TIME# 0.

POS	Y	W	V
1	0.1000	0.33746448E-05	0.20692991E-04
2	0.1062	0.34119216E-05	0.20718776E-04
3	0.1125	0.34475228E-05	0.20739736E-04
4	0.1187	0.34843457E-05	0.20756079E-04
5	0.1250	0.35225319E-05	0.20768109E-04
6	0.1312	0.35620049E-05	0.20776083E-04
7	0.1375	0.36027664E-05	0.20780215E-04
8	0.1437	0.36448435E-05	0.20780685E-04
9	0.1500	0.36882617E-05	0.20777655E-04
10	0.1562	0.37330427E-05	0.20771266E-04
11	0.1625	0.37792049E-05	0.20761642E-04
12	0.1687	0.38267649E-05	0.20748891E-04
13	0.1750	0.38757375E-05	0.20733114E-04
14	0.1812	0.39261360E-05	0.20714395E-04
15	0.1875	0.39779721E-05	0.20692816E-04
16	0.1937	0.40312561E-05	0.20668448E-04
17	0.2000	0.40859975E-05	0.20641353E-04
18	0.2062	0.41422040E-05	0.20611590E-04
19	0.2125	0.41998876E-05	0.20579214E-04
20	0.2187	0.42590712E-05	0.20544271E-04
21	0.2250	0.43197882E-05	0.20506810E-04
22	0.2312	0.43820152E-05	0.20466870E-04
23	0.2375	0.44454603E-05	0.20424484E-04
24	0.2437	0.45093253E-05	0.20379660E-04
25	0.2500	0.45729593E-05	0.20332367E-04
26	0.2750	0.48600310E-05	0.20121856E-04
27	0.3000	0.51667250E-05	0.19875611E-04
28	0.3250	0.54979076E-05	0.19594456E-04
29	0.3500	0.58538727E-05	0.19279341E-04
30	0.3750	0.62347294E-05	0.18931028E-04
31	0.4000	0.66405684E-05	0.18550131E-04
32	0.4250	0.70714654E-05	0.18137150E-04
33	0.4500	0.75274825E-05	0.17612503E-04
34	0.4750	0.80086718E-05	0.17216536E-04
35	0.5000	0.85150774E-05	0.16709545E-04
36	0.5250	0.90467366E-05	0.16171792E-04
37	0.5500	0.96036823E-05	0.15603463E-04
38	0.5750	0.10185942E-04	0.15004776E-04
39	0.6000	0.10793541E-04	0.14375883E-04
40	0.6250	0.11426501E-04	0.13716929E-04
41	0.6500	0.12084840E-04	0.13028041E-04
42	0.6750	0.12768576E-04	0.12309331E-04
43	0.7000	0.13477723E-04	0.11560899E-04
44	0.7250	0.14212294E-04	0.10782835E-04
45	0.7500	0.14972302E-04	0.99752186E-05
46	0.7750	0.15757743E-04	0.91361226E-05
47	0.8000	0.16568605E-04	0.82716112E-05
48	0.8250	0.17405914E-04	0.73757683E-05
49	0.8500	0.18276356E-04	0.64508583E-05
50	0.8562	0.18492419E-04	0.62149599E-05

OUTPUTS MISSILE AT LOCATION 0. TIME= 0.

POS	Y	W	V
51	0.8625	0.18710462E-04	0.59771924E-05
52	0.8687	0.18931338E-04	0.57375689E-05
53	0.8750	0.19154988E-04	0.54961058E-05
54	0.8812	0.19380871E-04	0.52528153E-05
55	0.8875	0.19608109E-04	0.50077005E-05
56	0.8937	0.19835470E-04	0.47607522E-05
57	0.9000	0.20061416E-04	0.45119458E-05
58	0.9062	0.20284466E-04	0.42612404E-05
59	0.9125	0.20504210E-04	0.40085861E-05
60	0.9187	0.20723260E-04	0.37539466E-05
61	0.9250	0.20950182E-04	0.34973493E-05
62	0.9312	0.21202806E-04	0.32389658E-05
63	0.9375	0.21510112E-04	0.29792183E-05
64	0.9437	0.21909107E-04	0.27188736E-05
65	0.9500	0.22431057E-04	0.24590421E-05
66	0.9562	0.23070183E-04	0.22009341E-05
67	0.9625	0.23729490E-04	0.19451722E-05
68	0.9687	0.24145927E-04	0.16904507E-05
69	0.9750	0.23814484E-04	0.14314628E-05
70	0.9812	0.21961226E-04	0.11563816E-05
71	0.9875	0.17657584E-04	0.84490962E-06
72	0.9937	0.10212593E-04	0.46903087E-06
73	1.0000	0.	0.

OUTPUTS   MISSILE AT LOCATION 0.   TIME= 0.

POS	Y	SIGMA-11,1	SIGMA-11,2	SIGMA-11,3	SIGMA-22,1	SIGMA-22,2	SIGMA-22,3
1	0.1000	-0.16791730E-04	-0.18030007E-04	-0.19455606E-04	0.19311907E-06	0.41193440E-08	-0.23171105E-06
2	0.1062	-0.18084501E-04	-0.19340359E-04	-0.20771372E-04	-0.82571720E-06	-0.10955022E-05	-0.14090763E-05
3	0.1125	-0.19200213E-04	-0.20463409E-04	-0.21889702E-04	-0.17836806E-05	-0.21316909E-05	-0.25204760E-05
4	0.1187	-0.20339691E-04	-0.21593119E-04	-0.22999214E-04	-0.27791499E-05	-0.31284539E-05	-0.35159244E-05
5	0.1250	-0.21487043E-04	-0.22731265E-04	-0.24119069E-04	-0.37374125E-05	-0.40823968E-05	-0.44632766E-05
6	0.1312	-0.22633800E-04	-0.23870723E-04	-0.25243206E-04	-0.46560609E-05	-0.49992690E-05	-0.53763673E-05
7	0.1375	-0.23779085E-04	-0.25009918E-04	-0.26369166E-04	-0.55419897E-05	-0.58843888E-05	-0.62588915E-05
8	0.1437	-0.24923291E-04	-0.26148878E-04	-0.27496471E-04	-0.64001885E-05	-0.67419467E-05	-0.71142067E-05
9	0.1500	-0.26066673E-04	-0.27287702E-04	-0.28624961E-04	-0.72342346E-05	-0.75754239E-05	-0.79456701E-05
10	0.1562	-0.27209377E-04	-0.28426433E-04	-0.29754475E-04	-0.80470191E-05	-0.83877041E-05	-0.87561360E-05
11	0.1625	-0.28351505E-04	-0.29565082E-04	-0.30884873E-04	-0.88410129E-05	-0.91812654E-05	-0.95480711E-05
12	0.1687	-0.29493139E-04	-0.30703660E-04	-0.32016026E-04	-0.96182880E-05	-0.99581645E-05	-0.10323502E-04
13	0.1750	-0.30634341E-04	-0.31842171E-04	-0.33147831E-04	-0.10380529E-04	-0.10720186E-04	-0.11084200E-04
14	0.1812	-0.31775197E-04	-0.32980643E-04	-0.34280220E-04	-0.11129633E-04	-0.11468901E-04	-0.11831701E-04
15	0.1875	-0.32915725E-04	-0.34119057E-04	-0.35413098E-04	-0.11866583E-04	-0.12205596E-04	-0.12567286E-04
16	0.1937	-0.34055968E-04	-0.35257421E-04	-0.36546403E-04	-0.12592667E-04	-0.12931456E-04	-0.13292127E-04
17	0.2000	-0.35195957E-04	-0.36395729E-04	-0.37680075E-04	-0.13308939E-04	-0.13647515E-04	-0.14007234E-04
18	0.2062	-0.36335652E-04	-0.37533955E-04	-0.38814075E-04	-0.14016116E-04	-0.14354641E-04	-0.14713620E-04
19	0.2125	-0.37475145E-04	-0.38672221E-04	-0.39948536E-04	-0.14714771E-04	-0.15053591E-04	-0.15412222E-04
20	0.2187	-0.38614919E-04	-0.39811005E-04	-0.41083912E-04	-0.15405632E-04	-0.15745086E-04	-0.16103746E-04
21	0.2250	-0.39756214E-04	-0.40951076E-04	-0.42220492E-04	-0.16091334E-04	-0.16429863E-04	-0.16787031E-04
22	0.2312	-0.40899701E-04	-0.42091573E-04	-0.43355864E-04	-0.16778783E-04	-0.17108871E-04	-0.17457064E-04
23	0.2375	-0.42039051E-04	-0.43224227E-04	-0.44479796E-04	-0.17475553E-04	-0.17782918E-04	-0.18107880E-04
24	0.2437	-0.43148762E-04	-0.44327519E-04	-0.45574704E-04	-0.18162712E-04	-0.18451314E-04	-0.18757024E-04
25	0.2500	-0.44214238E-04	-0.45385437E-04	-0.46623136E-04	-0.18841048E-04	-0.19110606E-04	-0.19396789E-04
26	0.2750	-0.48865071E-04	-0.50052566E-04	-0.51300437E-04	-0.21319054E-04	-0.21648265E-04	-0.21992570E-04
27	0.3000	-0.53417975E-04	-0.54606122E-04	-0.55849425E-04	-0.23862156E-04	-0.24199549E-04	-0.24550732E-04
28	0.3250	-0.57970725E-04	-0.59157979E-04	-0.60396013E-04	-0.26377229E-04	-0.26714884E-04	-0.27065234E-04
29	0.3500	-0.62523217E-04	-0.63709895E-04	-0.64943627E-04	-0.28858323E-04	-0.29196014E-04	-0.29545468E-04
30	0.3750	-0.67075353E-04	-0.68261730E-04	-0.69491953E-04	-0.31311869E-04	-0.31649634E-04	-0.31998361E-04
31	0.4000	-0.71627212E-04	-0.72813489E-04	-0.74040819E-04	-0.33743070E-04	-0.34080935E-04	-0.34429063E-04
32	0.4250	-0.76178863E-04	-0.77365191E-04	-0.78590118E-04	-0.36155882E-04	-0.36493862E-04	-0.36841492E-04
33	0.4500	-0.80730353E-04	-0.81916845E-04	-0.83139764E-04	-0.38553388E-04	-0.38891495E-04	-0.39238708E-04
34	0.4750	-0.85281717E-04	-0.86468461E-04	-0.87689693E-04	-0.40938019E-04	-0.41276261E-04	-0.41623124E-04
35	0.5000	-0.89832979E-04	-0.91020044E-04	-0.92239856E-04	-0.43311703E-04	-0.43650087E-04	-0.43996658E-04
36	0.5250	-0.94384153E-04	-0.95571591E-04	-0.96790206E-04	-0.45676010E-04	-0.46014541E-04	-0.46360867E-04
37	0.5500	-0.98935264E-04	-0.10012311E-03	-0.10134072E-03	-0.48032235E-04	-0.48370916E-04	-0.48717035E-04
38	0.5750	-0.10348631E-03	-0.10467462E-03	-0.10589138E-03	-0.50381425E-04	-0.50720260E-04	-0.51066208E-04
39	0.6000	-0.10803733E-03	-0.10922611E-03	-0.11044215E-03	-0.52724463E-04	-0.53063451E-04	-0.53409255E-04
40	0.6250	-0.11258830E-03	-0.11377758E-03	-0.11499303E-03	-0.55062087E-04	-0.55401231E-04	-0.55746918E-04
41	0.6500	-0.11713924E-03	-0.11832903E-03	-0.11954398E-03	-0.57394920E-04	-0.57734220E-04	-0.58079813E-04
42	0.6750	-0.12169015E-03	-0.12288047E-03	-0.12409503E-03	-0.59723502E-04	-0.60062960E-04	-0.60408475E-04
43	0.7000	-0.12624104E-03	-0.12743191E-03	-0.12864614E-03	-0.62048291E-04	-0.62387905E-04	-0.62733363E-04
44	0.7250	-0.13079192E-03	-0.13198332E-03	-0.13319730E-03	-0.64369675E-04	-0.64709445E-04	-0.65054858E-04
45	0.7500	-0.13534278E-03	-0.13653474E-03	-0.13774852E-03	-0.66688026E-04	-0.67027929E-04	-0.67373287E-04
46	0.7750	-0.13989350E-03	-0.14108601E-03	-0.14229964E-03	-0.69003629E-04	-0.69343650E-04	-0.69688951E-04
47	0.8000	-0.14444332E-03	-0.14563684E-03	-0.14685083E-03	-0.71314330E-04	-0.71656296E-04	-0.72003377E-04
48	0.8250	-0.14899776E-03	-0.15019486E-03	-0.15141182E-03	-0.73609895E-04	-0.73963773E-04	-0.74322614E-04
49	0.8500	-0.15362811E-03	-0.15421973E-03	-0.15603062E-03	-0.75971562E-04	-0.76299172E-04	-0.76631602E-04
50	0.8562	-0.15473319E-03	-0.15593071E-03	-0.15714737E-03	-0.76524362E-04	-0.76875956E-04	-0.77232334E-04

OUTPUTS MISSILE AT LOCATION 0. TIME* 0.

POS	Y	SIGMA-11,1	SIGMA-11,2	SIGMA-11,3	SIGMA-22,1	SIGMA-22,2	SIGMA-22,3
51	0.8625	-0.15584165E-03	-0.15704511E-03	-0.15826757E-03	-0.77076964E-04	-0.77452551E-04	-0.77832887E-04
52	0.8687	-0.15696640E-03	-0.15816946E-03	-0.15939139E-03	-0.77655396E-04	-0.78029288E-04	-0.78407896E-04
53	0.8750	-0.15810367E-03	-0.15930305E-03	-0.16052116E-03	-0.78247329E-04	-0.78606053E-04	-0.78969458E-04
54	0.8812	-0.15924823E-03	-0.16044158E-03	-0.16165352E-03	-0.78848784E-04	-0.79182823E-04	-0.79521510E-04
55	0.8875	-0.16039350E-03	-0.16157833E-03	-0.16278163E-03	-0.79460151E-04	-0.79759632E-04	-0.80063729E-04
56	0.8937	-0.16153012E-03	-0.16270417E-03	-0.16389656E-03	-0.80080215E-04	-0.80336419E-04	-0.80597205E-04
57	0.9000	-0.16264439E-03	-0.16380789E-03	-0.16498960E-03	-0.80698390E-04	-0.80912909E-04	-0.81131979E-04
58	0.9062	-0.16371873E-03	-0.16487895E-03	-0.16605724E-03	-0.81285647E-04	-0.81488509E-04	-0.81695893E-04
59	0.9125	-0.16473688E-03	-0.16591480E-03	-0.16711066E-03	-0.81786008E-04	-0.82062202E-04	-0.82342879E-04
60	0.9187	-0.16569748E-03	-0.16693483E-03	-0.16818999E-03	-0.82115756E-04	-0.82632650E-04	-0.83153994E-04
61	0.9250	-0.16663840E-03	-0.16800074E-03	-0.16938076E-03	-0.82180347E-04	-0.83198652E-04	-0.84221373E-04
62	0.9312	-0.16767194E-03	-0.16923904E-03	-0.17082372E-03	-0.81926606E-04	-0.83760244E-04	-0.85598272E-04
63	0.9375	-0.16902138E-03	-0.17085266E-03	-0.17270145E-03	-0.81445068E-04	-0.84320541E-04	-0.87200390E-04
64	0.9437	-0.17103694E-03	-0.17309692E-03	-0.17517442E-03	-0.81131266E-04	-0.84888320E-04	-0.88649755E-04
65	0.9500	-0.17414726E-03	-0.17618188E-03	-0.17823413E-03	-0.81882263E-04	-0.85480629E-04	-0.89083402E-04
66	0.9562	-0.17868247E-03	-0.18005618E-03	-0.18144771E-03	-0.85248069E-04	-0.86123643E-04	-0.87003670E-04
67	0.9625	-0.18449451E-03	-0.18404011E-03	-0.18360373E-03	-0.93366335E-04	-0.86848702E-04	-0.80335571E-04
68	0.9687	-0.19032622E-03	-0.18632895E-03	-0.18234968E-03	-0.10839836E-03	-0.87678991E-04	-0.66964118E-04
69	0.9750	-0.19297563E-03	-0.18350527E-03	-0.17405236E-03	-0.13109664E-03	-0.88601844E-04	-0.46111406E-04
70	0.9812	-0.18650636E-03	-0.17039808E-03	-0.15430561E-03	-0.15816261E-03	-0.89523772E-04	-0.20888883E-04
71	0.9875	-0.16209376E-03	-0.14089664E-03	-0.11971200E-03	-0.17834257E-03	-0.90212221E-04	-0.20849964E-05
72	0.9937	-0.10954704E-03	-0.90595940E-04	-0.71651922E-04	-0.16795564E-03	-0.90241753E-04	-0.12529630E-04
73	1.0000	-0.38831540E-04	-0.21999229E-04	-0.51669174E-05	-0.15532616E-03	-0.87996916E-04	-0.20667669E-04

GASL
1 7 **PROB 3** 6/26/59

INPUT

CLASS 10 N=72 HARMONIC= 0. ANG= 0.1489E-00 A= 1.0000E-01 THICK.= 0.2000E-02 NU= 0.2500E-00

SPRING CONS

TAU 0. TAU 1, TAU 2 0. 0.90E 04 0. 0.90E 04 0. 0. 0.90E 04

1.0000E-02 ±0. 0.8333E-03

INPUT TEMP FOR LOCATION= 1.

1.0000E-02	1.0000E-02	1.0000E-02	1.0000E-02	1.0000E-02	1.0000E-02	1.0000E-02	1.0000E-02	1.0000E-02
1.0000E-02	1.0000E-02	1.0000E-02	1.0000E-02	1.0000E-02	1.0000E-02	1.0000E-02	1.0000E-02	1.0000E-02
1.0000E-02	1.0000E-02	1.0000E-02	1.0000E-02	1.0000E-02	1.0000E-02	1.0000E-02	1.0000E-02	1.0000E-02
1.0000E-02	1.0000E-02	1.0000E-02	1.0000E-02	1.0000E-02	1.0000E-02	1.0000E-02	1.0000E-02	1.0000E-02
1.0000E-02	1.0000E-02	1.0000E-02	1.0000E-02	1.0000E-02	1.0000E-02	1.0000E-02	1.0000E-02	1.0000E-02
1.0000E-02	1.0000E-02	1.0000E-02	1.0000E-02	1.0000E-02	1.0000E-02	1.0000E-02	1.0000E-02	1.0000E-02
1.0000E-02	1.0000E-02	1.0000E-02	1.0000E-02	1.0000E-02	1.0000E-02	1.0000E-02	1.0000E-02	1.0000E-02
1.0000E-02	1.0000E-02	1.0000E-02	1.0000E-02	1.0000E-02	1.0000E-02	1.0000E-02	1.0000E-02	1.0000E-02
1.0000E-02	1.0000E-02	1.0000E-02	1.0000E-02	1.0000E-02	1.0000E-02	1.0000E-02	1.0000E-02	1.0000E-02
1.0000E-02	1.0000E-02	1.0000E-02	1.0000E-02	1.0000E-02	1.0000E-02	1.0000E-02	1.0000E-02	1.0000E-02
1.0000E-02	1.0000E-02	1.0000E-02	1.0000E-02	1.0000E-02	1.0000E-02	1.0000E-02	1.0000E-02	1.0000E-02
1.0000E-02	1.0000E-02	1.0000E-02	1.0000E-02	1.0000E-02	1.0000E-02	1.0000E-02	1.0000E-02	1.0000E-02
1.0000E-02	1.0000E-02	1.0000E-02	1.0000E-02	1.0000E-02	1.0000E-02	1.0000E-02	1.0000E-02	1.0000E-02
1.0000E-02	1.0000E-02	1.0000E-02	1.0000E-02	1.0000E-02	1.0000E-02	1.0000E-02	1.0000E-02	1.0000E-02
1.0000E-02	1.0000E-02	1.0000E-02	1.0000E-02	1.0000E-02	1.0000E-02	1.0000E-02	1.0000E-02	1.0000E-02
1.0000E-02	1.0000E-02	1.0000E-02	1.0000E-02	1.0000E-02	1.0000E-02	1.0000E-02	1.0000E-02	1.0000E-02
1.0000E-02	1.0000E-02	1.0000E-02	1.0000E-02	1.0000E-02	1.0000E-02	1.0000E-02	1.0000E-02	1.0000E-02
1.0000E-02	1.0000E-02	1.0000E-02	1.0000E-02	1.0000E-02	1.0000E-02	1.0000E-02	1.0000E-02	1.0000E-02
1.0000E-02	1.0000E-02	1.0000E-02	1.0000E-02	1.0000E-02	1.0000E-02	1.0000E-02	1.0000E-02	1.0000E-02
1.0000E-02	1.0000E-02	1.0000E-02	1.0000E-02	1.0000E-02	1.0000E-02	1.0000E-02	1.0000E-02	1.0000E-02
1.0000E-02	1.0000E-02	1.0000E-02	1.0000E-02	1.0000E-02	1.0000E-02	1.0000E-02	1.0000E-02	1.0000E-02
1.0000E-02	1.0000E-02	1.0000E-02	1.0000E-02	1.0000E-02	1.0000E-02	1.0000E-02	1.0000E-02	1.0000E-02
1.0000E-02	1.0000E-02	1.0000E-02	1.0000E-02	1.0000E-02	1.0000E-02	1.0000E-02	1.0000E-02	1.0000E-02
1.0000E-02	1.0000E-02	1.0000E-02	1.0000E-02	1.0000E-02	1.0000E-02	1.0000E-02	1.0000E-02	1.0000E-02
1.0000E-02	1.0000E-02	1.0000E-02						

OUTPUTS   MISSILE AT LOCATION 1.   TIME= 0.

POS	Y	W	V
1	0.1000	-0.13569444E-02	-0.90456785E-02
2	0.1062	-0.13569444E-02	-0.89645563E-02
3	0.1125	-0.14807626E-02	-0.88934351E-02
4	0.1187	-0.15056817E-02	-0.88303696E-02
5	0.1250	-0.15045805E-02	-0.87681416E-02
6	0.1312	-0.15029245E-02	-0.87057162E-02
7	0.1375	-0.15025696E-02	-0.86432049E-02
8	0.1437	-0.15026146E-02	-0.85806652E-02
9	0.1500	-0.15026489E-02	-0.85181696E-02
10	0.1562	-0.15026607E-02	-0.84556565E-02
11	0.1625	-0.15026651E-02	-0.83931443E-02
12	0.1687	-0.15026685E-02	-0.83306327E-02
13	0.1750	-0.15026721E-02	-0.82681221E-02
14	0.1812	-0.15026756E-02	-0.82056118E-02
15	0.1875	-0.15026788E-02	-0.81431022E-02
16	0.1937	-0.15026817E-02	-0.80805930E-02
17	0.2000	-0.15026846E-02	-0.80180844E-02
18	0.2062	-0.15026870E-02	-0.79555760E-02
19	0.2125	-0.15026895E-02	-0.78930681E-02
20	0.2187	-0.15026917E-02	-0.78305605E-02
21	0.2250	-0.15026939E-02	-0.77680533E-02
22	0.2312	-0.15026959E-02	-0.77055463E-02
23	0.2375	-0.15026978E-02	-0.76430397E-02
24	0.2437	-0.15026996E-02	-0.75805335E-02
25	0.2500	-0.15027016E-02	-0.75180271E-02
26	0.2750	-0.15027067E-02	-0.72680041E-02
27	0.3000	-0.15027115E-02	-0.70179844E-02
28	0.3250	-0.15027156E-02	-0.67679673E-02
29	0.3500	-0.15027189E-02	-0.65179520E-02
30	0.3750	-0.15027216E-02	-0.62679385E-02
31	0.4000	-0.15027242E-02	-0.60179263E-02
32	0.4250	-0.15027265E-02	-0.57679151E-02
33	0.4500	-0.15027281E-02	-0.55179048E-02
34	0.4750	-0.15027297E-02	-0.52678955E-02
35	0.5000	-0.15027311E-02	-0.50178867E-02
36	0.5250	-0.15027323E-02	-0.47678787E-02
37	0.5500	-0.15027333E-02	-0.45178711E-02
38	0.5750	-0.15027342E-02	-0.42678639E-02
39	0.6000	-0.15027350E-02	-0.40178571E-02
40	0.6250	-0.15027358E-02	-0.37678508E-02
41	0.6500	-0.15027364E-02	-0.35178447E-02
42	0.6750	-0.15027370E-02	-0.32678389E-02
43	0.7000	-0.15027375E-02	-0.30178335E-02
44	0.7250	-0.15027379E-02	-0.27678281E-02
45	0.7500	-0.15027383E-02	-0.25178231E-02
46	0.7750	-0.15027387E-02	-0.22678182E-02
47	0.8000	-0.15027390E-02	-0.20178135E-02
48	0.8250	-0.15027381E-02	-0.17678090E-02
49	0.8500	-0.15027348E-02	-0.15178046E-02
50	0.8562	-0.15027443E-02	-0.14553035E-02

OUTPUTS MISSILE AT LOCATION 1. TIME= 0.

POS	Y	W	V
51	0.8625	-0.15027620E-02	-0.13928027E-02
52	0.8687	-0.15027910E-02	-0.13305020E-02
53	0.8750	-0.15028294E-02	-0.12676017E-02
54	0.8812	-0.15028050E-02	-0.12053019E-02
55	0.8875	-0.15028571E-02	-0.11428021E-02
56	0.8937	-0.15027493E-02	-0.10803017E-02
57	0.9000	-0.15024511E-02	-0.10177969E-02
58	0.9062	-0.15018730E-02	-0.95529123E-03
59	0.9125	-0.15009694E-02	-0.89277543E-03
60	0.9187	-0.14999030E-02	-0.83024930E-03
61	0.9250	-0.14993268E-02	-0.76771446E-03
62	0.9312	-0.15002033E-02	-0.70516164E-03
63	0.9375	-0.15044042E-02	-0.64267725E-03
64	0.9437	-0.15142539E-02	-0.58024932E-03
65	0.9500	-0.15317213E-02	-0.51796746E-03
66	0.9562	-0.15564594E-02	-0.45590777E-03
67	0.9625	-0.15824093E-02	-0.39410955E-03
68	0.9687	-0.15931037E-02	-0.33249155E-03
69	0.9750	-0.15566945E-02	-0.27072161E-03
70	0.9812	-0.14252333E-02	-0.20805935E-03
71	0.9875	-0.11598059E-02	-0.14525214E-03
72	0.9937	-0.65705224E-03	-0.74461455E-04
73	1.0000	0.	0.

OUTPUTS MISSILE AT LOCATION 1. TIME= 0.

POS	Y	SIGMA-11.1	SIGMA-11.2	SIGMA-11.3	SIGMA-22.1	SIGMA-22.2	SIGMA-22.3
1	0.1000	-0.12092116E-01	-0.96399950E-02	-0.71878732E-02	-0.63125654E-02	0.14400157E-02	0.11192597E-01
2	0.1062	-0.10153656E-01	-0.92666017E-02	-0.65640666E-02	-0.36243052E-02	-0.15774214E-03	0.33488206E-02
3	0.1125	-0.52339655E-03	-0.12046213E-02	-0.16636463E-02	0.31955167E-02	0.41616603E-03	-0.23629407E-02
4	0.1187	0.34872570E-03	0.17983524E-03	0.10944670E-04	0.79624005E-03	0.68436621E-04	-0.65936229E-03
5	0.1250	0.83211609E-04	0.92534614E-04	0.10185770E-03	0.76994766E-05	-0.45996657E-05	-0.16898648E-04
6	0.1312	-0.18373714E-04	0.34964176E-05	0.25366549E-04	-0.44494168E-04	-0.41909510E-05	0.36112498E-04
7	0.1375	-0.26481226E-04	-0.11943663E-04	0.25935005E-05	-0.13633631E-04	-0.50722156E-06	0.12619186E-04
8	0.1437	-0.21466266E-04	-0.99174213E-05	0.16315607E-05	-0.27837022E-05	0.34400728E-06	0.34737166E-05
9	0.1500	-0.18724589E-04	-0.78761950E-05	0.29720832E-05	-0.17661395E-05	0.33271499E-06	0.24535693E-05
10	0.1562	-0.17495243E-04	-0.69823582E-05	0.35305274E-05	-0.21526357E-05	0.27663364E-06	0.27063069E-05
11	0.1625	-0.16613281E-04	-0.64596662E-05	0.36955089E-05	-0.22362010E-05	0.27706847E-06	0.27923379E-05
12	0.1687	-0.15798025E-04	-0.60140155E-05	0.37699938E-05	-0.21723099E-05	0.27671922E-06	0.27258647E-05
13	0.1750	-0.15033758E-04	-0.56002755E-05	0.38336909E-05	-0.20790612E-05	0.27765054E-06	0.26345951E-05
14	0.1812	-0.14325138E-04	-0.52165496E-05	0.38661553E-05	-0.19897707E-05	0.28009526E-06	0.25498446E-05
15	0.1875	-0.13679615E-04	-0.48765214E-05	0.39264560E-05	-0.19121216E-05	0.28172506E-06	0.24755716E-05
16	0.1937	-0.13066130E-04	-0.45661581E-05	0.39936972E-05	-0.18409919E-05	0.28475166E-06	0.24104957E-05
17	0.2000	-0.12535718E-04	-0.42830361E-05	0.39695296E-05	-0.17647398E-05	0.29033961E-06	0.23455359E-05
18	0.2062	-0.12031523E-04	-0.40277373E-05	0.39760469E-05	-0.16998965E-05	0.29825605E-06	0.22966415E-05
19	0.2125	-0.11564115E-04	-0.37961872E-05	0.39717415E-05	-0.16433495E-05	0.29103830E-06	0.22204221E-05
20	0.2187	-0.11129770E-04	-0.35629143E-05	0.39638253E-05	-0.15919795E-05	0.29313376E-06	0.21763635E-05
21	0.2250	-0.10725015E-04	-0.33662069E-05	0.39503539E-05	-0.15447149E-05	0.28633169E-06	0.21175947E-05
22	0.2312	-0.10343501E-04	-0.32054956E-05	0.39325096E-05	-0.14995457E-05	0.28044451E-06	0.20602019E-05
23	0.2375	-0.99663182E-05	-0.30371595E-05	0.39141160E-05	-0.14521047E-05	0.28321754E-06	0.20225998E-05
24	0.2437	-0.96330420E-05	-0.28788345E-05	0.38934895E-05	-0.14054821E-05	0.29220246E-06	0.19900035E-05
25	0.2500	-0.93235867E-05	-0.27171330E-05	0.38690666E-05	-0.13330633E-05	0.32794156E-06	0.19694214E-05
26	0.2750	-0.82711922E-05	-0.22617705E-05	0.37337677E-05	-0.12139790E-05	0.28661452E-06	0.17873244E-05
27	0.3000	-0.74079726E-05	-0.19050205E-05	0.35976155E-05	-0.11145605E-05	0.25972258E-06	0.16341218E-05
28	0.3250	-0.67030778E-05	-0.16234116E-05	0.34362549E-05	-0.10262965E-05	0.24051405E-06	0.15094411E-05
29	0.3500	-0.61164610E-05	-0.13995450E-05	0.33172540E-05	-0.93297582E-06	0.22538006E-06	0.14038523E-05
30	0.3750	-0.56215794E-05	-0.12192176E-05	0.31632600E-05	-0.86059615E-06	0.21117739E-06	0.13109529E-05
31	0.4000	-0.51989916E-05	-0.10716030E-05	0.30596694E-05	-0.83097257E-06	0.20035077E-06	0.12316741E-05
32	0.4250	-0.48340296E-05	-0.94935695E-06	0.29350631E-05	-0.76056473E-06	0.17010022E-06	0.11606356E-05
33	0.4500	-0.45157503E-05	-0.84692147E-06	0.28217909E-05	-0.73609408E-06	0.15679299E-06	0.10977[illegible]E-05
34	0.4750	-0.42351694E-05	-0.75949536E-06	0.27159695E-05	-0.69604721E-06	0.17241109E-06	0.10406694E-05
35	0.5000	-0.39878068E-05	-0.68560266E-06	0.26160851E-05	-0.66112261E-06	0.16402519E-06	0.98918099E-06
36	0.5250	-0.37671996E-05	-0.62258714E-06	0.25221579E-05	-0.62017052E-06	0.15774276E-06	0.94377701E-06
37	0.5500	-0.35685953E-05	-0.56662620E-06	0.24349429E-05	-0.59709419E-06	0.15320255E-06	0.90320640E-06
38	0.5750	-0.33898977E-05	-0.51665026E-06	0.23525208E-05	-0.56880526E-06	0.14577676E-06	0.86653566E-06
39	0.6000	-0.32274984E-05	-0.47602225E-06	0.22755703E-05	-0.54389230E-06	0.14368934E-06	0.83155464E-06
40	0.6250	-0.30801166E-05	-0.43676935E-06	0.22028107E-05	-0.52107498E-06	0.13911031E-06	0.79950750E-06
41	0.6500	-0.29456569E-05	-0.40582381E-06	0.21342421E-05	-0.49977098E-06	0.13515819E-06	0.77008735E-06
42	0.6750	-0.28221402E-05	-0.37825432E-06	0.20696316E-05	-0.48102811E-06	0.13026675E-06	0.74156560E-06
43	0.7000	-0.27085189E-05	-0.35006087E-06	0.20086300E-05	-0.46147034E-06	0.12817327E-06	0.71761087E-06
44	0.7250	-0.26029501E-05	-0.32564649E-06	0.19514700E-05	-0.44577521E-06	0.12549372E-06	0.69463023E-06
45	0.7500	-0.25057234E-05	-0.30494240E-06	0.18978754E-05	-0.42675763E-06	0.12155760E-06	0.67171041E-06
46	0.7750	-0.24156179E-05	-0.28533395E-06	0.18449500E-05	-0.41365047E-06	0.11862721E-06	0.65122731E-06
47	0.8000	-0.23309840E-05	-0.26775524E-06	0.17994753E-05	-0.39732349E-06	0.11604615E-06	0.63073821E-06
48	0.8250	-0.22603199E-05	-0.26018824E-06	0.17397106E-05	-0.38160942E-06	0.11431962E-06	0.61013270E-06
49	0.8500	-0.22510067E-05	-0.27322676E-06	0.17042059E-05	-0.51315874E-06	0.11590494E-06	0.74028533E-06
50	0.8562	-0.21636022E-05	-0.19776963E-06	0.17879065E-05	-0.60673666E-06	0.10558870E-06	0.81816688E-06

OUTPUTS MISSILE AT LOCATION 1. TIME= 0.

POS	Y	SIGMA-11,1	SIGMA-11,2	SIGMA-11,3	SIGMA-22,1	SIGMA-22,2	SIGMA-22,3
51	0.8625	-0.20521693E-05	-0.57974830E-07	0.15362196E-05	-0.69173984E-06	0.10660927E-06	0.90536196E-06
52	0.8687	-0.17974526E-05	0.16822014E-06	0.21537764E-05	-0.62247273E-06	0.11327211E-06	0.64913330E-06
53	0.8750	-0.13905810E-05	0.46298373E-06	0.23166649E-05	-0.21175947E-06	0.12642704E-06	0.46484638E-06
54	0.8812	-0.87625813E-06	0.71991235E-06	0.23159664E-05	0.79150777E-06	0.14994293E-06	-0.49162190E-06
55	0.8875	-0.46403147E-06	0.67916699E-06	0.16223634E-05	0.25676796E-05	0.18405262E-06	-0.22194581E-05
56	0.8937	-0.62747858E-06	-0.11639438E-06	0.59045699E-06	0.51163160E-05	0.22677705E-06	-0.46648783E-05
57	0.9000	-0.21798769E-05	-0.23142201E-05	-0.24480799E-05	0.76757276E-05	0.26042107E-06	-0.71548857E-05
58	0.9062	-0.62198378E-05	-0.65404992E-05	-0.66735934E-05	0.83774794E-05	0.24260953E-06	-0.78923767E-05
59	0.9125	-0.13774144E-04	-0.12971810E-04	-0.12169475E-04	0.36780257E-05	0.11071097E-06	-0.34566037E-05
60	0.9187	-0.24937326E-04	-0.20384672E-04	-0.15832251E-04	-0.11701486E-04	-0.21746382E-06	0.11266442E-04
61	0.9250	-0.37319958E-04	-0.24929991E-04	-0.12539909E-04	-0.43702312E-04	-0.82002953E-06	0.42062253E-04
62	0.9312	-0.43841311E-04	-0.18685939E-04	0.64696651E-05	-0.95680123E-04	-0.16951235E-05	0.92289992E-04
63	0.9375	-0.50413153E-04	0.11071563E-04	0.52556396E-04	-0.16197434E-03	-0.26462366E-05	0.15668175E-03
64	0.9437	0.25045709E-04	0.80371741E-04	0.13569766E-03	-0.21761959E-03	-0.31256678E-05	0.21156785E-03
65	0.9500	0.14954817E-03	0.20244321E-03	0.25533615E-03	-0.20700262E-03	-0.20654406E-05	0.20287186E-03
66	0.9562	0.36386190E-03	0.37417129E-03	0.38448092E-03	-0.32554495E-04	0.21778978E-05	0.36710174E-04
67	0.9625	0.65855507E-03	0.55309199E-03	0.44762902E-03	0.44019601E-03	0.11570868E-04	-0.41705416E-03
68	0.9687	0.95421821E-03	0.62622385E-03	0.29822939E-03	0.13463285E-02	0.27575413E-04	-0.12911776E-02
69	0.9750	0.10487942E-02	0.37939590E-03	-0.29000244E-03	0.27335821E-02	0.49409922E-04	-0.26347624E-02
70	0.9812	0.56787545E-03	-0.51175942E-03	-0.15913944E-02	0.43957561E-02	0.71232440E-04	-0.42532910E-02
71	0.9875	-0.10448460E-02	-0.24310566E-02	-0.38172676E-02	0.56280803E-02	0.78482088E-04	-0.54711162E-02
72	0.9937	-0.44313754E-02	-0.56562235E-02	-0.68810716E-02	0.49466320E-02	0.44516055E-04	-0.48576002E-02
73	1.0000	-0.89695318E-02	-0.10033201E-01	-0.11096872E-01	0.41218723E-02	-0.13280764E-03	-0.43874876E-02

REFERENCE

1. Love, A. E. H., Mathematical Theory of Elasticity,

Dover Publications, 4th Edition.

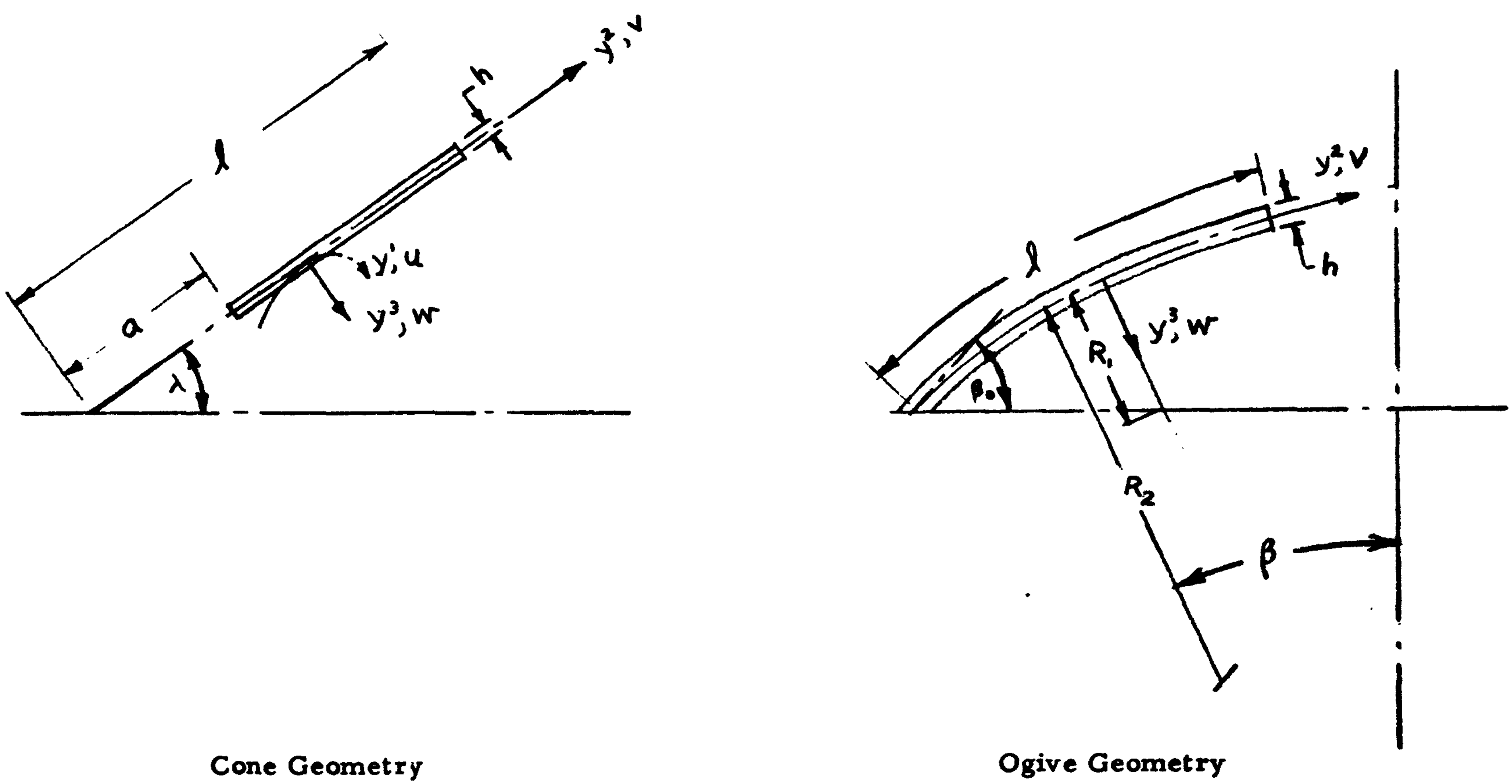

Figure 1. Shell Geometries for the Cone and Ogive Digital Programs

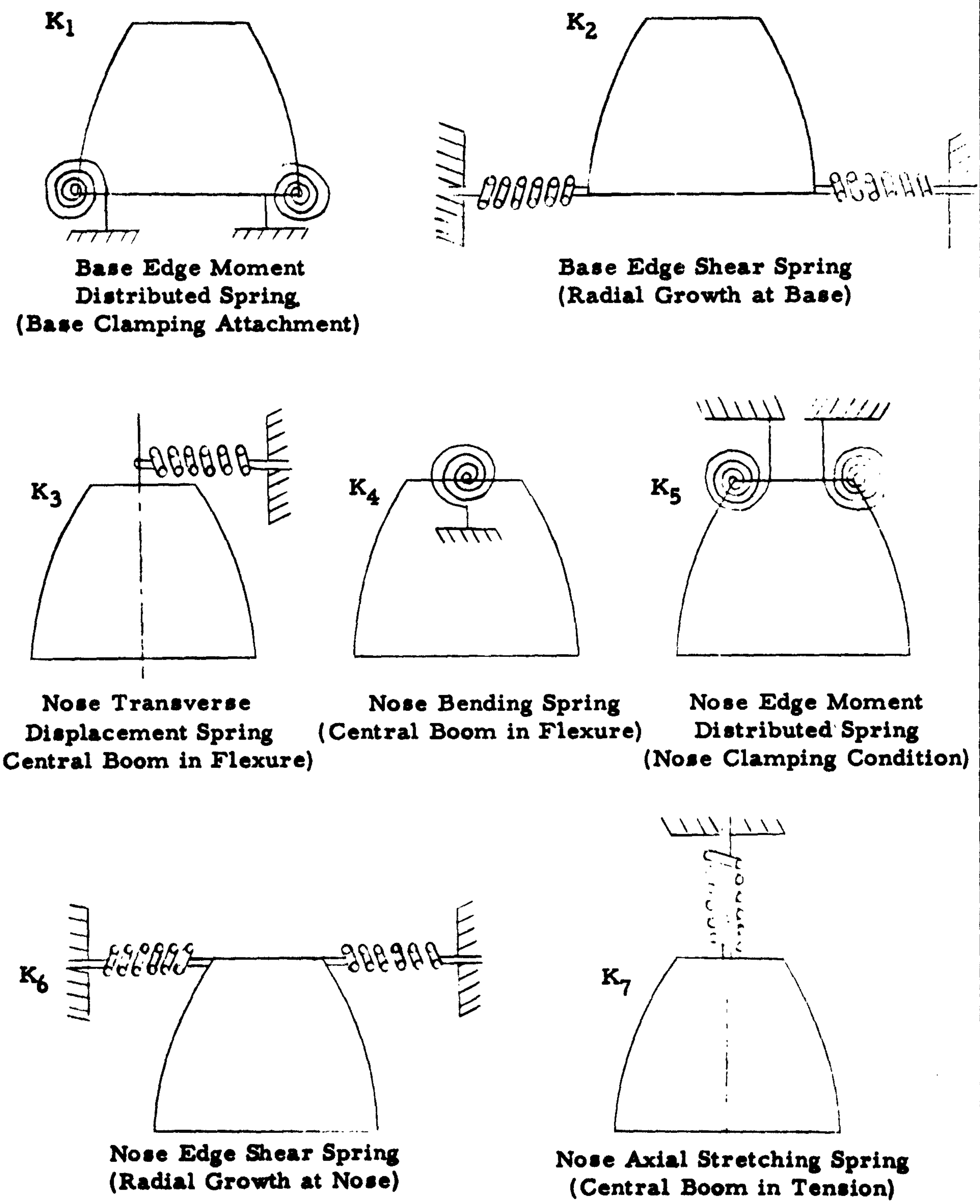

FIG. 2 - SPRING RESTRAINT SCHEME FOR BOUNDARY CONDITIONS

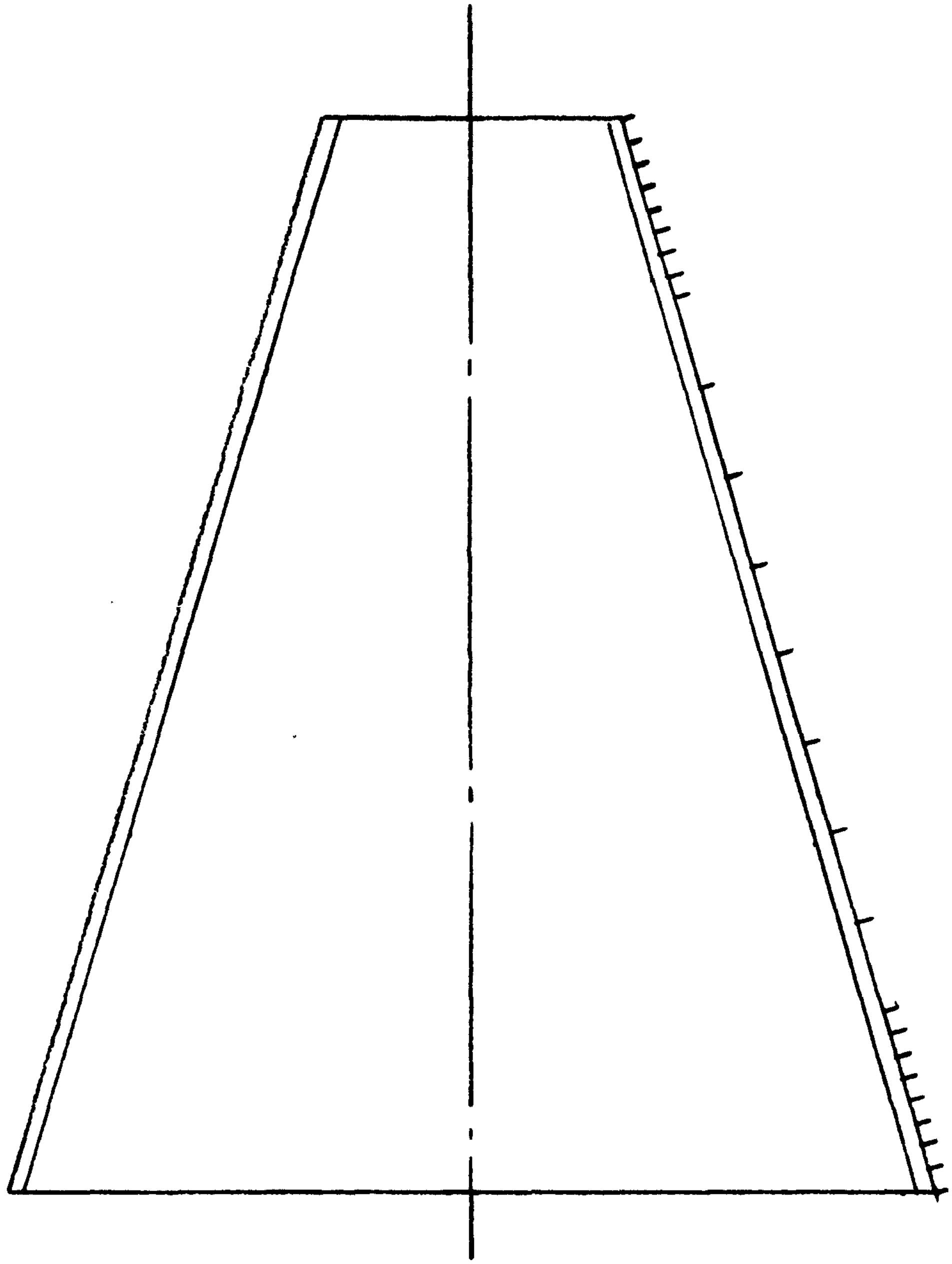

Figure 3. Spacing of Mesh Points Along the Generator of the Cone for n = 24.

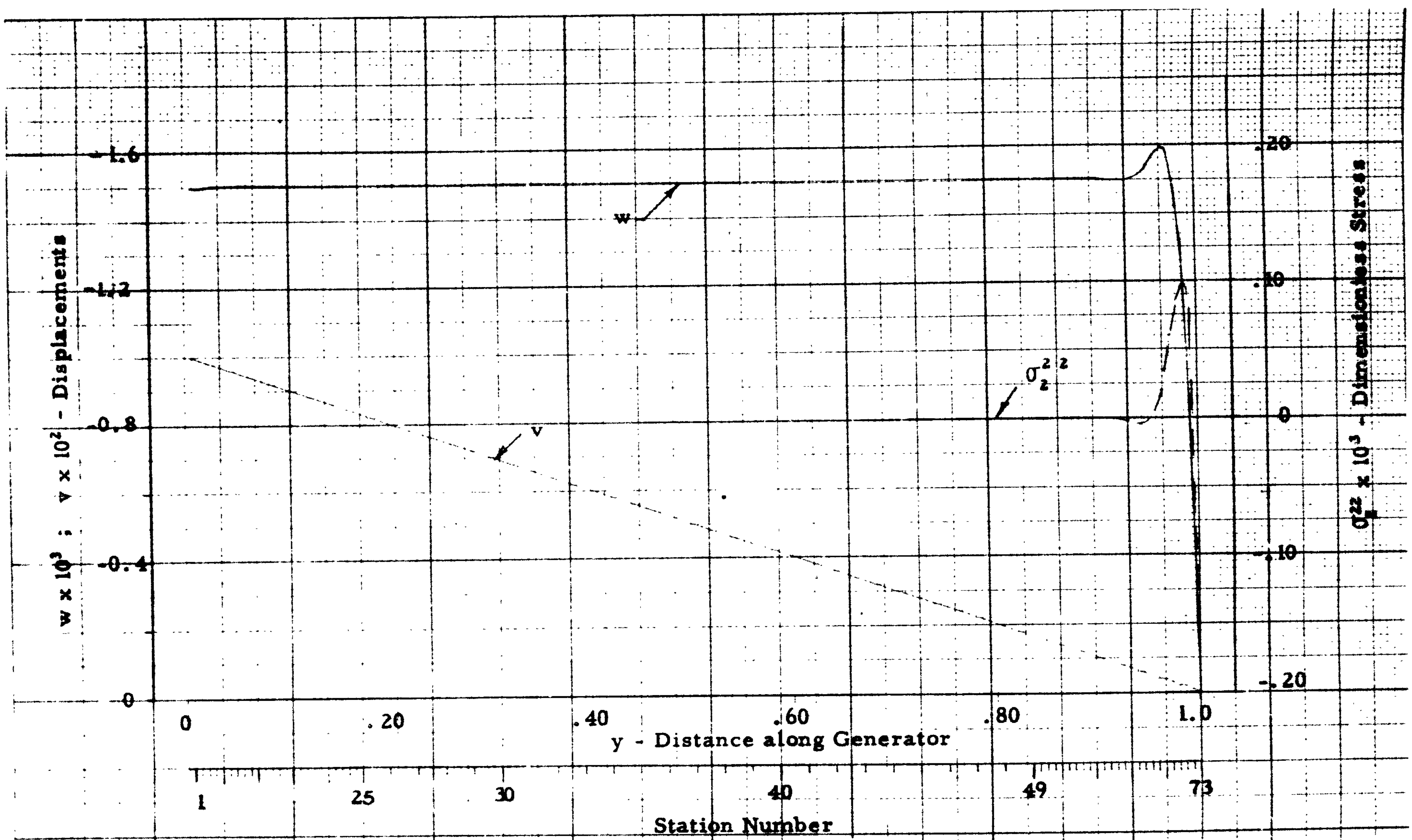

Figure 4. Displacements and Stress Vs. Station for Problem 1;
The Closed Cone With Thermal Loading; $K_1 = 0$; $K_2 = \infty$; $\alpha = 10^{-5}$; $\delta = .0276$

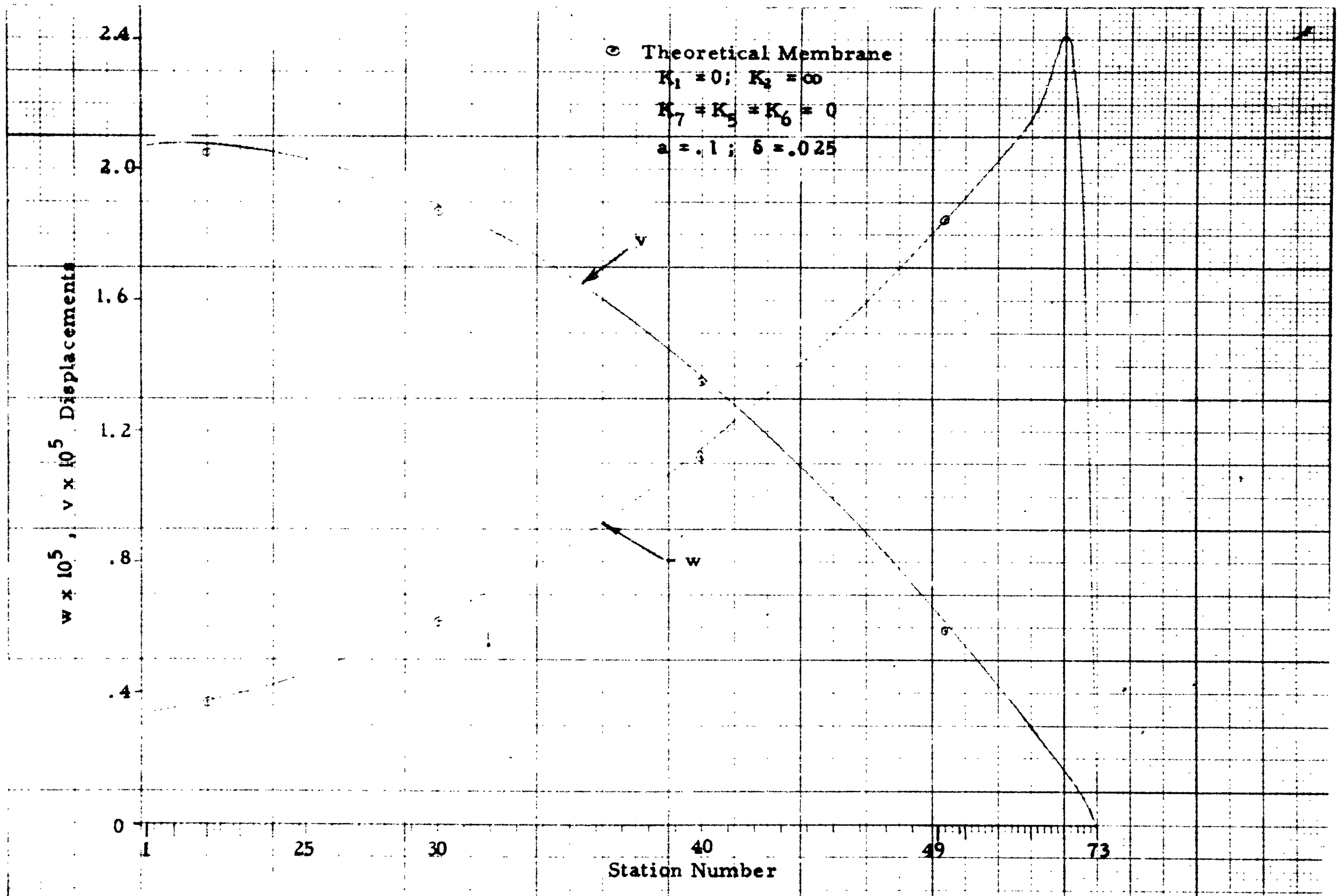

Figure 5. Displacements Vs. Station Number for Problem 2; Uniform Pressure Loading.

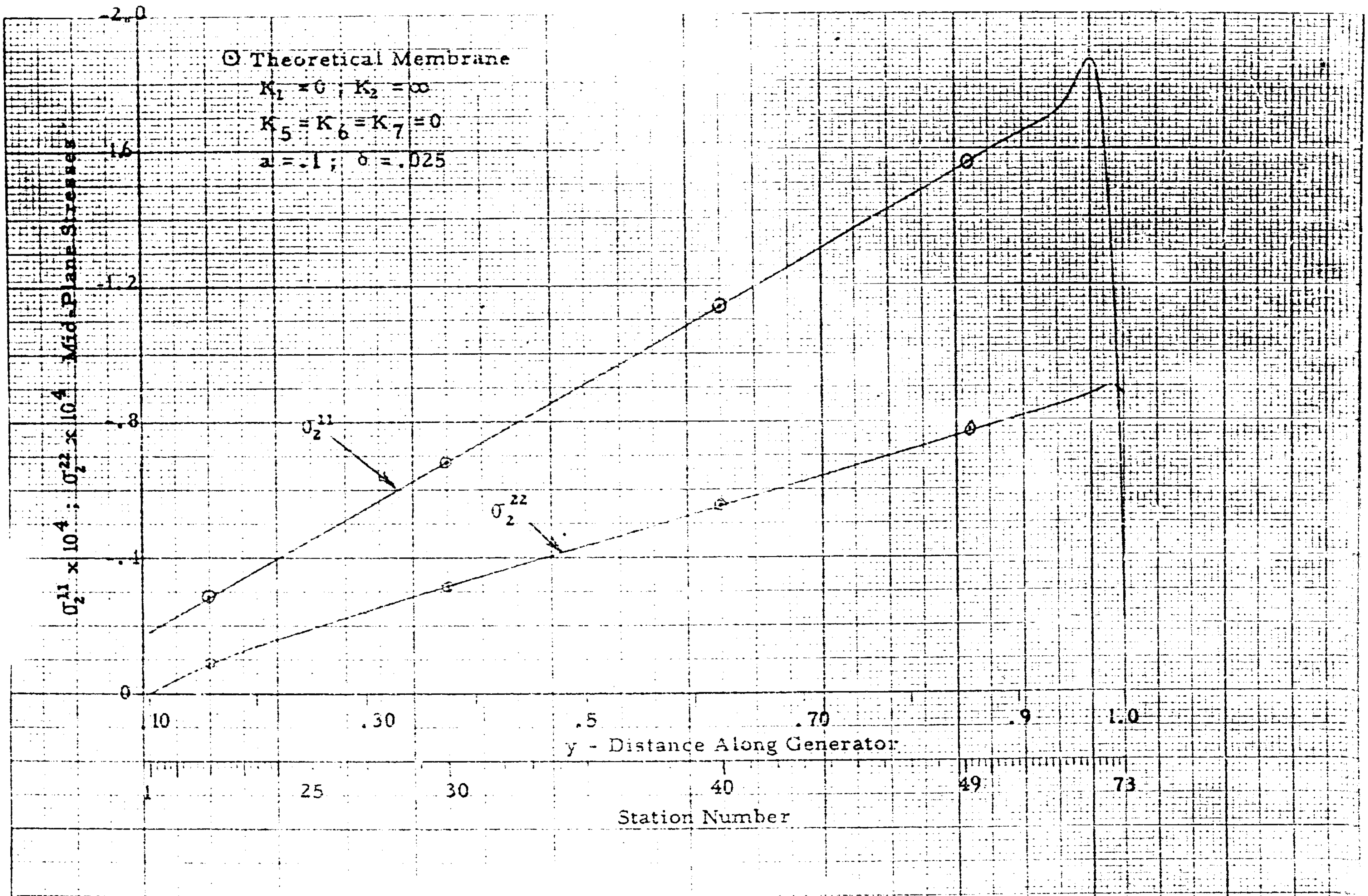

Figure 6. Mid-Plane Stresses Vs. Distance Along Generator for Problem 2; Uniform Pressure Loading.

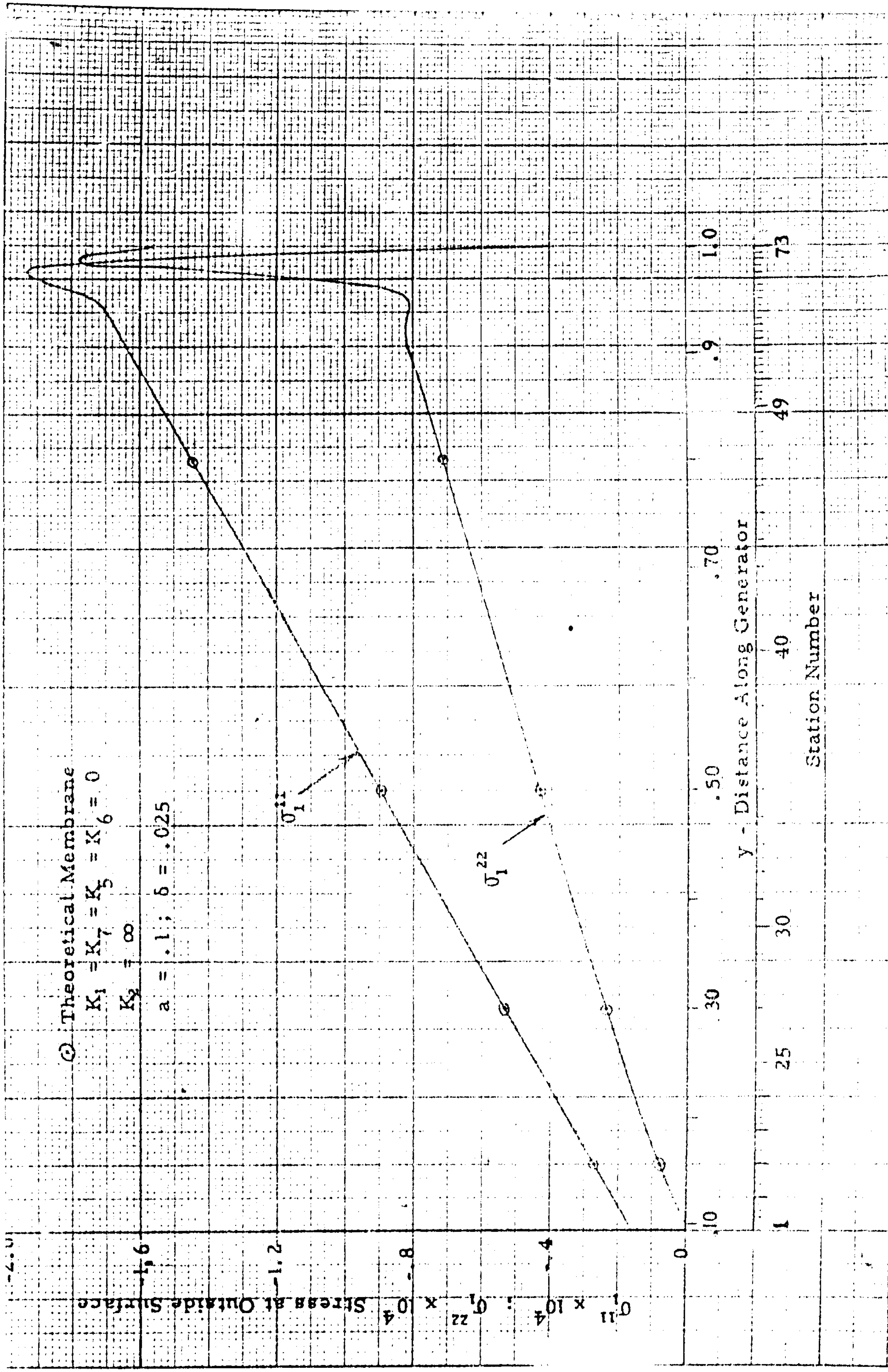

Figure 7. Stress Vs. Distance Along the Generator for Problem 2; Uniform Pressure Loading

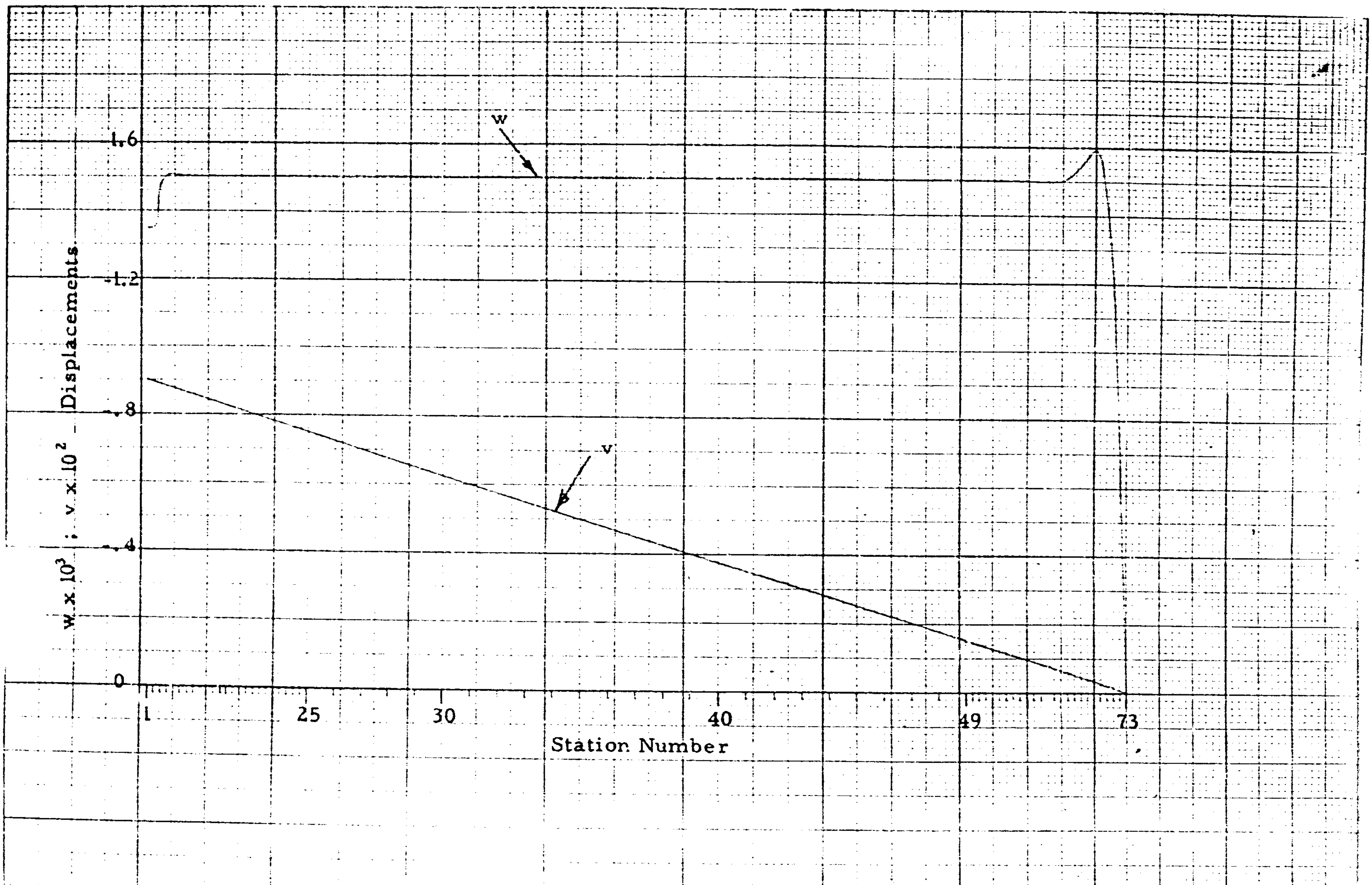

Figure 8. Mid-Plane Displacements Vs. Station Number for Problem 3; Truncated Cone With Thermal Loading; $K_2 = K_5 = K_6 = \infty$; $K_1 = 0$; $a = .1$; $\delta = .025$; $\alpha = 10^{-5}$

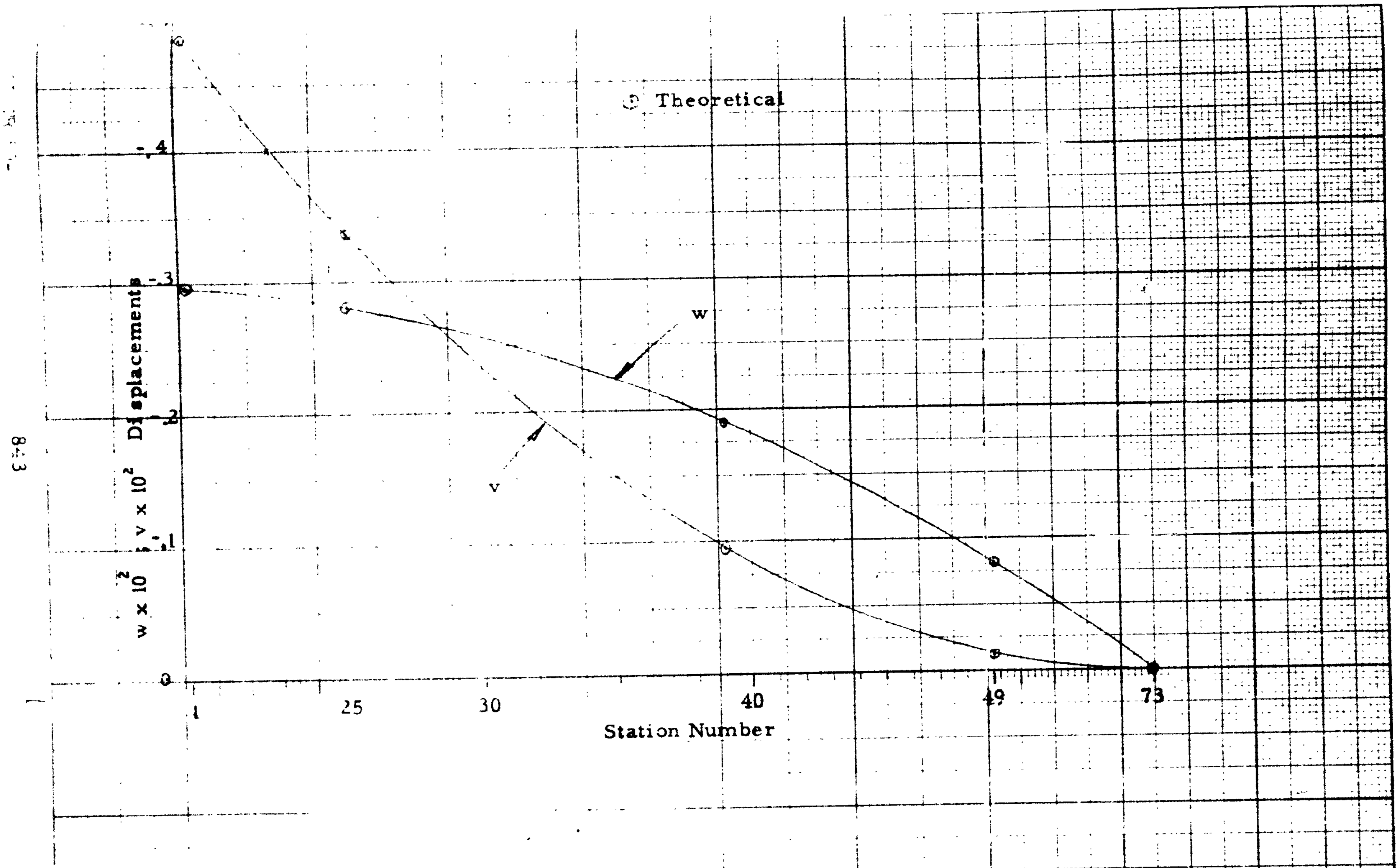

Figure 9. Mid-Plane Displacements Vs. Station Number for Problem 4; Truncated Cone With a Linear Temperature Distribution; $K_5 = K_6 = K_7 = K_1 = 0$; $K_2 = \infty$; $a = .1$; $\delta = .025$; $\alpha = 12 \times 10^{-}$

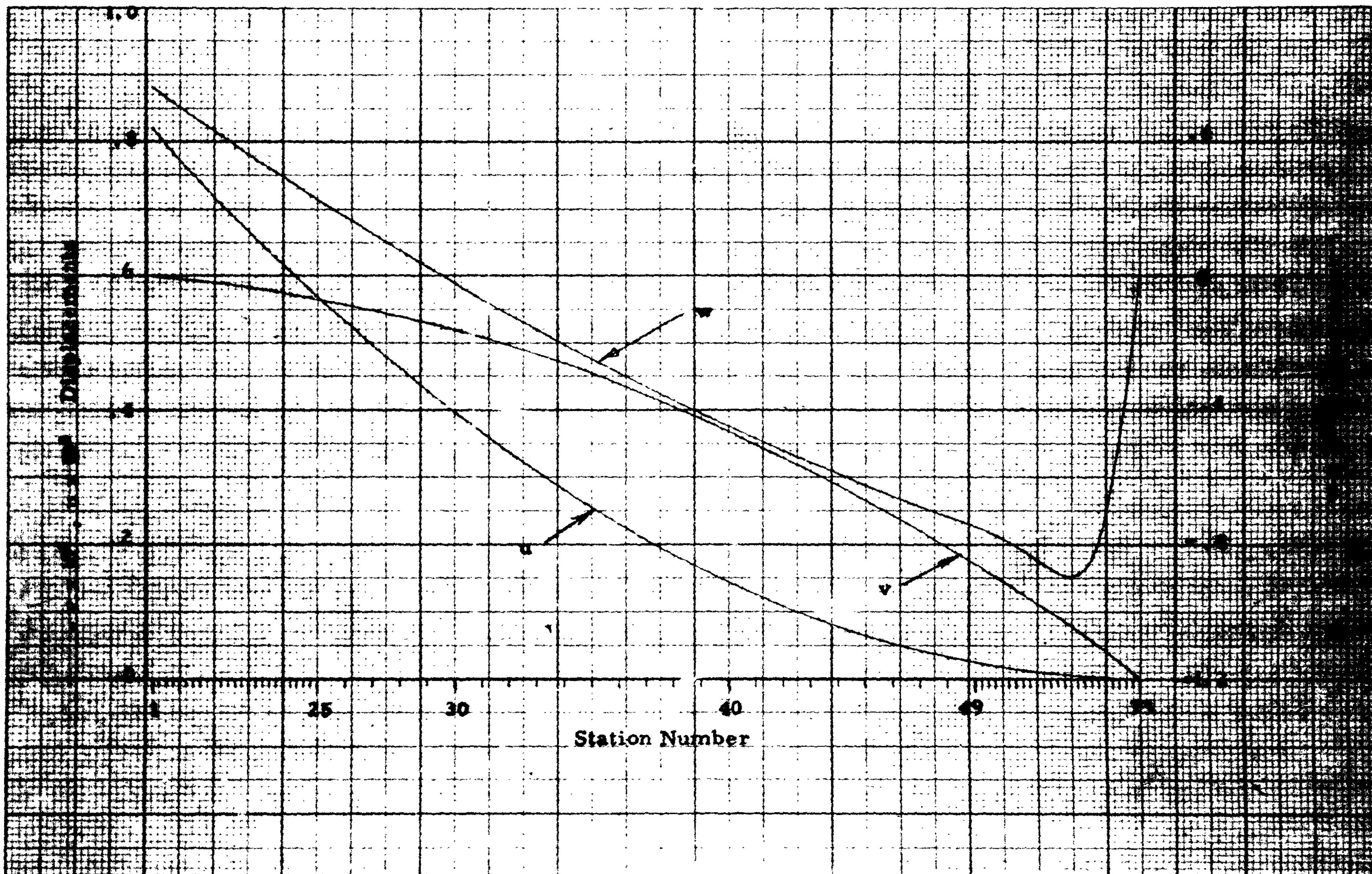

Figure 10. Displacements Vs. Station Number for Problem 5; Truncated Cone With Linear Temperature Distribution and $m = 1$, $K_1 = K_3 = K_4 = 0$; $K_2 = \infty$; $a = .1$; $\delta = .025$; $\alpha = 12 \times 10^{-6}$

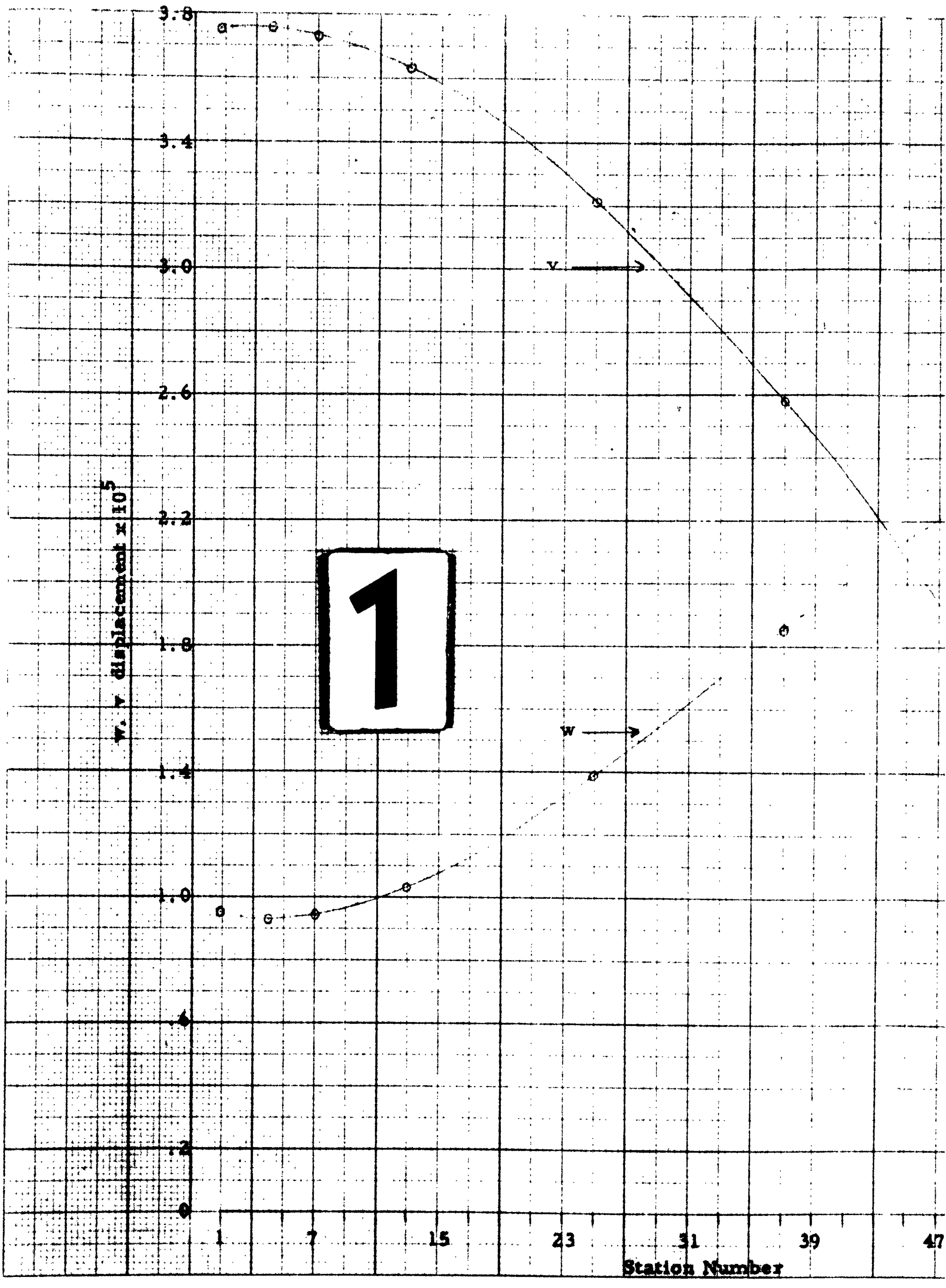
3.8
3.4
3.0
2.6
2.2
1.8
1.4
1.0
.6
.2
0
1
7
15
23
31
39
47
v
w
1
w, v displacement x 10^5
Station Number

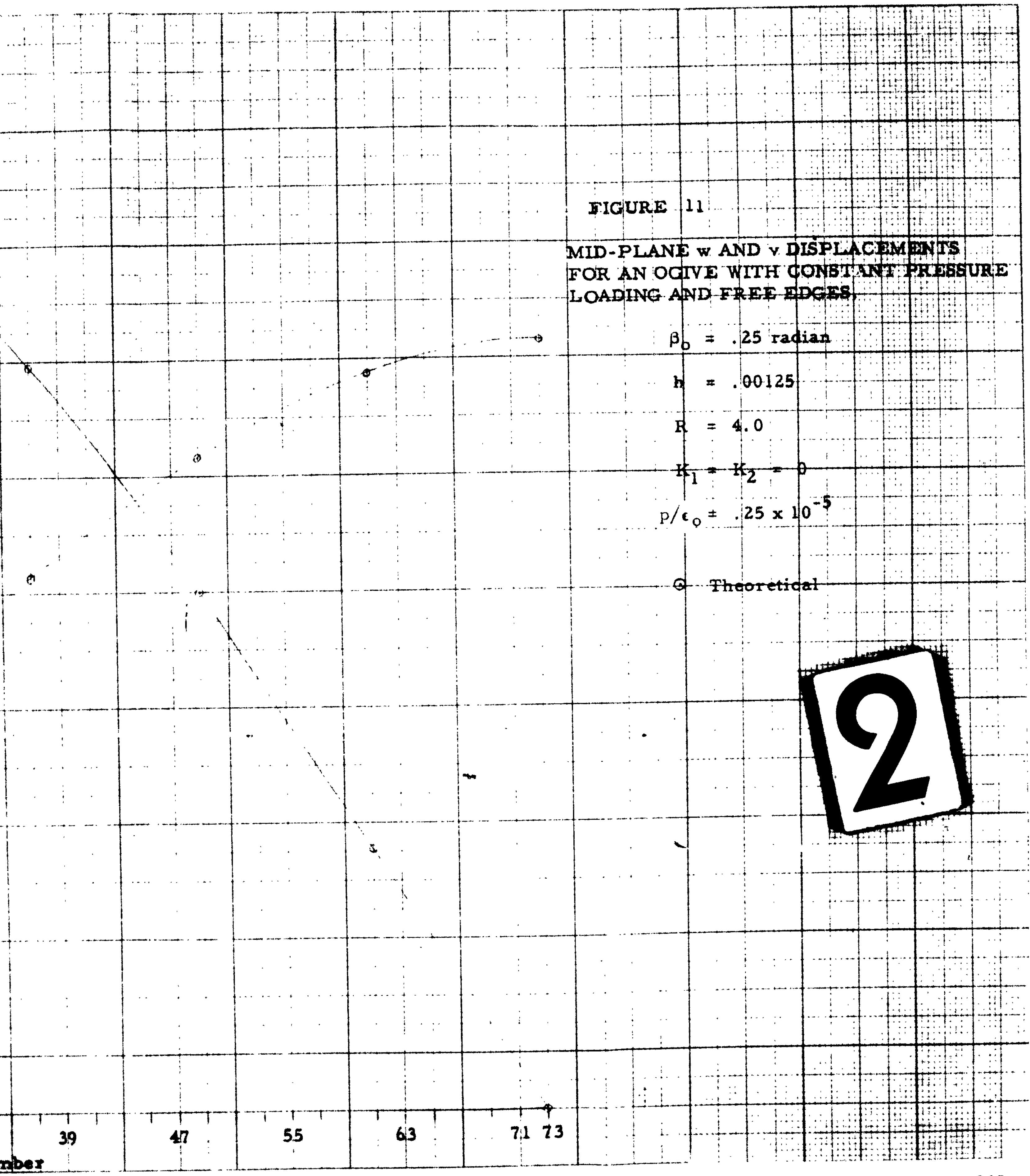

FIGURE 11

MID-PLANE w AND v DISPLACEMENTS FOR AN OGIVE WITH CONSTANT PRESSURE LOADING AND FREE EDGES.

CHAPTER IV - PART E

ANALYSIS OF SANDWICH SHELLS

by Frank Lane

ANALYSIS OF SANDWICH SHELLS

TABLE OF CONTENTS

LIST OF SYMBOLS

p	pressure
ϵ	Young's modulus of face material
α	thermal expansion coefficient of face material
ν	Poisson's ratio of face material
ϵ_c	Young's modulus of core material
α_c	thermal expansion coefficient of core material
ν_c	Poisson's ratio of core material
τ^{ij}	stress tensor
η_{ij}	strain tensor
ξ^i	displacement vector (tensor quantity)
a_{ij}, a^{ij}	metric tensor (covariant, contravariant)
u^i	physical displacements
σ^{ij}	physical stresses
h_c	core thickness
h_-	outer face thickness
h_+	inner face thickness
ΔT	temperature relative to a datum level
J	volume element or Jacobian
$\tilde{\tilde{J}}$	value of J at $y^3 = 0$ (= surface area element on shell mid-surface)
F	free energy
W	virtual work

$y^1\ y^2\ y^3$	curvilinear shell coordinates, y^1 = circumferential, y^2 = meridional, y^3 = normal, inward
θ	alternate symbol for y^1 = longitude angle
$i\,j\,k$	indices ranging over 1, 2, 3
$\alpha\,\beta\,\gamma\,\delta$	indices ranging over 1, 2
$(\ )$	(no subscript) pertaining to face material
$(\ )_c$	pertaining to core material
$(\ )_\pm$	pertaining to (inner/outer) face shell
$_m(\ )$	pertaining to mth Fourier coefficient

1. INTRODUCTION AND PRESENTATION OF SANDWICH SHELL ASSUMPTIONS

Following is an extension of the analysis of homogeneous shells described in Part A of Chapter IV to shells of sandwich type construction. The geometry considered is that of Figure 1; i.e., a shell of revolution with core material of thickness h_c and with an outer face-shell of thickness h_- and an inner face-shell of thickness h_+. The coordinate system $y^1\ y^2\ y^3$ is the same as that used in the homogeneous shell analysis.

In accordance with the accepted practice for shell theory and for sandwich construction, the following assumptions are made. First, in the face plates

$$\tau^{33} = \text{small of high order} \tag{1}$$

$$\eta_{\alpha 3} = \text{small of high order .} \tag{2}$$

In the core, infinite rigidity is assumed in the normal direction

$$\text{i.e.,} \quad \eta_{33} = 0 \tag{3}$$

and

$$\tau^{33} = \text{small of high order .} \tag{4}$$

Zero rigidity is assumed in the tangential directions;

$$\text{i.e.,} \quad \tau^{11} = \tau^{12} = \tau^{22} = 0 \tag{5}$$

and the only core stresses of importance are $\tau^{\alpha 3}$, $\alpha = 1,\ 2$.

In accordance with the usual assumptions of sandwich theory, the face shells are assumed to be thin in comparison with the core and, therefore, all terms depending on the cube of the face thicknesses, h_+^3 or h_-^3, are neglected.

2. FORMULATION OF THERMOELASTIC PROBLEMS BY MEANS OF FREE ENERGY

Assumptions (1) and (2) for the face shells imply that the same shell stress-strain law applies to the face-shells as to homogeneous shells. For the tangential stresses, this law is as follows:

$$T^{\alpha\beta} = \frac{\epsilon}{1+\nu}\left(a^{\alpha\delta}a^{\beta\gamma} + \frac{\nu}{1-\nu}a^{\alpha\beta}a^{\delta\gamma}\right)\eta_{\gamma\delta} - \frac{\epsilon\,a\,a^{\alpha\beta}}{1-\nu}\Delta T \; . \qquad (6)$$

$$\alpha,\beta = 1,\ 2$$

This is simply Duhamel's thermal stress-strain law generalized to curvilinear coordinates and then specialized to incorporate the vanishing of T^{33}. In the core, we must revert to the more general relation giving T^{ij} and then specialize to $T^{\alpha 3}$ since these shear stresses are the only core stresses of importance in the analysis.

$$T^{\alpha 3} = \frac{\epsilon_c}{1+\nu_c}\left(a^{\alpha\beta}\right)\eta_{\beta 3} \qquad (7)$$

where use has been made of the geometric relations derived in the homogeneous shell theory section of Part A of this chapter:

$$a^{33} = a_{33} = 1 \qquad (8)$$

$$a^{\alpha 3} = a_{\alpha 3} = 0 \qquad \alpha = 1,\ 2. \qquad (9)$$

Now the thermoelastic problem for sandwich shells, as for the case of homogeneous shells, is formulated through the use of the so-called free energy, F.

This free energy may be defined in general as

$$F = \frac{1}{2}\iiint J\, dy^1\, dy^2\, dy^3 \left(T^{ij}\eta_{ij} - \frac{\epsilon\, a\, \Delta T}{1-2\nu}\, a^{ij}\, \eta_{ij} \right) . \tag{10}$$

In the present context, no consideration need be given to the physical nature of this quantity. Rather, F may be thought of as the integral, the vanishing of whose first variation with respect to displacements leads to the proper equilibrium equations and natural boundary conditions for the thermoelastic problem. Now from the assumed vanishing of T^{33} it follows from the general thermal stress-strain law that

$$0 = \frac{\epsilon}{1+\nu}\left(\eta_{33} + \frac{\nu}{1-2\nu}\left[a^{\alpha\beta}\eta_{\alpha\beta} + \eta_{33} \right] \right) - \frac{\epsilon\, a\, \Delta T}{1-2\nu} . \tag{11}$$

This may be solved for η_{33} to give:

$$\eta_{33}\left(\frac{1-\nu}{1-2\nu}\right) + \frac{\nu a^{\alpha\beta}}{1-2\nu}\,\eta_{\alpha\beta} = \frac{(1+\nu)}{1-2\nu}\, a\Delta T$$

(12)

or

$$\eta_{33} = \frac{-\nu}{1-\nu}\, a^{\alpha\beta}\eta_{\alpha\beta} + \left(\frac{1+\nu}{1-\nu}\right) a\Delta T .$$

Substituting this into the integrand of (10) and eliminating the contribution of τ^{33}, the integrand of the free energy, F, becomes:

$$J\left\{\tau^{ij}\,\eta_{ij} - \frac{\epsilon\,\alpha\Delta T}{1-2\nu}\,a^{ij}\,\eta_{ij}\right\} = J\left\{\tau^{\alpha\beta}\eta_{\alpha\beta} + \tau^{\alpha 3}\,\eta_{\alpha 3}\right. \tag{13}$$

$$\left. - \frac{\epsilon\,\alpha\Delta T}{1-2\nu}\left[a^{\alpha\beta}\,\eta_{\alpha\beta} - \frac{\nu}{1-\nu}\,a^{\alpha\beta}\eta_{\alpha\beta} + \frac{1+\nu}{1-\nu}\,\alpha\Delta T\right]\right\} .$$

The term involving $(\Delta T)^2$ makes no contribution to the variation operation and, hence, is dropped. The remainder of the right-hand side of (13) reduces to:

$$\tau^{\alpha\beta}\eta_{\alpha\beta} + \tau^{\alpha 3}\,\eta_{\alpha 3} - \frac{\epsilon\,\alpha\Delta T}{1-\nu}\,a^{\alpha\beta}\,\eta_{\alpha\beta} \,. \tag{14}$$

Thus, the free energy expression, subject only to the restriction that $\tau^{33} = 0$, is given by:

$$F = \frac{1}{2}\iiint J\,dy^1\,dy^2\,dy^3\left(\tau^{\alpha\beta}\eta_{\alpha\beta} + \tau^{\alpha 3}\,\eta_{\alpha 3} - \frac{\epsilon\,\alpha\Delta T}{1-\nu}\,a^{\alpha\beta}\,\eta_{\alpha\beta}\right) . \tag{15}$$

Now the contribution of the two face-shells to F is clear. Recognizing the insignificance of $\tau^{\alpha 3}$ in the face-shells, this contribution becomes:

$$F_{\text{face shells}} = F_{(+)} + F_{(-)} = \frac{1}{2}\iiint_{\text{face shells' volume}} J\,dy^1dy^2dy^3\left(\tau^{\alpha\beta}\,\eta_{\alpha\beta} - \frac{\epsilon\,\alpha\Delta T}{1-\nu}\,a^{\alpha\beta}\,\eta_{\alpha\beta}\right)$$

$$= \iiint_{\text{face shells' volume}} J\,dy^1dy^2dy^3\left(\frac{\epsilon}{2(1+\nu)}\left(a^{\alpha\delta}a^{\beta\gamma} + \frac{\nu}{1-\nu}\,a^{\alpha\beta}a^{\gamma\delta}\right)\eta_{\alpha\beta}\eta_{\gamma\delta} - \frac{\epsilon\,\alpha\Delta T}{1-\nu}\,a^{\alpha\beta}\eta_{\alpha\beta}\right) . \tag{16}$$

For the core, the term $\tau^{\alpha\beta}\eta_{\alpha\beta}$ drops out of the integrand of (15) due to the assumed insignificance of core in-plane stresses $\tau^{\alpha\beta}$. However, it is necessary to evaluate the core in-plane strains $\eta_{\alpha\beta}$ which enter the thermal term in (15). This is done as follows: First, since τ^{33} is assumed insignificant in the core, the thermal stress-strain law for the core in-plane stresses is the same as for the face shells (6) but with core properties ϵ_c , ν_c replacing ϵ, ν . Thus, the vanishing of $\tau^{\alpha\beta}$ in the core implies:

$$0 = \frac{\epsilon_c}{1+\nu_c}\left(a^{\alpha\delta}a^{\beta\gamma} + \frac{\nu_c}{1-\nu_c}\; a^{\alpha\beta}a^{\delta\gamma}\right)\eta_{\gamma\delta} - \frac{\epsilon_c\,\alpha_c\, a^{\alpha\beta}\,\Delta T}{1-\nu_c} \quad . \tag{17}$$

We require, for F, the expression for $a^{\alpha\beta}\eta_{\alpha\beta}$. This is found by multiplying (17) through by $a_{\alpha\beta}$, contracting on α and recalling that the metric tensors are symmetric and that the contravariant and covariant forms of the metric tensors are inverses of each other; i.e.,

$$a_{\alpha\beta}a^{\beta\gamma} = \delta^{\gamma}_{\beta} \begin{cases} = 0 & \gamma \neq \beta \\ = 1 & \gamma = \beta \end{cases} \quad . \tag{18}$$

Performing this multiplication and contraction we find (noting that $\delta^{\beta}_{\beta} = 2$ since we are effectively in 2-space when summing over Greek indices)

$$\frac{2\,\alpha_c\,\Delta T}{1-\nu_c} = \frac{1}{1+\nu_c}\left(a^{\delta\gamma} + \frac{2\nu_c}{1-\nu_c}\; a^{\delta\gamma}\right)\eta_{\gamma\delta} = \frac{1}{1-\nu_c}\; a^{\alpha\beta}\,\eta_{\alpha\beta} \quad . \tag{19}$$

Thus, we have the required expression $a^{\alpha\beta}\,\eta_{\alpha\beta}$ for the core.

Now this together with (7) is introduced into expression (15) to get the core contribution to F.

$$F_{core} = \frac{1}{2}\iiint_{core} J\,dy^1\,dy^2\,dy^3\left(\frac{\epsilon_c}{1+\nu_c}\,a^{\alpha\beta}\,\eta_{\beta 3}\,\eta_{\alpha 3} - \frac{2\epsilon(a_c\Delta T)^2}{1-\nu_c}\right)$$

$$\underset{(effective)}{F_{core}} = \iiint_{core} J\,dy^1 dy^2\,dy^3\left(\frac{\epsilon_c}{2(1+\nu_c)}\,a^{\alpha\beta}\,\eta_{\alpha 3}\,\eta_{\beta 3}\right) \tag{20}$$

where the $(a_c\Delta T)^2$ term is dropped since it makes no contribution in the process of forming a first variation with respect to the displacements.

The final effective expression for free energy F is thus given by:

$$F = F_{face\ shells} + F_{core} \tag{21}$$

or

$$F = \iiint_{\substack{face\ shells' \\ volume}} J\,dy^1 dy^2\,dy^3\left(\frac{\epsilon}{2(1+\nu)}\left(a^{\alpha\delta}a^{\beta\gamma} + \frac{\nu}{1-\nu}\,a^{\alpha\beta}a^{\delta\gamma}\right)\eta_{\alpha\beta}\,\eta_{\gamma\delta} - \frac{\epsilon\,a\Delta T}{1-\nu}\,a^{\alpha\beta}\,\eta_{\alpha\beta}\right) \tag{22}$$

$$+ \iiint_{core} J\,dy^1 dy^2\,dy^3\left(\frac{\epsilon_c}{2(1+\nu_c)}\,a^{\alpha\beta}\,\eta_{\alpha 3}\,\eta_{\beta 3}\right).$$

Assuming face shell strains, temperatures, and metric elements to be replaceable by their mean values (at the face shell mid-surfaces) and using ($\pm$) notation to denote inner and outer face shells, respectively, this becomes:

$$F = \iint \int_{y^3 = -\frac{h_c}{2}}^{\frac{h_c}{2}} J\, dy^1\, dy^2\, dy^3 \left(\frac{\epsilon_c}{2(1+\nu_c)}\, a^{\alpha\beta}\, \eta_{\alpha 3}\, \eta_{\beta 3} \right)$$

$$+ h_{(+)} \iint J_{(+)}\, dy^1\, dy^2 \left(\frac{\epsilon}{2(1+\nu)} \left[a^{\alpha\delta}_{(+)}\, a^{\beta\gamma}_{(+)} + \frac{\nu}{1-\nu}\, a^{\alpha\beta}_{(+)}\, a^{\gamma\delta}_{(+)} \right] \eta_{\alpha\beta_{(+)}}\, \eta_{\gamma\delta_{(+)}} - \frac{\epsilon \alpha \Delta T_{(+)}}{1-\nu}\, a^{\alpha\beta}_{(+)}\, \eta_{\alpha\beta_{(+)}} \right)$$

$$+ h_{(-)} \iint J_{(-)}\, dy^1\, dy^2 \left(\frac{\epsilon}{2(1+\nu)} \left[a^{\alpha\delta}_{(-)}\, a^{\beta\gamma}_{(-)} + \frac{\nu}{1-\nu}\, a^{\alpha\beta}_{(-)}\, a^{\gamma\delta}_{(-)} \right] \eta_{\alpha\beta_{(-)}}\, \eta_{\gamma\delta_{(-)}} - \frac{\epsilon \alpha \Delta T_{(-)}}{1-\nu}\, a^{\alpha\beta}_{(-)}\, \eta_{\alpha\beta_{(-)}} \right) . \qquad (23)$$

If the face shell thicknesses $h_{(+)}$, $h_{(-)}$ vary along the meridian, it is merely necessary to keep these quantities inside their respective integrals.

Thus, in the core, integration through the core thickness (with respect to y^3) is required while in the face shells, mean values (values at the face-shell mid-surfaces) are used. More will be said subsequently about the meaning of the face-shell mean temperatures $\Delta T_{(+)}$ and $\Delta T_{(-)}$ which are called for in the free energy.

The possible presence of external pressure $p(y^1, y^2)$ requires the formulation of a work term W as follows:

$$W = \iint dy^1\, dy^2\, \tilde{\tilde{J}}(y^1, y^2)\; p(y^1, y^2)\; u^3(y^1, y^2)\ . \tag{24}$$

The variational formulation of the problem of sandwich shell response to both mechanical (pressure) and thermal loads is then simply the following:

$$\delta\,(F - W) = 0 \tag{25}$$

where the variation is performed with respect to displacements and where $p(y^1, y^2)$ is constant with respect to the variation operation.

3. DISPLACEMENT AND STRAIN EXPRESSIONS, AND REDUCTION TO A TWO-SPACE PROBLEM

In accordance with usual shell theoretical assumptions, it is presumed that the tangential physical displacements are approximable by first-order polynomials in y^3 and the normal displacement is independent of y^3.

$$u^\alpha = u^\alpha_{(o)}(y^1, y^2) + y^3 u^\alpha_{(1)}(y^1, y^2)$$

$$u^3 = u^3_{(o)}(y^1, y^2) \, . \tag{26}$$

The relation between tensor and physical displacements is:

$$u^i = \xi^i \sqrt{a_{ii}} = \xi_i \sqrt{a^{ii}} \tag{27}$$

no sum on i

where ξ_i is the contravariant form of the displacement vector . Thus,

$$u^\alpha = \xi^\alpha \sqrt{a_{\alpha\alpha}} \qquad \text{no sum on } \alpha$$

$$u^3 = \xi^3 \tag{28}$$

The strain-displacement expression within the assumption of linear elasticity is

$$\eta_{ij} = \frac{1}{2}(\xi_{i,j} + \xi_{j,i}) \tag{29}$$

commas denoting covariant derivatives. Following from (28) and (29), together with the orthogonality of the curvilinear coordinate system and the independence of metric elements a_{ij} on y^1, it can be shown that:

$$\eta_{11} = \sqrt{a_{11}}\,\frac{\partial u^1}{\partial y^1} + \frac{u^2}{2}\,\sqrt{a^{22}}\,\frac{\partial a_{11}}{\partial y^2} + \frac{u^3}{2}\,\frac{\partial a_{11}}{\partial y^3}$$

$$\eta_{22} = \sqrt{a_{22}}\,\frac{\partial u^2}{\partial y^2} + \frac{u^3}{2}\,\frac{\partial a_{22}}{\partial y^3}$$

$$\eta_{12} = \frac{1}{2}\,\sqrt{a_{22}}\,\frac{\partial u^2}{\partial y^1} - \frac{u^1}{4}\sqrt{a^{11}}\,\frac{\partial a_{11}}{\partial y^2} + \frac{1}{2}\,\sqrt{a_{11}}\,\frac{\partial u^1}{\partial y^2}$$

$$\eta_{13} = \frac{1}{2}\,\sqrt{a_{11}}\,\frac{\partial u^1}{\partial y^3} + \frac{1}{2}\,\frac{\partial u^3}{\partial y^1} - \frac{u^1}{4}\,\sqrt{a^{11}}\,\frac{\partial a_{11}}{\partial y^3}$$

$$\eta_{23} = \frac{1}{2}\sqrt{a_{22}}\,\frac{\partial u^2}{\partial y^3} + \frac{1}{2}\,\frac{\partial u^3}{\partial y^2} - \frac{u^2}{4}\,\sqrt{a^{22}}\,\frac{\partial a_{22}}{\partial y^3}\ . \tag{30}$$

Substituting into (30) from (26) the strains are expressed in terms of $u^i_{(0)}$ and $u^i_{(1)}$.

$$\eta_{11} = \sqrt{a_{11}}\left(\frac{\partial u^1_{(0)}}{\partial y^1} + y^3\,\frac{\partial u^1_{(1)}}{\partial y^1}\right) + \frac{\sqrt{a^{22}}}{2}\,\frac{\partial a_{11}}{\partial y^2}\left(u^2_{(0)} + y^3 u^2_{(1)}\right) + \frac{u^3_{(0)}}{2}\,\frac{\partial a_{11}}{\partial y^3}$$

$$\eta_{22} = \sqrt{a_{22}}\left(\frac{\partial u^2_{(0)}}{\partial y^2} + y^3\,\frac{\partial u^2_{(1)}}{\partial y^2}\right) + \frac{u^3_{(0)}}{2}\,\frac{\partial a_{22}}{\partial y^3}$$

$$\eta_{12} = \frac{1}{2}\sqrt{a_{22}}\left(\frac{\partial u^2_{(0)}}{\partial y^1} + y^3\,\frac{\partial u^2_{(1)}}{\partial y^1}\right) + \frac{1}{2}\sqrt{a_{11}}\left(\frac{\partial u^1_{(0)}}{\partial y^2} + y^3\,\frac{\partial u^1_{(1)}}{\partial y^2}\right) - \frac{\sqrt{a^{11}}}{4}\,\frac{\partial a_{11}}{\partial y^2}\left(u^1_{(0)} + y^3 u^1_{(1)}\right)$$

$$\eta_{13} = \frac{1}{2}\,\sqrt{a_{11}}\,u^1_{(1)} + \frac{1}{2}\,\frac{\partial u^3_{(0)}}{\partial y^1} - \frac{\sqrt{a^{11}}}{4}\,\frac{\partial a_{11}}{\partial y^3}\left(u^1_{(0)} + y^3\,u^1_{(1)}\right)$$

$$\eta_{23} = \frac{1}{2}\,\sqrt{a_{22}}\,u^2_{(1)} + \frac{1}{2}\,\frac{\partial u^3_{(0)}}{\partial y^2} - \frac{\sqrt{a^{22}}}{4}\,\frac{\partial a_{22}}{\partial y^3}\left(u^2_{(0)} + y^3\,u^2_{(1)}\right). \tag{31}$$

These expressions for strain now permit the evaluation of $\eta_{ij_{(+)}}$ and $\eta_{ij_{(-)}}$ in an obvious manner. As in the expressions for geometrical quantities $a^{ij}_{(+)}$, $a^{ij}_{(-)}$, etc., it is merely necessary to substitute for y^3 the values $\left(\frac{h_c+h_{(+)}}{2}\right)$and $-\left(\frac{h_c+h_{(-)}}{2}\right)$in the respective integrands of $F_{(+)}$ and $F_{(-)}$.

Now the metric tensor elements a_{ij} and a^{ij} are known functions of y^1, y^2, y^3 as is the Jacobian J. Thus, integration with respect to y^3 through the core thickness is possible in the core contribution to F. The core contribution may be integrated with respect to y^3 either analytically or by quadratures, whichever is more convenient in the numerical program. The result, in either case, is a formulation (25) in which now both F and W are 2-space integrals (over y^1 and y^2).

It is important to note that, unlike the homogeneous shell analysis, the sandwich shell theory places no restriction on the shear strains $\eta_{\alpha 3}$ in the core material. Thus, the displacement slopes $u^{\alpha}_{(1)}$ cannot be evaluated a priori in terms of the $u^{i}_{(o)}$ but must be found as a result of the overall calculation. This implies that five functions $u^{\alpha}_{(o)}$, $u^{\alpha}_{(1)}$, $u^{3}_{(o)}$ are being sought in the sandwich problem, whereas only three were required in the homogeneous shell problem. Hence, variations must be performed with respect to all five of these functions in the present case. Furthermore, it should be noted that ΔT appears only in the face-shell contributions to F, so that it is unnecessary to introduce the $T^{(o)}$ $T^{(1)}$ $T^{(2)}$ integral expressions which appeared in the homogeneous shell analysis.

4. REDUCTION TO A SET OF ONE-DIMENSIONAL PROBLEMS BY FOURIER ANALYSIS.

As in the homogeneous shell problem, the sandwich shell problem is transformed by Fourier analysis from a two-space problem to a set of one-dimensional problems for the Fourier coefficients of the displacements, strains, and stresses. This Fourier analysis proceeds in a manner similar to that used in the homogeneous shell problem. It is assumed first that $\alpha\Delta T$ and p may be decomposed into Fourier cosine series in y^1 (or, equivalently, in θ). If $\alpha\Delta T$ and p are symmetric about different θ-values, then we need merely superimpose the stresses, strains, and displacements of two separate responses with the proper angular displacement, since the present analysis is a linear one. With this in mind, we express $\alpha\Delta T$ and p in the form:

$$\alpha\Delta T = \sum_{m=o}^{\infty} {}_mT \cos m\theta$$

$$p = \sum_{m=o}^{\infty} {}_mp \cos m\theta \; . \qquad (32)$$

Corresponding to these forms in the forcing phenomena, the appropriate forms for displacements and strains are:

$$u^1_{(o)} = \sum_{1}^{\infty} {}_mu^1_{(o)} \sin m\theta \qquad u^1_{(1)} = \sum_{1}^{\infty} {}_mu^1_{(1)} \sin m\theta$$

$$u^2_{(o)} = \sum_{0}^{\infty} {}_mu^2_{(o)} \cos m\theta \qquad u^2_{(1)} = \sum_{0}^{\infty} {}_mu^2_{(1)} \cos m\theta$$

$$u^3_{(o)} = \sum_{0}^{\infty} {}_mu^3_{(o)} \cos m\theta \qquad (33)$$

$$\eta_{11} = \sum_{0}^{\infty} {}_m\eta_{11} \cos m\,\theta$$

$$\eta_{22} = \sum_{0}^{\infty} {}_m\eta_{22} \cos m\,\theta$$

$$\eta_{12} = \sum_{1}^{\infty} {}_m\eta_{12} \sin m\,\theta$$

$$\eta_{13} = \sum_{1}^{\infty} {}_m\eta_{13} \sin m\,\theta$$

$$\eta_{23} = \sum_{0}^{\infty} {}_m\eta_{23} \cos m\,\theta\,. \tag{34}$$

Analogous expressions apply for the corresponding stress components, i.e., τ^{11} is a cosine series, etc.

The detailed expressions for the strain components are as follows:

$${}_m\eta_{11} = \sqrt{a_{11}}\left(m\,{}_m u^1_{(0)} + y^3\, m\,{}_m u^1_{(1)}\right) + \frac{\sqrt{a^{22}}}{2}\,\frac{\partial a_{11}}{\partial y^2}\left({}_m u^2_{(0)} + y^3\,{}_m u^2_{(1)}\right) + \frac{{}_m u^3_{(0)}}{2}\,\frac{\partial a_{11}}{\partial y^3}$$

$${}_m\eta_{22} = \sqrt{a_{22}}\left(\frac{\partial\,{}_m u^2_{(0)}}{\partial y^2} + y^3\,\frac{\partial\,{}_m u^2_{(1)}}{\partial y^2}\right) + \frac{{}_m u^3_{(0)}}{2}\,\frac{\partial a_{22}}{\partial y^3}$$

$${}_m\eta_{12} = -\frac{\sqrt{a_{22}}}{2}\left(m\,{}_m u^2_{(0)} + y^3\, m\,{}_m u^2_{(1)}\right) + \frac{\sqrt{a_{11}}}{2}\left(\frac{\partial\,{}_m u^1_{(0)}}{\partial y^2} + y^3\,\frac{\partial\,{}_m u^1_{(1)}}{\partial y^2}\right) - \frac{\sqrt{a^{11}}}{4}\,\frac{\partial a_{11}}{\partial y^2}\left({}_m u^1_{(0)} + y^3\,{}_m u^1_{(1)}\right)$$

$${}_m\eta_{13} = \frac{1}{2}\sqrt{a_{11}}\;{}_m u^1_{(1)} - \frac{m}{2}\,{}_m u^3_{(0)} - \frac{\sqrt{a^{11}}}{4}\,\frac{\partial a_{11}}{\partial y^3}\left({}_m u^1_{(0)} + y^3\,{}_m u^1_{(1)}\right)$$

$${}_m\eta_{23} = \frac{1}{2}\sqrt{a_{22}}\;{}_m u^2_{(1)} + \frac{1}{2}\,\frac{\partial\,{}_m u^3_{(0)}}{\partial y^2} - \frac{\sqrt{a^{22}}}{4}\,\frac{\partial a_{22}}{\partial y^3}\left({}_m u^2_{(0)} + y^3\,{}_m u^2_{(1)}\right)\,. \tag{35}$$

As may be seen by inspection of the free energy expression (23) and the work integral (24), the harmonics all decouple and it suffices to consider each Fourier component separately. The $m = 0$ component corresponds to axisymmetric loading; $m = 1$, to the simplest case of asymmetric loading, and so on. The linearity of the analysis then permits superposition of the Fourier components with the appropriate $\cos m\theta$ or $\sin m\theta$ multipliers to give total displacements, strains, or stresses as required.

5. NUMERICAL ANALYSIS

The sandwich shell response to thermal and/or mechanical loading is to be solved starting from the formulation (25) together with expressions (23) and (24) for F and W, respectively. As noted earlier, the core contribution to F is integrated numerically or analytically. This leaves the expression F-W in the form of a two-space integral with integrand involving the known geometry (a_{ij}, etc.) and the five unknown functions of y^1 and y^2 $(u^{\alpha}_{(o)}, u^{\alpha}_{(1)}, u^3_{(o)})$. Resolution into Fourier components then reduces the (F-W) integral to a set of one-dimensional integrals over y^2, the meridional variable, and reduces the entire analysis to a set of uncoupled problems.

$$\delta\ ({}_mF - {}_mW) = 0 \tag{36}$$

for the functions $({}_mu^{\alpha}_{(o)}, {}_mu^{\alpha}_{(1)}, {}_mu^3_{(o)})$.

This may be handled by any one of a number of techniques: (a) A direct variational method may be used in which each of the unknown displacement functions is expanded in a series of boundary-condition satisfying functions and the variation is formed with respect to the coefficients of these functions. (b) Alternatively, the direct variational method may be applied with respect to the point values of the displacements and displacement slopes at a set of mesh points along the shell meridian. (This corresponds to the method which has been programmed for homogeneous shells.) (c) Another possibility is to form the required variation analytically, thereby deriving the differential equations and natural boundary conditions of the problem. These could then be solved numerically. Inasmuch as this corresponds closely to the direct variational method (b) and method (b) insures the positive definite nature of the matrix for the difference equations, method (b) is preferred. Furthermore, method (b) eliminates the necessity for deriving the Euler equations analytically and, at the same time, automatically introduces natural boundary conditions at free or simply supported edges in proper finite-difference form. Under this method, the required integrals are evaluated by quadratures in terms of the mesh-point values of the unknown functions. The result leads directly to the matrix and the forcing vector for the numerical determination of these point values. The matrix algebra problem is then solved for these point values, and strains and stresses are calculated from them using finite difference approximations to the required derivatives.

6. NUMERICAL DETERMINATION OF TEMPERATURES ΔT_+ and ΔT_-

The required mean temperature increments ΔT_+ and ΔT_- in the inner and outer face shells may be determined by a quasi-one-dimensional numerical analysis. A suitable technique may be described as follows: Consider the one-dimensional composite slab as shown in the sketch. The face and core thicknesses are those of the sandwich shell

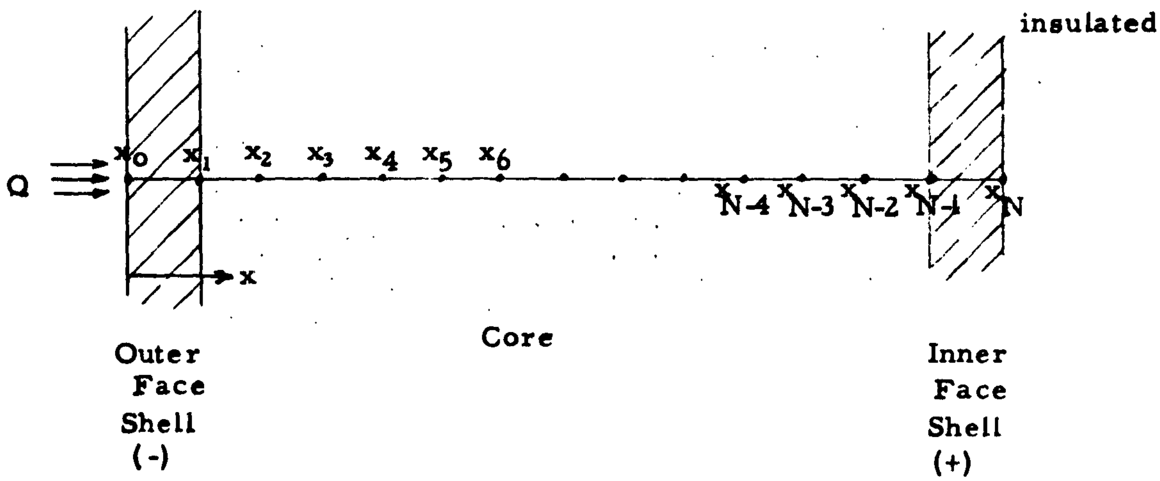

Let the heat flux into the outer face at some point (y^1 y^2) be denoted by Q and assume an insulated inner face. It is required to calculate the mean temperature in each of the face sheets. This may be done by calculating the temperatures at the mesh points shown at a set of equal time increments Δt and then defining

$$\Delta T_{(+)}(\nu\Delta t) = \Delta T_+^\nu = \frac{T_N^\nu + T_{N-1}^\nu}{2} - T_{reference}$$
$$\Delta T_{(-)}(\nu\Delta t) = \Delta T_-^\nu = \frac{T_1^\nu + T_0^\nu}{2} - T_{reference} \tag{37}$$

where $T_m^{\nu} = T(x_m, \nu\Delta t)$.

The heat flux Q depends on time, on $(y^1\ y^2)$, and on the outer wall temperature T_o^{ν} itself. The quasi-one-dimensional analysis must, therefore, be performed at a number of space points $(y^1\ y^2)$ depending upon the nature of the physical problem. If only axisymmetric conditions are of interest in a particular application, then no y^1-dependence of Q occurs. The reason that Fourier analysis is not suggested for the heat problem lies in the essentially non-linear character of the outer wall boundary conditions; i.e., radiation is frequently important, and this involves $(T_o^{\nu})^4$, and convective heat transfer also involves T_o^{ν} in a non-linear manner. Thus, the functions ΔT_+ and ΔT_- must be calculated first as functions of (y^1, y^2, t) and then the quantities $\alpha\Delta T_+$, $\alpha\Delta T_-$ may be Fourier analyzed giving Fourier components which depend on y^2 and time. The thermal stress analysis is then carried out at a number of fixed values of time.

A mesh is chosen for the core, and the heat equation for the composite material is written in difference form. These difference equations may be put in explicit difference form with a strict upper limit on permissible time step Δt for stability. Alternatively, they may be written in implicit form with no stability limitation on Δt. The implicit form requires solution of $(N + 1)$ simultaneous equations, but the tri-diagonal nature of the associated matrix permits rapid and efficient solution. A more serious problem which arises in connection with the implicit scheme is the necessity to iterate in order to express heat flux Q at the latest time. This is not a major drawback, however, and much numerical experience has been accumulated in this respect. The large gain to be realized in time-step size Δt recommends the use of the implicit scheme. The difference equations for the heat problem are well-known and need not be reproduced herein.

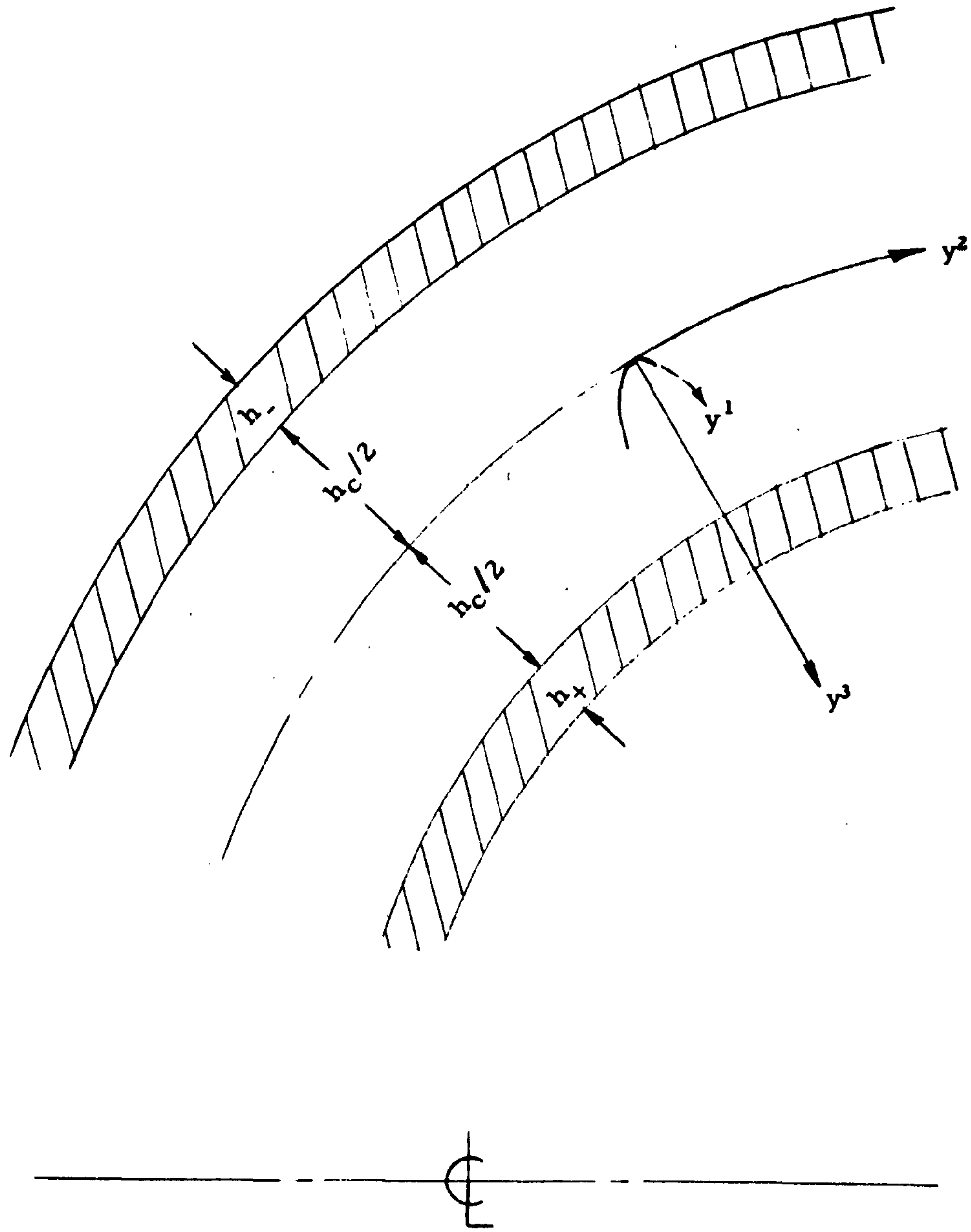

Figure 1. Geometry of Sandwich Shell